ARTICLE IN PRESS

BBA - General Subjects xxx (xxxx) xxxx

Contents lists available at ScienceDirect

BBA - General Subjects

journal homepage: www.elsevier.com/locate/bbagen

Gold nanomaterials as key suppliers in biological and chemical sensing, catalysis, and medicine

Mojtaba Falahati[a,*], Farnoosh Attar[b], Majid Sharifi[a,c], Ali Akbar Saboury[d], Abbas Salihi[e,f], Falah Mohammad Aziz[e], Irena Kostova[g], Clemens Burda[h], Peter Priecel[i], Jose A. Lopez-Sanchez[i], Sophie Laurent[j,k], Nasrin Hooshmand[l], Mostafa A. El-Sayed[l]

[a] Department of Nanotechnology, Faculty of Advanced Science and Technology, Tehran Medical Sciences, Islamic Azad University, Tehran, Iran
[b] Department of Biology, Faculty of Food Industry & Agriculture, Standard Research Institute (SRI), Karaj, Iran
[c] Department of Animal Science, Faculty of Agriculture, University of Tabriz, Tabriz, Iran
[d] Institute of Biochemistry and Biophysics, University of Tehran, Tehran, Iran
[e] Department of Biology, College of Science, Salahaddin University-Erbil, Kurdistan Region, Iraq
[f] Department of Medical Analysis, Faculty of Science, Tishk International University, Erbil, Iraq
[g] Department of Chemistry, Faculty of Pharmacy, Medical University, 2 Dunav St., Sofia 1000, Bulgaria
[h] Department of Chemistry, Case Western Reserve University, 10900 Euclid Avenue, Cleveland, OH 44106, United States
[i] Stephenson Institute for Renewable Energy, Department of Chemistry, University of Liverpool, Crown Street, L69 7ZD Liverpool, United Kingdom
[j] General, Organic and Biomedical Chemistry, NMR and Molecular Imaging Laboratory, University of Mons, Avenue Maistriau, 19, B-7000 Mons, Belgium
[k] Center for Microscopy and Molecular Imaging (CMMI), Rue A. Bolland, 8 B-6041 Gosselies, Belgium
[l] Laser Dynamics Laboratory, School of Chemistry and Biochemistry, Georgia Institute of Technology, Atlanta, GA 30332, United States

ARTICLE INFO

Keywords:
Gold NPs
Colorimetry
Sensing
Catalysis
Imaging
Photothermal therapy

ABSTRACT

Background: Gold nanoparticles (AuNPs) with unique physicochemical properties have received a great deal of interest in the field of biological, chemical and biomedical implementations. Despite the widespread use of AuNPs in chemical and biological sensing, catalysis, imaging and diagnosis, and more recently in therapy, no comprehensive summary has been provided to explain how AuNPs could aid in developing improved sensing and catalysts systems as well as medical settings.

Scope of review: The chemistry of Au-based nanosystems was followed by reviewing different applications of Au nanomaterials in biological and chemical sensing, catalysis, imaging and diagnosis by a number of approaches, and finally synergistic combination therapy of different cancers. Afterwards, the clinical impacts of AuNPs, future application of AuNPs, and opportunities and challenges of AuNPs application were also discussed.

Major conclusions: AuNPs show exclusive colloidal stability and are considered as ideal candidates for colorimetric detection, catalysis, imaging, and photothermal transducers, because their physicochemical properties can be tuned by adjusting their structural dimensions achieved by the different manufacturing methods.

General significance: This review provides some details about using AuNPs in sensing and catalysis applications as well as promising theranostic nanoplatforms for cancer imaging and diagnosis, and sensitive, non-invasive, and synergistic methods for cancer treatment in an almost comprehensive manner.

1. Introduction

Recently, the properties of metal NPs have been the subject of intense research due to the interesting properties of their SPR. Plasmonic metal NPs exhibit unique absorption, scattering, and surface localized electric-field intensities. The effect of NP size, shape, composition and inter-particle separation distance on SPR, have received significant attention with regards to finding optimal NP dimensions with high

Abbreviation: computed tomography, CT; doxorubicin, DOX; gadolinium, Gd; localized surface plasmon resonance, LSPR; magnetic resonance imaging, MRI; monolayer protected clusters, MPCs; nanocages, NC; Nanoparticle, NP; nanorods, NR; near infrared, NIR; optical imaging, OI; photoacoustic, PA; photodynamic therapy, PDT; photothermal therapy, PTT; platinum, Pt; polyethylene glycol, PEG; positron-emission tomography, PET; radiofrequency ablation, RFA; silica, SiO_2; silver, Ag; single-photon emission computed tomography, SPECT; surface plasmon resonance, SPR; surface-enhanced Raman spectroscopy, SERS; surface-enhanced resonance Raman scattering, SERRS; ultrasound, US; X-ray fluorescence computed tomography, XFCT

* Corresponding author.
E-mail address: Mojtaba.falahati@alumni.ut.ac.ir (M. Falahati).

https://doi.org/10.1016/j.bbagen.2019.129435
Received 2 June 2019; Received in revised form 11 September 2019; Accepted 11 September 2019

sensitivity in the field of material chemistry [1,2]. NPs are typically of a size comparable to bio-macromolecules and can be employed for several implementations like chemical and biological sensing, catalysis, accurate imaging, and personalized cancer treatment [1,3]. After establishing interdisciplinary nanotechnology fields, it may be believed that nanomaterial will combine with chemically and clinically applicable fields in the next generation of chemical and medical platforms. Most of the applications of nanotechnology are in sensing, catalysis and biomedicine. The well-studied nanosystems include nanomicelles, nanoliposomes, carbon nanotubes, quantum dots, dendrimers, and metallic NPs [4].

The application of AuNPs has gained a potential attention in the main branches of chemistry, physics, and medicine. AuNPs have also been extensively implemented in medicinal and biological studies due to their distinctive optical features deriving from their SPR properties [1,3,4]. Applications linked to plasmon resonance are countless, ranging from chemical and biological sensing or photothermal agents to cell imaging and killing [5,6]. The physicochemical features of AuNPs are dramatically changed by their diameter and morphology due to their unique electronic structure [5]. AuNPs are excellent candidates in developing analytical tools for specific applications such as detection, catalyst, diagnosis, and therapy [1,4,5,7,8]. Here, we provide the general review of the most recent applications of AuNPs in chemical and biological sensing, catalysis, clinical imaging, and therapy. To date, the published papers have been focused on biosensorics, immunoassays, bioimaging, cancer cells killing, and targeted drug delivery. This critical overview is focused on the chemistry of AuNPs and their applications for chemical and biological detection, catalytic agents, their conjugations for biomedical diagnostics and imaging, and finally as therapeutic agents.

2. Chemistry of gold NPs

There are several current reviews devoted to AuNPs [5,9–17]. Among their first applications, AuNPs were used for their therapeutic properties as colloidal Au [18]. In recent decades, there is an increase in the number of studies devoted to the synthesis of modified AuNPs. One motivation for the extensive interest in Au nanotechnology is that Au is the most electronegative metal and a good heat- and electric conductor with a face-centered cubic crystal lattice making it soft and plastic.

2.1. Synthetic protocols

A variety of synthetic protocols with the intention of controlling the size, shape, morphology and crystal structures of AuNPs has been observed and described in the literature [19]. AuNPs display significant stability and can be obtained in various methods in order to optimize their size and properties. Their chemical modification can be done by the interaction of the surface atoms with different ligands [20]. The synthetic methods used to produce AuNPs range from the classical reduction of $HAuCl_4$ to the reduction of Au complexes $[Au^{III}Cl_4]^-$ and stabilization with various ligands [20].

Au(III) ions are reduced by trisodium citrate and by sodium borohydride ($NaBH_4$). The second route can be classified in three steps: (i) Phase transfer by tetra-butyl-ammonium bromide; (ii) Reduction of Au(III) by the thiols; (iii) Reduction of Au(I) by $NaBH_4$ in the presence of thiols and/or sulfur-group compounds that cause the fabrication of AuNPs. Other techniques such as micro-emulsion [21], copolymer micelles [22] or seeding growth [23] have also been utilized to synthesize AuNPs.

2.2. Size and surface functionalization

Depending on their size and surface modification, AuNPs are usually divided into three key groups: colloids, NPs protected by an organic MPCs, and small clusters [24]. Au colloids have a size ranging from 10 to 100 nm. They can be obtained by chemical reduction of Au(III) salts with mild reducing agents [25]. For AuNPs, many synthetic methods have been developed. First of all, metallic AuNPs are typically produced by using $HAuCl_4$ and its reduction to Au^0 [26]. For the stabilization of Au colloids the adsorption of a wide range of compounds such as monolayers induced by salts or green synthesis route to reduce van der Waals and electrostatic forces on the surface of AuNPs is used [27–30]. Secondly, covering the MPCs involves the synthesis of particles with an Au core and a size between 1–10 nm surrounded by chemically adsorbed ligands as a monolayer [31]. In comparison with colloid NPs, MPCs show good stabilization when dissolved or in the solid state. The monolayer passivation prevents irreversible aggregation and conveys solubility in aqueous solutions and in biological medium. Between the models of ligand-capped clusters, $Au_{55}[(C_6H5)_3P]_{12}C_{l6}$ has been extensively studied [32]. Another cluster is Au_{20} possessing a stable naked tetrahedral form [33]. It was established that NPs containing the so-called "magic numbers" of Au atoms, like Au_{55} demonstrate better stability than others [34]. Many additional nanoclusters of different nuclearities have been realized, such as $Au_{25}(glutathione)_{18}$ [35], $Au_{38}(SPhX)_{24}$ [36], $Au_{40}(SR)_{24}$ [37], $Au_{52}(SR)_{32}$ [37], and $Au_{103}S_2(S\text{-}Nap)_{41}$ [38] obtained by reduction of clusters. It should be mentioned that the cluster of Au_{13} is the smallest member of the particle classification but larger particles containing 55, 147, 309, 561, 923 or more atoms are also possible. The third group, covering the small Au clusters, represents the "lower bound" of MPCs. The small Au clusters are molecular structures involving some atoms which are normally monodispersed. Their monodispersity allows their crystallization and the X-ray analysis particularly in the case of Au-thiolate clusters which is not possible for larger MPCs.

Classification of the different forms of AuNPs at the nanoscale and the respective synthesis techniques have been systematically reported [39]. Overall, success in developing plasmonic activities of AuNPs requires confidence in the methods of fabrication and accuracy. AuNPs are produced by different methods including photolithography, biosynthetic organisms, chemical synthesis, polymer intermediates, US, and lasers. with varying sizes and morphologies [40]. However, chemical synthesis seems to be a very much simpler form of AuNP fabrication and cost effective among all fabrication routes. Besides, diverse synthesis approaches of AuNPs, have no effect on their plasmonic features. But other factors such as the dielectric environment, size and

Table 1
Summary of the synthesis and SPR features AuNPs [40].

Shape	Size	Synthesis method	SPR peak
Spheres	5–150 nm	Seed-mediated growth	520–650 nm
Rods	20 nm	Electrochemical or Photochemical reduction, Seed-mediated growth, Bioreduction, Solvothermal reduction, etc.	600–1800 nm
Plate and Disks	40–1000 nm with 5–50 nm thickness	Electrochemical reduction, Microwave- or US-assisted reduction, Photo-induced reduction.	700–1300 nm
Shells	10–400 nm	Templated-directed synthesis	520–900 nm
Cage and hollows	20–200 nm	Galvanic replacement reaction	400–1200 nm
Stars	45–300 nm	Seed-mediated growth	550–800 nm
Polyhedral	20–270 nm	Polyol process, Seed-mediated growth	560–1000 nm

shape, composition, assembly, and physicochemical properties of the NPs affect their plasmonic activities [40]. The most popular forms are NRs, nanoshells and nanospheres (Table 1). However, there are some other shapes such as triangles, boxes, cages, semi-shells etc., each of them having its own specific properties and applications [41]. Mesoporous sponges and thin films of AuNPs have also received a significant share of interest [42].

In the case of AuNPs, the most important applications arise from their remarkable surface properties. The functionalization of AuNPs surface plays an essential role in their stability, dispersity and solubility. The most remarkable illustration of NPs surface modification and functionalization is their coupling with biomolecules. The surface composition of AuNPs can be adapted to contain a range of functional groups or mixtures of functional groups; this represents a good way for regulating their optical, electronic or catalytic properties, turning NPs into very useful nanostructures in a variety of practical fields. With this in mind, the main challenge in the production of metal nanodispersions is the low stability of NPs in solutions and the tendency to form aggregates. To prepare stable NPs of fixed size and shape as colloidal solutions, the existence of stabilizing agents that adsorb on the particle surface hence preventing further association is required. Different sulfur-containing organic substances (thiols, sulfides, disulfides, thiourea derivatives, xanthates, dithiocarbamates, etc.) have often been used as such stabilizers [43–45]. Although, there is still no general agreement on the thiol interaction mechanism with the Au surface, most scientists believe that this interaction is joined with the S-H bond cleavage in the thiol molecule and the resulting alkanethiolate becomes bound to the surface of the metal [45–47]. The adsorption of disulfides on the surface of Au is accompanied by the S-S bond cleavage to afford Au thiolate, identical with the thiol reaction. While, coupling by S atom is undoubtedly the most leading binding mode, various elements (hydrogen, halogens, nitrogen, phosphorus, arsenic, antimony, oxygen, selenium, tellurium, carbon etc.) may also be used to bind to Au [48]. Therefore, Au surfaces offer an appropriate platform on which it is possible to accumulate monolayer structures of different organic molecules. Modifying AuNPs with various organic ligands (amines, thiocyanates, carboxylates, etc.) makes it possible to impart their anticipated properties. Presently, the attention is focused on ligands containing a "functional" group (fluorophore, chromophore, receptor or electrochemically active group) bound to a sulfur-containing group through a linker, for instance. Finally, among the many synthetic methods reported in the literature, AuNPs can be established using coordination chemistry strategies combining metal NPs and coordination complexes [49]. It has to be taken into consideration that atoms at the NP surface, which are most important for its chemical and physical properties, exhibit incomplete valence, meaning that they are coupled to the inner atoms, thus leaving peripheral atoms available for donor-acceptor interaction with appropriate ligands. Accordingly, the coordination chemistry of AuNPs can be explained by using the concept of hard and soft acid-base. The interaction with metal ions and the synthesis and application of AuNPs with metal complexes attached to the surface is a contemporary and alternative way to prevent the NP aggregation [50]. Coordination or complexation blocks the chelating fragment in the molecule thus preventing the irreversible aggregation of NPs. A very noteworthy aspect is the opportunity for the stabilization control of AuNPs dispersions by using the targeting coupling of charged coordination complexes like $[Fe(CN)5L]^{3-}$. Pentacyanoferrate(II) ions are useful for this point because they have high charge density and appropriate kinetic and thermodynamic properties [49]. The cyanide ions in the complex $[Fe(CN)_5]^{3-}$ are inert in substitution reactions, keeping only one coordination position for reaction with donor atoms. The chemical properties of these complex ions depend on the nature of the ligand L and typically they show a strong affinity for nitrogen and sulphur containing ligands. Several interesting systems have been described by using different ligands: $[Fe(CN)_5(2\text{-mpy})]^{3-}$, $[Fe(CN)_5(4\text{-mpy})]^{3-}$, $[Fe(CN)_5(pzt)]^{3-}$, $[Fe(CN)_5(dmso)]^{3-}$, where 2-mercaptopyridine (2-mpy), 4-mercaptopyridine (4-mpy), pyrazine-2-ethanethiol (pzt) and dimethyl sulfoxide (dmso) [28]. So far several reports were devoted to AuNPs modified with coordination compounds and their applications [49,51,52]. The review of Beloglazkina et al. [53] summarizes the data on the synthesis and practical use of AuNPs bearing metal ions coordinated on their surface to the terminal donor groups of organic ligands that stabilize the NPs. Modified NPs may serve for the design of new functional hybrid materials and supramolecular structures. From the numerous literature reports, it can be assumed that the common synthetic method for obtaining NPs with metal complexes is the use of functionalized thiols that form stable bonds with the metal surface [53]. Among other ligands, nitrogen-donor molecules prevail however oxygen- and phosphor-donor ligands have also been explored. Coordination complexes have occasionally been used for surface functionalization of metal NPs despite their consequences in catalysis. Many studies have described AuNPs functionalization with metal complexes depending on the phase transfer [54].

3. Chemical and biological sensing

AuNP has attracted a great deal of interest in sensing analysis due to their well-characterized colorimetric properties. In sensor technology, utilizing an instrument with high sensitivity yields expensive settings. By tuning the interparticle distance and trapping analytical molecules in the hot spots region, we can fabricate improved sensing devices. At nanoscale separations, the hot spots produced in these composite frameworks exhibit noteworthy enhancements in Raman scattering, fluorescence emission, and IR absorption. This has been useful in a variety of applications including biological imaging, selective PTT, SERS, optical wave guiding, and biochemical sensing [55,56]. Colloidal NPs may reveal different colors upon interaction with aggregated or conjugated species due to the alteration of Au's LSPR at the nanoscale. Therefore, different interactions between ligand and NP may change the optical signals, followed by detection of different sensing approaches. A wide number of studies have been focused on the design and progress of plasmonic sensors by ligand-inspired colorimetric changes of AuNPs. In this section, we overview a number of approaches that have been studied to monitor the colorimetric features of AuNPs after the addition of different ligands such as nucleic acids, proteins, organic and inorganic molecules.

The strong absorption of AuNPs offers interesting optical properties with a high potential application in the colorimetric study of analytes-NP interaction and biodiagnostic assays [1,4,5,57]. For instance, an optical colorimetric sensor was developed by application of Ag and AuNPs for quantitative detection of H_2O_2 and H_2 [58–60]. Also, Yang et al. [61] reported an analyte-induced autocatalytic amplification using AuNPs probes for colorimetric determination of heavy metal ions. Besides, Han et al. [62] and Sadani et al. [63] developed an Au chip-based nanozyme for colorimetric determination of mercury ions (Fig. 1A). On the other hand, Priyadarshini and Pradhan [64] reviewed AuNPs as cost-effective sensors in colorimetric determination of toxic metal ions. Moreover, Thatai et al. [65] and Boruah and Biswas [66] studied the colorimetric determination of Pb^{2+} using Au nanocomposites and AuNPs. Likewise, Zhang et al. [67] reported a green fabrication route of AuNPs with pectinase as a distinctive colorimetric approach for Mg^{2+}. As well, Xu et al. [68] designed a uniform Au nanobipyramids for sensitive colorimetric determination of influenza virus. In the same way, Weerathunge et al. [69] provided Au nanozymes based on the colorimetric method to detect human norovirus by increasing the detection limit to 3 viruses per assay equivalent to 30 viruses/mL of sample. Furthermore, Wei et al. [70] and Chang et al. [71] suggested an AuNPs conjugates with DNA for colorimetric discrimination of proteins and pollen allergens. Also, Shokri et al. [72] designed a unique method for the colorimetric detection of disulfide-induced self-assembled DNAs/RNAs via bare AuNPs (Fig. 1B). The novelty of this work was derived from the hybridization of DNA target

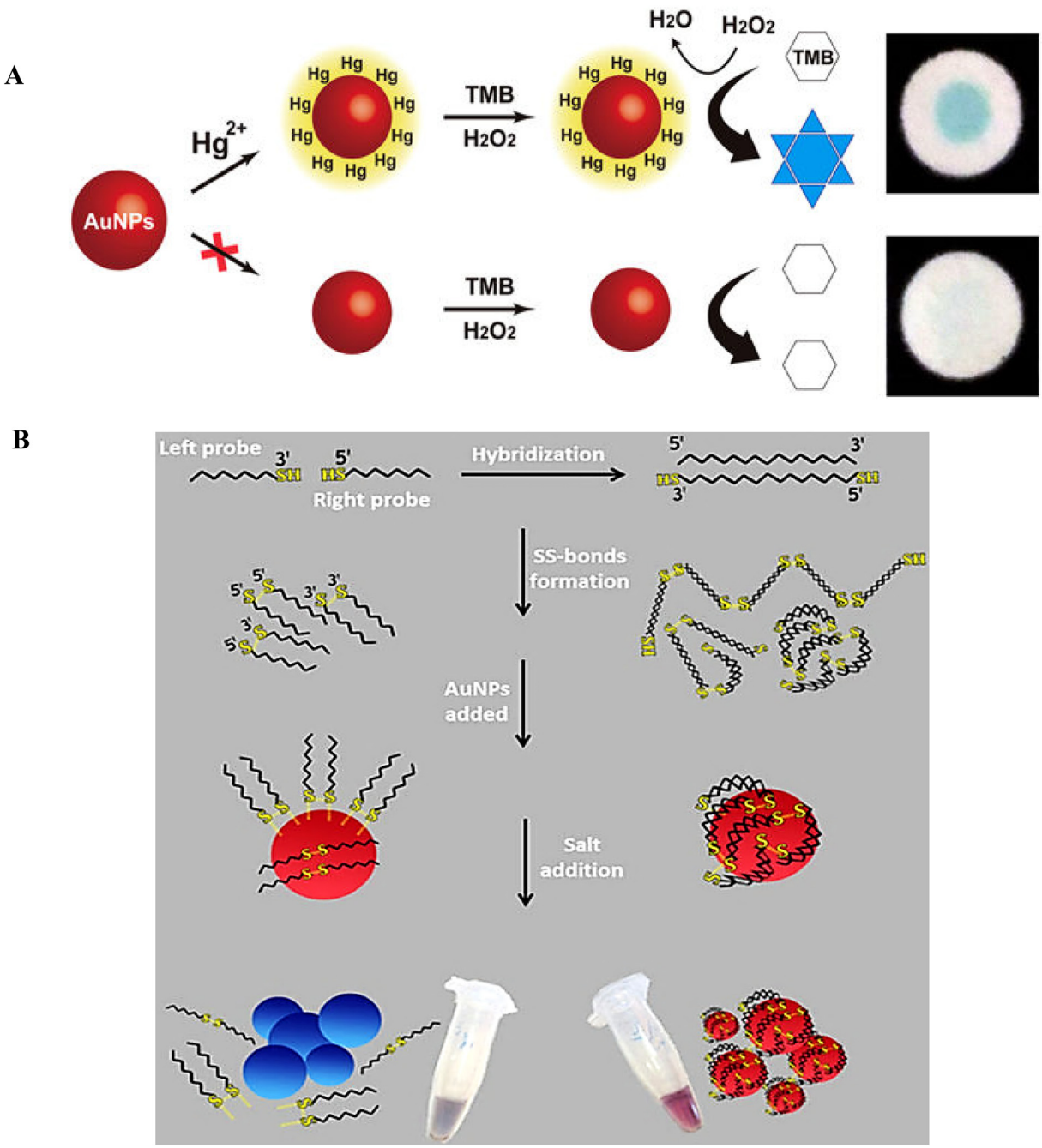

Fig. 1. Chemical and biological sensing. (A): Schematic illustration of the Au nanozyme-based analytical devices (AuNZ-PAD) colorimetric sensing mechanism for Hg^{2+} ions based on the Hg^{2+}-promoted nanozyme activity of AuNPs. When Hg^{2+} ions are introduced onto the AuNZ-PAD, the tetramethylbenzidine (TMB) chromogenic peroxidase substrate with H_2O_2 catalytic reaction is highly increased by the formation of Au–Hg combination, leading to blue staining of the paper chip [62]. (B): Schematic representation of the colorimetric determination by AuNPs using disulfide inspired self-assembling of nucleic acid targets with thiolated probes [72]. Reproduced under the terms of the Creative Commons Attribution License (CC BY).

with thiolated probes and the capability of DNA target to assemble at both ends and form long S-rich species. These species can be strongly attached on AuNPs surface by disulfide bonds with Au atoms. Some other colorimetric AuNPs applications were also reported in Table 2.

Table 2 summarizes the diversity of analytes that the AuNPs can detect for a variety of applications. It is clear that AuNPs can be applied to detect several molecules such as amino acids, drugs, proteins, heavy metals, ions, viruses, DNA, RNA, and other molecules. AuNPs are also attracting interest in the areas of cleaner production, sensing, therapeutics and diagnostics and offer themselves as supreme candidates for applications as platforms in designing biosensors, introducing a number of advantages over state of the art classical sensors.

4. Catalytic applications

Despite the many papers and reviews dedicated to the synthesis and properties of AuNPs of all shapes and forms, (5–14) in catalysis, the focus has been in the study of spherical AuNPs. This is well-documented and the triumphant emergence of the Au catalysis field has been well documented and revised by some excellent reviews on Au catalysis in general [73–92] or more specifically in homogeneous catalysis [93] photocatalysis [94] or oxidation reactions [95–97].This bias in the

Table 2
Some colorimetric AuNP applications for chemical and biological sensing.

NP	colorimetric assay	Ref.
AuNP	Aptasensors for determination of streptomycin in blood and milk	[359]
AuNP	Determination of DNA from the disassembly of DNA–AuNP species	[360]
Citric acid-coated AuNP	Recognition of pesticide dimethoate	[361]
AuNP	Cyanide detection	[362]
functionalized AuNP	In-situ colorimetric recognition of arylamine	[363]
PEG-modified AuNP	Detection of miRNA	[364]
AuNP	Sensing assays for enzymatic decarboxylation	[365]
AuNP	Protein sensing	[366]
AuNP	Chiral discrimination and determination of S-citalopram	[367]
AuNP	Imaging and counting single NPs	[368]
AuNP	Detection of plasmodiumvivax in urine	[369]
AuNP	Aggregation assay for arsenic (III)	[370]
AuNP	Detection of protein contents in artificial urine	[371]
AuNP	Detection of picomolar mercury ion	[372]
AuNP	Detection of single nucleotide polymorphisms	[373]
AuNP	Recognition of creatinine with good selectivity and sensitivity	[374]
AuNP	Detection of human papillomavirus (genotypes 16 and 18)	[375]
AuNP	Detection of urea and urease	[376]
AuNP	Aptasensors for detection of cancer cells	[377]
Graphene/AuNP hybrids	Determination of miRNA-21	[378]
AuNP	Sensing of Ag ion	[379]
AuNP	Detection of cucumber green mottle mosaic virus	[380]
Gallic acid capped AuNP	Determination of Cr (III) and Cr (VI)	[381]
AuNP	Determination of polyphosphates	[382]
AuNP	Detection of bisphenol A	[383]
AuNP	Aptasensors for detection of adenosine triphosphate	[384]
PEGylated AuNP	Detection of nitrite ions	[385]
AuNP and SiO_2 –Au nanocomposites	Detection of Pb^{2+}	[65]
functionalized AuNP	Detection of aluminum (III)	[386]
AuNP	Determination of micro-RNAs	[387]
AuNP	Measurement of Fe^{3+}	[388]
chitosan stabilized AuNP	Measurement of mercury (II)	[389]
AuNP	Immunosensor for Aβ (1–42)	[390]
AuNP	Aptasensor for determination of human estrogen receptor α	[391]
AuNP	Sensor array for discrimination of organophosphate pesticides	[392]
Au- nanobipyramids	Detection of influenza virus	[68]
Glutathione modified AuNP	Measurement of Pb^{2+} ions	[393]
AuNP	Measurement of aluminum and fluoride in water	[394]
AuNP	measurement of heavy-metal ions	[61]
AuNP	Chiral recognition of α-amino acids	[395]
AuNP	Determination of DNA oxidation	[396]
AuNP	Measurement of chromium (VI) ions	[397]
AuNP	Aptasensor for the detection of S. typhimurium	[398]
AuNP	Aptasensor for detection of adenosine triphosphate	[399]
Graphene-AuNP	Determination of oxytetracycline	[400]
AuNP	Detection of bacterial contamination water	[401]
AuNP	Detection of Hg^{2+} ions	[402]
AuNP	Detection of micro-RNA	[403]

catalysis field for the simpler preparative techniques that offer little NP control strongly contrasts with the refinement and synthetic control that the techniques used in other fields discussed in this review exhibit.

Traditionally, heterogeneous Au catalysts are prepared by simple synthetic methods such as impregnation or deposition-precipitation that involve the impregnation of the metal salt before or during the reduction process that result in the formation of the metal NPs in different dimensions and morphologies. In this regard, Hajfathalian et al. [98] by deforming the AuCu photocatalytic structures from spherical to triangular based on the vapor phase assembly method, enhanced the catalytic activity of the NPs by improving plasmon resonance in the visible spectrum with the amplification of the near field at the tip of the triangle. At the same time, it was also determined that the AuCu nanocluster alloys (50:50) enhanced the photocatalytic activity of AuCu compared to Au or Cu colloidal NPs [99]. More recently, the preparation of colloidal NPs and their subsequent immobilization on the surfaces of porous supports paved the way towards the enhanced AuNP-dimension control and promisingimproved activity and implications in many reactions [95,100–103].

Due to the extensive literature available on catalysis by spherical AuNPs and multitude of excellent recent review, we will put particular focus in the utilization of anisotropic AuNPs which have been extensively discussed in this review but are little explored within the field of Au catalysis. We hope that doing so, we can help build bridges across scientists in different disciplines with an interest in catalysis. For anisotropic AuNPs there are excellent reviews for detailed synthesis [28,104–123], properties [78,105,109,114,121,123–133] and various applications [10,105,109,111,112,114–116,122,127,128,134–138]. Recently, we reviewed in detail the catalytic applications of Au shaped as rods, polyhedrons, stars, flowers, urchins, cages, plates, wires or belts in chemo-, photo- and electrocatalysis [139]. In this short section, we will concisely explore the relevant literature on the newly emerged studies that contributed to the field of anisotropic Au catalysis as implications of the properties such as SPR are shared between catalysis, sensing, imaging, and therapy.

Anisotropic NPs are typically synthesized in colloidal form which offers control over multiple parameters affecting their size, shape or purity/yield. For catalytic applications, AuNPs can be used in this form [140–149], although one might argue this can limit their utilization and full potential, especially in industrial context with regards to

Table 3
Overview of publications from the literature that discuss various anisotropic AuNPs either in colloidal, core@shell or supported form for chemo-, photo- or electrocatalytic applications. For core@shell, the core is typically metal (in our case Au) and shell metal oxides, such as TiO_2, SiO_2 or CeO_2 but could be also other metal oxides.

Shape	Catalyst form	System type	Ref.
Rods, dumbbells, rattles, bipyramids	Colloidal	Chemo	[140–142,144,145,188–191,197,404–407]
Polyhedra (prims, pyramids, cubes, cages)	Colloidal	Chemo	[141–149,189,192,194,195,237,408–412]
Stars, flowers, urchins, dendrites	Colloidal	Chemo	[193,196,413–419]
Foams, porous networks, belts, tubes	Colloidal	Chemo	[186,187,420–423]
Rods	Core@shell	Chemo	[150,157,158,405]
Dendrites	Core@shell	Chemo	[199]
Icosahedra	Core@shell	Chemo	[159]
Rods	Supported	Chemo	[213,424–426]
Polyhedral	Supported	Chemo	[170,426–428]
Dendrimers	Supported	Chemo	[177,429]
Tubes	Supported	Chemo	[430,431]
Rods, dumbbells, rattles	Colloidal	Photo	[168,180,190,198,234,407,432]
Polyhedra (prims, pyramids, cubes, cages, discs, triangles)	Colloidal	Photo	[167,237,432–435]
Dendrites	Colloidal	Photo	[236]
Rods, dumbbells, bipyramids	Core@shell	Photo	[152–155,160,161,175,211,219,221,235,436,437]
Cages, cubes	Core@shell	Photo	[156,200,235]
Stars	Core@shell	Photo	[175,220]
Rods, bipyramids	Supported	Photo	[169,171–176,178,223,438]
Cubes, pyramids, prims, hexagons/triangles	Supported	Photo	[176,178,223,439]
Stars	Supported	Photo	[174,175,178]
Rods	Colloidal	Electro	[201,202]
Tubes	Colloidal	Electro	[440]
Triangular prism network	Colloidal	Electro	[206]
Neuron-like nanostructures, nanoporous network	Colloidal	Electro	[441,442]
Rods	Supported	Electro	[161,171,178–181,443]
Prisms, cubes, polyhedral, plates	Supported	Electro	[178,183,203,207,444,445]
Stars, dendrites, flowers, multipods, urchins,	Supported	Electro	[178,182–185,204,205,214–218,446–459]
Porous networks, belts, combs, wires/chains	Supported	Electro	[208–210,444,460–464]

separation, recyclability and stability. This is however circumstantial and advances in nanotechnology and synthetic methods offer great promise in the application of anisotropic NPs in catalysis. Therefore, multiple authors attempted to coat AuNPs by a layer of metal oxide such as TiO_2 [150–156], SiO_2 [157–159], CeO_2 [160,161], all of which are typically used as porous supports in catalysis [162–166]. However, possibilities are limitless and other oxides such as Cu_2O [167] or Fe_xO_y [168] were applied to perform as a shell. All these particles are termed core@shell in this part of the review. The shell generally changes the activity of the produced material but mostly also serves to protect from the agglomeration of the individual NPs. The last type is supported catalyst, which has metal NPs immobilized on the surface of the support. The function is the same as in the case of core@shell type although particle size of the support is typically bigger than the resulting core@shell particles. Depending on the application, metal oxides [169–175], carbon [176,177]or electrodes [178–185] can be used to hold and disperse AuNPs. Table 3 presents some publications studying the catalytic activity of different shapes and forms of monometallic Au and multi-metallic alloys and core@shell structures including AuNPs. These systems are classified following their type of catalysis (chemo-, photo- or electro-) and their form (colloidal, core@shell or supported).

A wide variety of reactions have been studied with anisotropic AuNPs, including simple gas phase reactions [186,187], reduction of nitrophenol or other nitro compound [140,145,147,148,158,188–197] by sodium or potassium borohydride, degradation [154,167,198–200] or oxidation [181,185,201–209]of small organic molecules or hydrogen evolution [152,172,210,211]. The reaction choice appears to be related to the ease of carrying out some of the catalytic tests (e.g. gas phase reaction, reduction of nitrophenol for room temperature reaction and analysis by UV-vis spectrometer, degradation of dyes for ease of analysis) and the fact that they can be good examples or model reactions for some of the industrial transformations, such as selective or total oxidation or wastewater treatment.

Regarding catalytic activity and NP morphology, the number and the type of the exposed planes are well-known to be highly relevant for chemo (thermo)-catalytic activity [139]. Several authors were able to confirm that high energy planes such as (110) or (100) give rise to the higher activity that some of the anisotropic AuNPs display as they contain these planes in a higher proportion as compared spherical AuNPs that display a higher ratio of low energy (111) planes [141,146,147,212]. However, this seems to be a subject of great controversy and the opposite has also been argued for some morphologies/reactions where (111) planes gave higher activity [159], also supported by DFT calculations [213]. This suggests that further specific investigations combined with theoretical calculations are required to shed more light on the source of activity difference between different anisotropic NPs when compared to spherical NPs. Most certainly, other variables such as the use of different preparation methods, ligands, and residues from synthetic precursors play a role which is difficult to evaluate considering the limited amount of research carried out to date in Au catalysis with anisotropic NPs. Similarly to chemocatalysis, electrocatalytically driven reactions over anisotropic shapes such as nanoflowers [182,183] were shown to offer higher oxidation/reduction activity owing to the high-index planes. Other authors seemed to take advantage of dendritic shapes offering both higher surface area, more high-energy planes and a strong increase of the electric field in comparison with the surface of the normal Au electrode [214–218], somehow complicating attribution of the activity increase to the specific property of the anisotropic structures.

Nevertheless, it is arguable that the most relevant application of anisotropic AuNPs in catalysis might be in photocatalysts. This is due to the extraordinary plasmonic properties that AuNPs have, which offers the opportunity of using natural light as the only source of energy during the photocatalytic transformations. Careful control of particle morphology and surface during synthesis appears a suitable tool for tuning the plasmon band and thus giving rise to the tuneable differences in photocatalytic activity. In addition to the activation of the plasmonic feature of the Au or bimetallic NPs alone, these are typically combined with photo-active support such as TiO_2 [94,154,172–175,219–221]. Nevertheless, other suitable supports such

as CeO_2 [161], reduced GO [176,222], MoS_2 [223] and even other carbon-based materials [224–231] were explored as carriers/catalysts for photocatalytic reactions. The advantage of this type of catalysis employing anisotropic Au is that by fine-tuning morphology and dimension of the nanocrystals the plasmonic response can be directly tailored from UV to NIR region as it is required by the reaction system [176,211,232–234]. Au nanocrystals can be further functionalized by the addition of second metal which can broaden the light-induced range and enhance the catalytic response [220,234–237].

Inspection of the recent literature shows that catalysis by anisotropic AuNPs is booming. In our review in 2016 [139] we found 90 papers studying anisotropic Au from the time between 2008 and 2016. Since then, more than 60 publications have appeared that contribute to the understanding of the relationship between properties of different shapes of Au nanocrystals and their chemo-, electro- and photocatalytic activities. Anisotropic NPs are expected to further contribute to catalysis as synthetic procedures for different shapes are developed and improved and so to offer higher tuneability, electronic and optical properties. Although light-driven reactions could be correlated to their plasmon-based properties, other variables such as support interactions come into play in photocatalysis, which further complicates the available studies and selectivity in these cases is not ideal and needs to be studied and improved [238]. For chemo- and electrocatalysis, more studies are necessary which will not only improve the activity or compare it to the standard catalyst or spherical AuNPs, but also analyse the reason behind observed enhancements in activity.

5. Medical applications

The successful implementation of AuNPs in medicine is based on cost-effective and simple methods of generating NPs having high colloidal stability, favorable morphology, suitable size, and surface modifications. Biological systems are composed of cells with a diameter of around 10 μm. However, the cell organelles demonstrate a nanosized diameter. This simple size comparison yields an idea of using NPs as very small probes that would lead to investigate interactions at the cellular level without introducing too much interference. Clearly, a profound exploring the medical systems at the nanoscale level is a benefit behind the design and development of nanotechnology based on Au particles. Physical properties of nanomaterials such as optical and magnetic effects are the most used features for their medical applications. Another fundamental aspect of AuNPs in their application in medicine is their inherent low toxicity towards biological systems [239,240]. Therefore, their applications in medicine have received potential interests in recent years. Hence, we outlined the distinctive characteristics of AuNPs involved in medicinal implementations with a focus on cancer imaging, diagnostics and therapeutics. For that reason, the properties of AuNPs, their applicability to diagnostics and therapeutics of cancers are addressed in the next chapters.

5.1. Imaging and diagnosis

AuNPs have shown several unique characteristics that inspire them ideal candidates for medicinal implementations. AuNPs are considered to show low adverse effect against biological systems. The surface of AuNPs can be modified for selective applications including targeted drug delivery. AuNPs can adopt larger form upon interaction with polymeric NPs or micelles that carry specific drugs for increased diagnostic improvement and imaging probes. This array of properties can be detected by CT-scan, MRI, PET, SPECT, US, and OI (Fig. 2) [3,241]. This section reviews recent papers on AuNPs utilization for imaging and diagnostics.

5.1.1. CT-scan

CT is known as a distinguished diagnostic tool for biomedical imaging. CT uses X-rays photons and a computer to drive comprehensive images of the inside human body.

5.1.1.1. Targeted molecular imaging. CT shows several disadvantageous, such as lack of selective imaging and limited imaging time. For this reasons, the application of multifunctional NPs for selective CT imaging of prostate cancer cells was done by modified AuNPs [242]. In one study, AuNPs were modified with a prostate-specific membrane antigen (PSMA) RNA aptamer that specifically attach to prostate cancer cells [243]. The designed PSMA aptamer-conjugated AuNPs exhibited greater CT signal for a selective tumor due to its targeted binding and contrasting properties. Also, Li et al. [244] synthesized fluorescent modified with diatrizoic acid and nucleolin-targeted AS1411 aptamer (AS1411-DA-AuNPs). The (AS1411-DA-AuNPs) conjugates showed high hydrophilicity, excellent biocompatibility in animals, strong fluorescence, and X-ray attenuation signals. AS1411-DA-AuNP was employed as a decent contrast conjugate to determine the accurate tumor border in CL1–5 tumor-bearing mice (Fig. 3A). Likewise, the fluorescence intensity emitting from the AS1411-DA-AuNPs in the CL1–5 cancer cells can be detected readily by the naked eyes (Fig. 3B). Also, Khademi et al. [245], by designing a AuNPs-based imaging molecule containing cysteamine-folic acid to targeting, were able to obtain a higher contrast compared to the conventional iodine method. Based on the same method and by loading the epidermal growth factor receptor (EGFR) on the Au nanoplates, Zhao et al. [246] not only provided more appropriate CT scan of lung cancer compared to previous methods, but also provided the appropriate timing for PTT using AuNPs. In this regard, Popovtzer et al. [247] and Khademi et al. [245] optimized standard clinical CT and described a targeted molecular imaging platform that enabled cancer determination. This method used Au nanoprobes accumulated in the vicinity of the target tumor and causing well-defined contrast in CT imaging by enhanced X-ray attenuation [245]. Previously, Popovtzer et al. [247] showed that targeted cells in head and neck cancer cells provide an attenuation coefficient five times higher than that of control cancer cells or normal cells. They concluded that this unique imaging approach may result in remarkable advancement in tumor therapy due to the faster and more accurate detection of tumors.

5.1.1.2. Quantitative imaging. Quantitative imaging biomarkers are defined as a target typically derived from an *in vivo* image calculated on a ratio or interval scale as an index of normal biological systems, pathogenic activities or a response to a therapeutic intervention. Manohar et al. reported the quantitative imaging of AuNPs accumulation in tumor-bearing mice by benchtop XFCT (Fig. 3C). As illustrated in Fig. 3C, photon irradiation of AuNPs leads to the induction of secondary electrons, scattering, and XRF photons. Therefore, when a mouse injected with AuNPs irradiated by an x-ray beam, Au XRF photons can be revealed by XFCT imaging [248].

The *in vivo* CT scan before injection of AuNPs revealed that the kidney and tumor cells could not be detected by contrast (Fig. 3D). The post-injection *in vivo* CT scan demonstrated remarkable contrast increment in the kidneys due to AuNPs accumulation. However, no contrast enhancement was observed elsewhere, including the tumor cells. The postmortem CT scan revealed an even higher contrast in the kidneys, however no contrast magnification in the tumor cells. These results indicate the limited capability of conventional x-ray CT to induce potential contrast and sensitivity. After processing and reconstruction of the images, each raw XFCT image, shown in Fig. 3D. The images demonstrated that the current XFCT system distinctly yields the system to detect and visualize AuNPs in the kidneys and in the tumor region [248].

5.1.2. MRI

MRI with contrast materials has several advantages for imaging of tissues with spesified disorderes. Indeed, due to the inherent low discrimination of the contrast material in the tissues which reduces

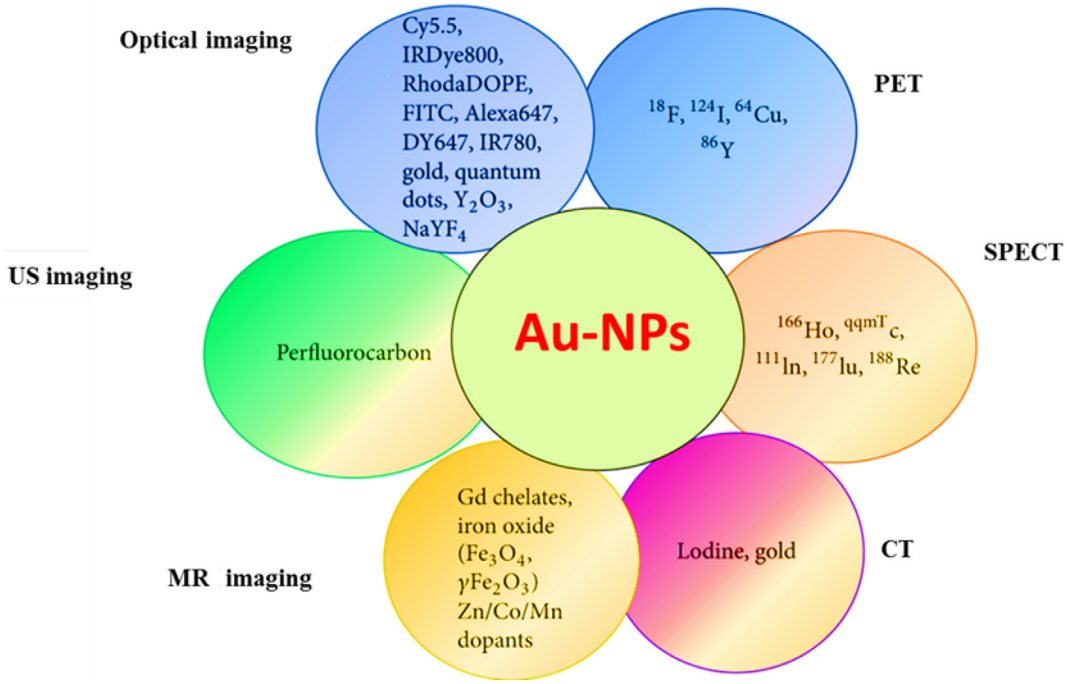

Fig. 2. Incorporation of multicomponent imaging agents with AuNPs for multimodal imaging. Reproduced under the terms of the Creative Commons Attribution License (CC BY) from Ref. [241].

potential tissue recognition, the low stability of the contrast material in the tissue and the lack of complete intelligibility of the contrast material as well as the lack of synchronization of therapeutic activity, the apl-lication of NPs, especially AuNPs with high biocompatibility has attracted a wide range of interest instead of using contrast agents [249].

5.1.2.1. T1 MRI contrast. Holbrook et al. [250] developed a system to increase T_1 MRI contrast with internalized Gd(III) incorporating into a metal-based NP having a Au and SiO_2 NP layers. They showed that the designed Gd(III)-encapsulating Au, SiO_2 NPs demonstrate excellent MRI T_1 enhancement [250]. Besides, Rammohan et al. [251] developed a system for imaging of the pancreas by fabricating Gd(III)-Au nanoconjugate for T_1-weighted MRI. They synthesized new dithiolane-Gd(III)-AuNP complex and showed that the nanoconjugates provide high signal outputs. They provided MRI of pancreatic tissue (Fig. 4A), post-mortem bioaccumulation investigation, and pancreatic tissue examination of NP distribution. Outstanding contrast signal was detected leading to the sharp observation of the pancreas. Rammohan et al. developed Gd (III)-Au nanoconjugates to exhibit remarkable labeling and imaging breast cancer cells for high field MRI [252]. Recently, for dual activities, Henderson et al. [253] with the design of the Au@SiO_2@Au multilayer core-shell nanostructure known as a nanomatryoshka, in addition to increasing the contrast of T1 MRI imaging, caused promising responses to NIR PTT.

5.1.3. US imaging

US or PA imaging is considered as a unique imaging method using laser-produced US. Among imaging techniques, US imaging has shown certain advantages because of its real-time, low cost, high safety, and ease of integration with other portable techniques. The clarity and sensitivity of clinical US imaging greatly improves by using AuNPs as US contrast agents [40].

5.1.3.1. Bimodal ultrasound/MRI guided photothermal tumor ablation. In this field, Ke et al. [252] developed Au nanocapsules for dual modal US/MRI targeted photothermal cancer cells ablation. They prepared nanocapsules by incorporating perfluorooctyl bromide (PFOB) and iron NPs into polymer nanocapsules modified by, PEGylated Au nanoshell (Fig. 4B). The synthesized modified nanocapsules were identified to show a nanotheranostic ability to confer significant bimodal US/ MRI guided photothermal ablation of cancerous cells. Such a designed system including a single theranostic agent, bimodal US and MR imaging can act as a potential candidate to confer more profound diagnostic data and dynamics of disease spread for the precise ablation of tumor tissue and demonstrating pronounced contrast imaging-guided PTT [252]. Moreover, Jin et al. [254] used graphene oxide (GO)-polymer-Au nanoconjugates for US/CT dual modal imaging-guided PTT therapy. Additionally, Moon et al. enhanced PA efficiency and photothermal stability of GO-Au nanoconjugates for improved PA imaging [255]. Also, Xu et al. [256] synthesized and evaluated the targeted delivery of Au nanoshelled polymeric NPs having anti p53 antibody to breast cancer MCF-7 as a theranostic platform for US contrast imaging and PTT therapy. Also, for multiple activities such as imaging, PTT, and drug delivery in MCF-7 cancerous cells, Zhao et al. [257] using liposomes coated with Au nanoshells and connected to sulfydryl modified with AS1411 and S2.2 aptamers, not only enhanced the activity of docetaxel delivery and PTT under 808 nm laser irradiation in cancerous cells, but also provided a promising approach for US imaging simultaneously through bubble generation.

5.1.4. PET

PET is defined as a nuclear imaging approach with a great potential for the clear determination of metabolic activity in the body.

5.1.4.1. Dynamic distribution patterns. Goel et al. [258] studied the dynamic distribution patterns of AuNPs by labelling them with copper-64. They concluded that the dynamic PET imaging of AuNPs-Cu conjugate not only overcomes the current limitation in precisely and non-invasively obtaining the organ kinetics, but also significantly extends to have high potential as a tool for investigating renal clearance mechanism, as well as the diagnosis of kidney disorders.

5.1.4.2. Dual modality imaging. Tsoukalas et al. [259] designed a system to assess AuNP *in vitro* and *in vivo* dual modality imaging with

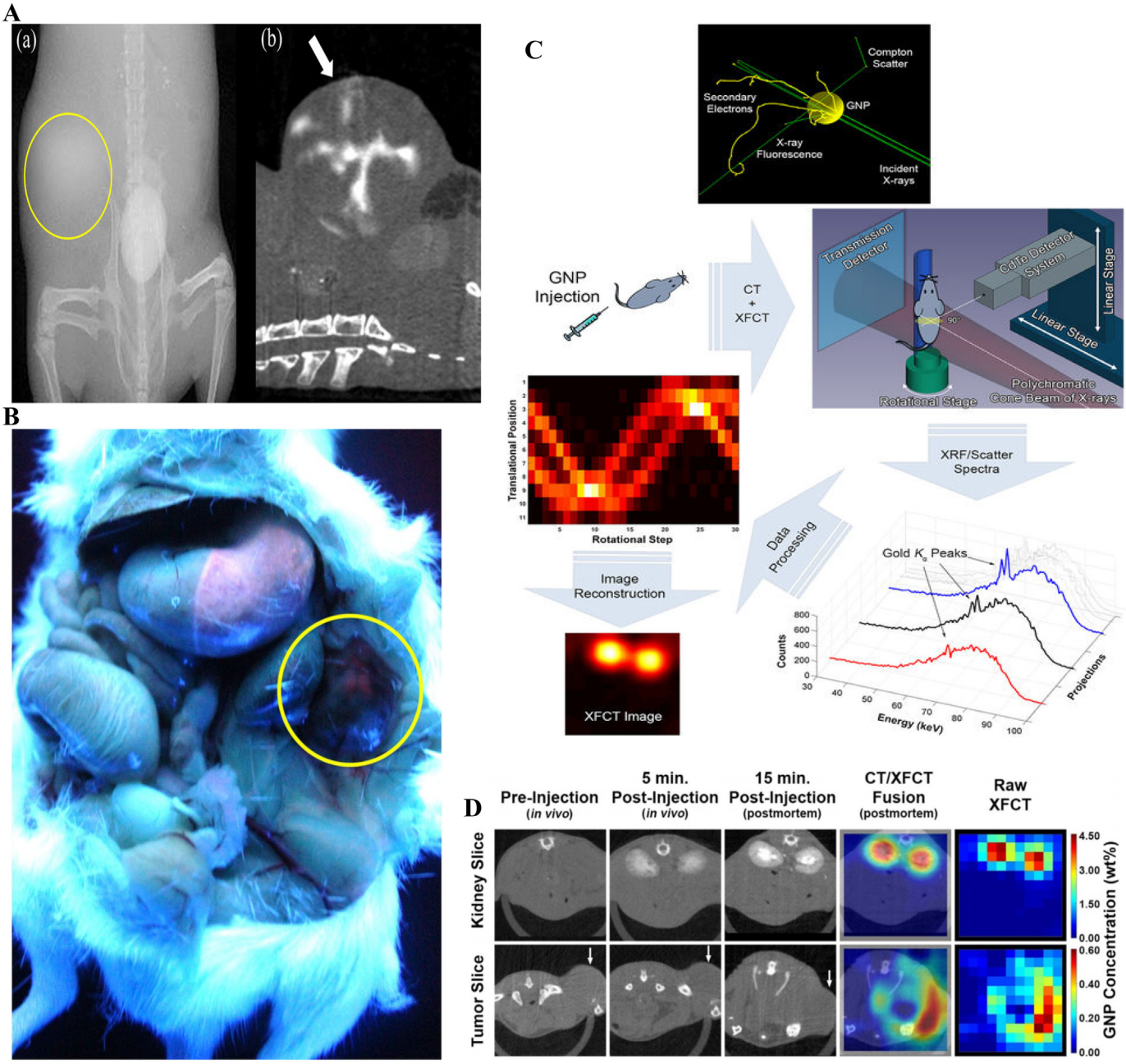

Fig. 3. CT-scan. (A): (a) CT image of the CL1-5 tumor-bearing mouse after injection of AuNPs conjugates. Yellow circle demonstrates the location of CL1-5tumor. (b) axial CT image of CL1-5 tumor. The white arrow shows the border of CL1-5 tumor [244]. (B): The yellow circle determines the border of the CL1-5 tumor [244]. (C): Mouse was irradiated by X-rays and detector collected the XRF/scatter spectrum. The acquired images were processed to recreate axial XFCT images [248]. (D): Reconstructed axial CT images at various time-scales and XFCT images of the kidneys and tumor (white arrow) [248]. Reproduced under the terms of the Creative Commons Attribution License (CC BY).

radiolabeled Gd chelate coated AuNPs for Gd-based MRI and PET contrast agents. This basic data may hold great promise for the requirement of the further design of radiolabeled Gd chelate coated AuNPs, as possible bimodal PET/MRI imaging nanosystems. Recently, in order to detect prostate cancer with the development of AuNPs decorated with a NIR dye and NODAGA chelator for complexation with ^{64}Cu radiolable, Pretze et al. [260] in addition to improving the quality of dual optical and PET imaging, caused chemical stability of NPs up to 95% for long-term imaging. Analogously, Lee et al. [261] with the development of PEGylated crushed Au shell@radioiodine-labeled core NPs for dual imaging PET and luminescence, were able to imaging the lymph nodes in mice model with the highest contrast without causing toxicity and reduced immune system along with mapping for surgical guidance.

5.1.4.3. Whole-body non-invasive imaging. Wall et al. designed a nanosystem that can be applied to image the whole-body in a non-invasive, high sensitivity and resolution manner. Indeed, SERRS holds great promise for the pre and intra-operative imaging [262]. They suggested that probing the ultrabright SERRS AuNPs with a potential Raman reporter dye would result in pre-operative detection of tumors by combined PET-SERRS tissue imaging (Fig. 5A).

5.1.5. SPECT

Distinct from PET that only is sensitive to 511 keV gamma ray pairs, SPECT is sensitive to a wide range of wavelengths, and hence can be

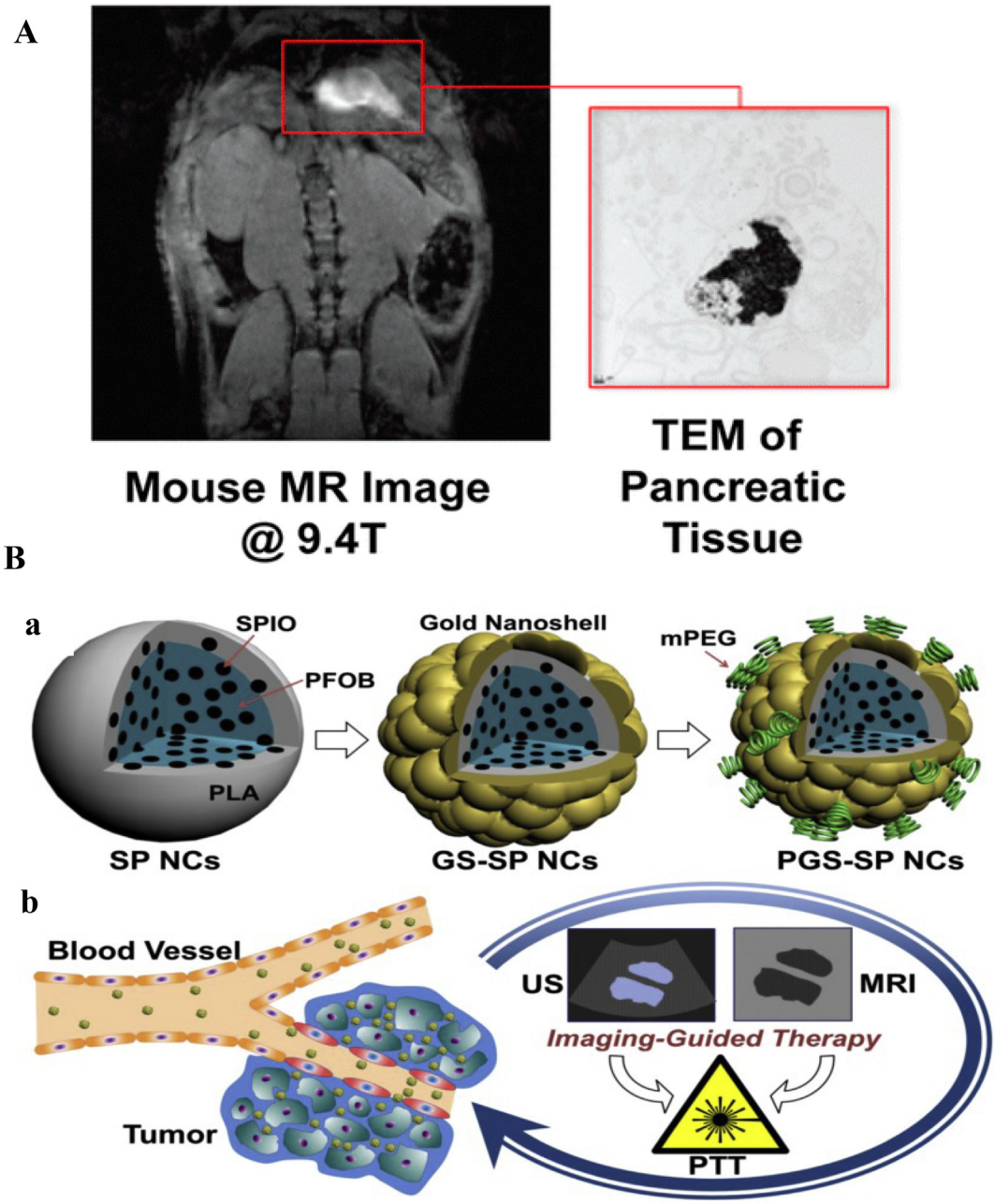

Fig. 4. MRI and US imaging. (A): Gd(III)-dithiolane Au nanohybrid as a contrast system for MRI of the pancreas [251]. (B): (a) Schematic presentation of the preparation route of nanocapsules; (b) The dual modal US/MRI guided tumor PTT procedure utilizing the nanotheranostic materials [252]. Reproduced under the terms of the Creative Commons Attribution License (CC BY).

used in multipurpose diagnosis with various radionuclides. When correctly joined with NP labels, this independent tracking system can assist to identify potential *in vivo* details such as radiolabeling efficiency and biological features such as enzyme assay.

5.1.5.1. Dual-modal imaging. Black et al. used dual-radiolabeled AuNPs with two distinct radionuclides grafted within specific peptides, which were then employed as an *in vivo* multispectral SPECT imaging contrast agent [263] (Fig. 5B). Li et al. tried to realize the precise accumulation and vulnerability evaluation of atherosclerotic plaques based on bimodal imaging [264]. AuNP were fully functionalized and conjugated to prepare targeted SPECT/CT imaging agent. They suggested that targeting molecules result in more potent accumulation of imaging agent in apoptotic macrophages. Indeed, CT leads to control the lesions boarder more precisely, meantime, SPECT imaging signal is in good agreement with pathological changes. Likewise, Zhou et al. [265] using a 99mTc-labeled arginine-glycine-aspartic acid–polyethylenimine conjugates with AuNPs platform in an orthotopic hepatic carcinoma model, were able to study SPECT/CT images of cavities and accumulation of NPs. Recently, in order to imaging malignant glioma with indistinct margins in surgery, Zhao et al. [266] provided a appropriate and targeted SPECT/CT image using 131I-labeled CTX-functionalized Au polyethylenimine nanoprobe in a subcutaneous tumor model.

5.1.5.2. Targeted cancer imaging. In this regard, Zhao et al. [267] used ^{199}Au atoms-doped AuNPs for selective imaging of tumor tissue in breast cancer model mice by SPECT. They found that when AuNPs are conjugated with specific peptide, they can act as a potential sensitive nanosystem for the targeted and selectively determination of both

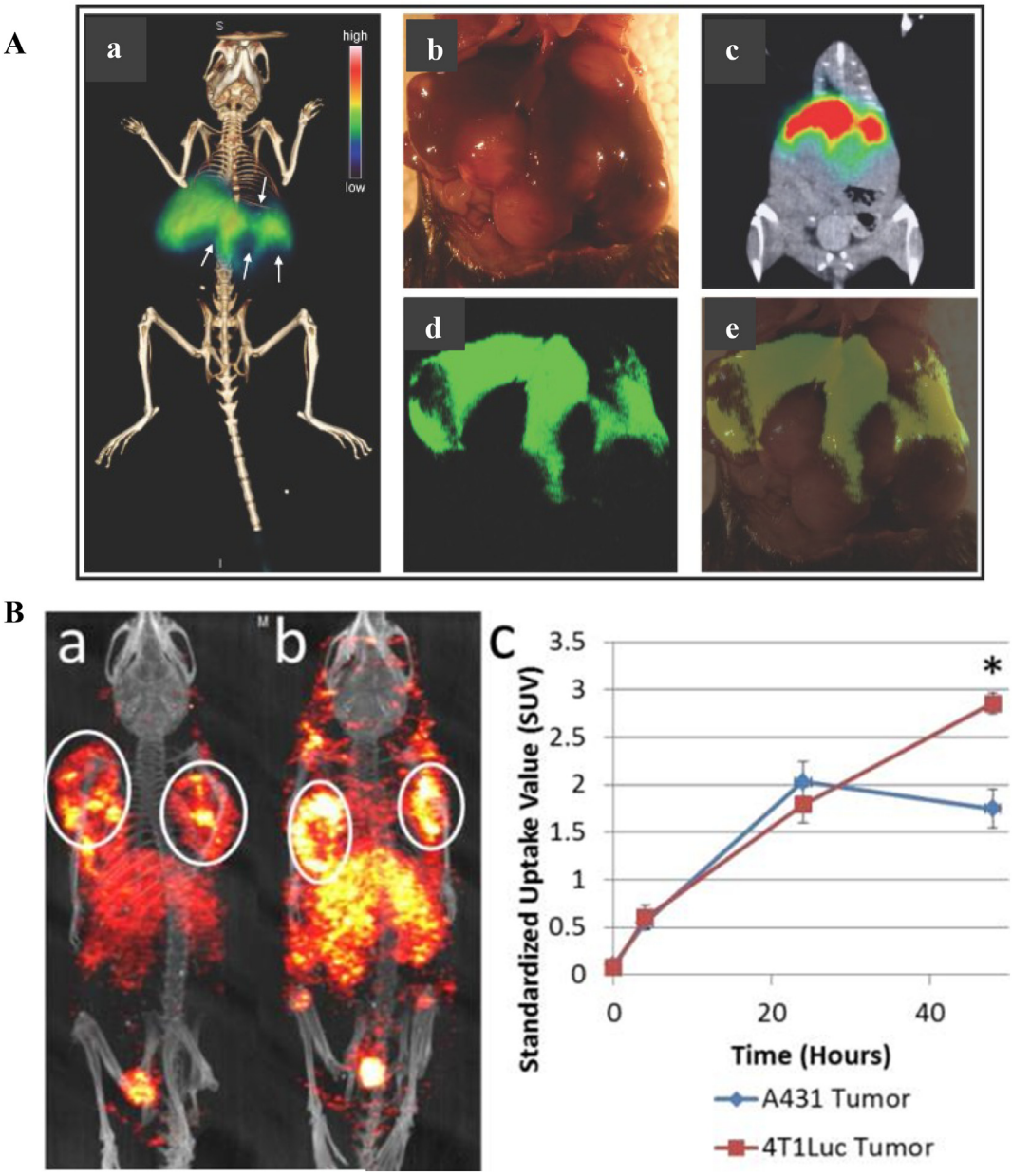

Fig. 5. PET and doul-modal imaging. (A): Imaging of liver tumor with PET-SERRS labeled AuNPs. (a) Arrows show the filling defects in the liver by PET-CT image. (b) White light image of the liver with visible tumors (c) PET imaging, exhibiting normal liver with high signal and tumors with low signals (d) SERRS imaging shows the position and average size of the tumors. (e) Overlay of photograph b and d [262]. (B): Tumor diagnosis with dual-radiolabeled AuNPs. SPECT/CT images of bilateral (a) A431 and (b) 4T1Luc tumors (circled)-bearing mice 48 h post injection. (c) Tumor standardized uptake values (SUVs) of ^{111}In over the time course of 48 h post injection [263]. Reproduced under the terms of the Creative Commons Attribution License (CC BY).

tumor and its metastasis in breast cancer model mice.

5.1.6. Optical imaging and scattering

Strong electric fields at the surface of AuNPs can hold a distinctive potential of developing unique optically active systems for imaging of tumor tissues.

5.1.6.1. Malignant cells and the nonmalignant cells. AuNRs with tunable aspect ratios can vibrate and scatter dramatically in the IR region and act as a distinctive contrast nanosystem for both molecular diagnosis and PTT [268]. AuNRs-monoclonal antibodies nanoconjugates were incubated with benign and malignant cell lines. The antibody-conjugated AuNRs accumulated selectively in the vicinity of malignant-type cells and dramatically scattered IR from AuNRs to distinguish malignant cells from the benign cells [268]. Using a simple and inexpensive method, El-Sayed et al. recorded scattering images and SPR bands from both AuNP and Au-antibody nanoconjugate after incubation with nonmalignant and malignant epithelial cell lines [269]. The antibody conjugated AuNPs selectively accumulated at the surface of cancerous cells. This specific binding was detected by different SPR absorptions and a red-shifted maximum. These data demonstrated that SPR scattering imaging generated from antibody conjugated AuNPs can hold great promise in molecular diagnosis for the detection and exploring of oral tumor cells [269].

5.1.6.2. Cancer biomarkers. Mani et al. [270] suggested a densely packed AuNP-antibody bioconjugate employed as the platform for a sensitive electrochemical immunosensor to detect prostate cancer biomarkers in human serum. Human oral cancer cells showed to aggregate antibody-conhugated AuNRs. Immunoconjugated AuNRs

and nanospheres can show a great Rayleigh scattering potential for imaging. Moreover, Huang et al. [271] showed that molecules near the AuNRs led to a Raman spectrum that is substantially increased with sharp and polarized signals. These properties can be referred to as diagnostic approach for detection of cancer cells [271]. Ambrosi et al. [272] developed an ELISA immunoassay for the detection of tumor-associated antigens CA15–3. AuNPs were employed as a platform to strengthen the amplification of the signal and resultant sensitivity. In a cellular model, Zhao et al. [246] with the modification of the surface of the AuNPs by EGFR peptide due to their 5-fold presence in cancerous cells, were able to result in CT and PA imaging from lung cancerous cells. Therefore, it may be concluded that application of AuNPs to the commercially available test can be useful to improve potential immunoanalysis methods where more certain data are needed. Besides, Suo et al. [273] using the biomarker of anti-HER2 in AuNPs along with 5-aminolevulinic acid and Cy7.5, in addition to increasing the targeting of AuNPs in the tracing of breast cancer cells, allowed multiple activities, including increased cellular uptake, imaging, and PTT/PDT.

5.2. Therapy

PDT is defined as a potential tumor-ablative medical intervention in which a photosensitizer agent is excited with potential high energy electromagnetic waves. This excitation releases vibrational energy (heat) in tumor environment to induce the formation of cytotoxic singlet oxygen, which results in the killing of tumorous cells. This approach is comparable with PTT that converts the electromagnetic radiations such as NIR, visible light, radiofrequency waves, microwaves, and US waves into heat through a photosensitizer conjugated with a NP to destroy the cancer cells. These electromagnetic waves are less energetic relative to other ultraviolet and X-ray electromagnetic waves and therefore are not toxic to healthy cells. When AuNPs is excited by NIR light, the vibration of electrons causes the production of heat [274].

5.2.1. Physicochemical characteristic of AuNPs

Any alteration in the size and shape of AuNPs results in changes in their absorption spectrum [274]. The selected wavelength range is 700–1000 nm, due to the inability of biological tissues to absorb light at these wavelengths [275]. The SPR intensity is correlated with the physicochemical characteristics of the AuNPs such as morphology and dimension [274,275]. Electron-electron collisions after excitation by NIR like pulsed laser lead to the release of energy as phonons which elevate the environmental temperature of the AuNPs [274–286].

5.2.2. Gold colloids

Au colloids (nanospheres) can be fabricated by and biologically-inspired routes [20]. The dimension of the Au colloids can be controlled by the concentration of Au salt, the temperature of medium and incubation time. Generally, a greater amount of Au salt can form larger Au colloids. More recently, the unique optoelectronic properties of Au colloid have attracted great interest in medicinal applications [287–291]. The potential heat production and simple bioconjugation of AuNPs have received great interests in their application as unique photothermal NPs in therapy.

5.2.2.1. Photothermal therapy. El-Sayed et al. [292] demostrated the use of AuNPs in the targeted PTT of epithelial carcinoma with bioconjugated AuNPs. In their study, two oral malignant cell lines and one benign epithelial cell line were treated with bioconjugated AuNPs, followed by irradiation (514 nm). It was revealed that by subsequent incubation of both malignant and benign cells with bioconjugated AuNPs, the malignant cells were more sensitive to be destroyed by the laser than the benign cells [292]. Therefore, it may be suggested that PTT therapy with the application of AuNPs required low laser power owing to the SPR features of AuNPs [293]. Furthermore, Nam et al. [294] designed a smart AuNP that tends to be agglomerated in acidic intracellular microenvironments by functionalized active surface. AuNPs with different surface moieties can demonstrate different charges. The pH-triggered induction of AuNPs agglomerates shifts the resonance to the longer wavelength of NIR. Indeed, aggregation and reduced exocytosis of AuNPs followed by their surface modification can be considered as an important route to affect the cancerous cells. AuNPs showed well-organized ablation of tumor cells through thermal destruction [294]. Also, Cheng et al. [295] by providing photocross-linkable AuNPs and changing the surface decoration with photolabile diazirin, were able to change the SPR of the AuNPs to NIR regions for increasing the phototherapy performance *in vitro* and *in vivo*. This method increased the PTT activity and PA imaging of tumors *in vivo*. At the same time, Panikkanvalappil et al. [279] in the human oral squamous cell carcinoma-3 and human keratinocyte models, showed that by inducing the accumulation of spherical AuNPs to cluster forms in the nucleus of cells by using PEG, they can enhance the activity of PTT by transferring to NIR region. Recently, in a computational model and then in the model of breast cancer mice, Hu et al. [296] described that the major defect in light scattering in the NIR region is corrected in AuNPs through the growth of multibranched AuNPs with a core size of 25 nm and a tip number of 5 with height of 40 nm. In this method, Multibranched AuNPs have the highest light-to-heat conversion efficiency in the PTT process in the NIR zone.

5.2.2.2. TNF-α and cancer therapy. Tumor necrosis factor-α is a toxic agent that can remarkably increase hyperthermic damage. Consequently, Visaria et al. [297] used a nanosystem contained PEG-AuNPs-TNF-α to enhance tumor destruction and reduce systemic exposure to the side effect of TNF-α. SCK mammary carcinomas of A/J mice were injected with PEG-AuNPs-TNF-α at 42.5 °C (Fig. 6A). Tumor growth was decreased for both treated groups; however, the most considerable effect was reported in the combination system. Therefore, they concluded that thermally mediated tumor ablation was increased by pretreatment with decorated nanohybrid of TNF-α when administered by intravenous injection at the correct dosage and timing [297]. Similarly, Shao et al. [298] to intensify the cancer therapy activities in a mice cancerous model, with the development of AuNPs decorated with TNF-α, not only enhanced the cell death of cancerous cells by inducing TNF-α overexpression, but also through PTT and heat increase significantly reduced the activity of cancerous cells.

5.2.2.3. Photodynamic therapy. AuNPs can be implemented in PDT because singlet oxygen can be produced by Au nanocrystals under laser irradiation directly and be employed as productive PDT agents *in vivo*. Accordingly, Cheng et al. [287] reported a nanocarrier containing PEG and AuNPs for the targeted hydrophobic drug delivery in PDT. The dynamics of *in vitro* and *in vivo* drug release proved the efficacy of the designed nanoconjugate. With the aim of this nanoconjugate, the drug delivery time required for PDT was decreased dramatically. In this line, Pang et al. [299] with covalently attachments of photoprecursor Pc 227 to AuNPs, in addition to increasing the ability to transfer the drug to the target tissue, allowed the release of drug only in the target tissue through PDT at 608 nm.

5.2.2.4. RFA. RFA technique is known as a needle placement and is limited by the restricted precision of targeting. Therefore, Nikzad et al. [300] explored the impact of RFA with AuNPs, as a new route for renal cell carcinoma (RCC) therapy. Outcomes indicated that RFA with AuNPs can be potentially employed for RCC therapy as an alternative to nephrectomy. They concluded that more detailed *in vivo* investigations are required to reveal the efficiency of the reported route for medical implementations.

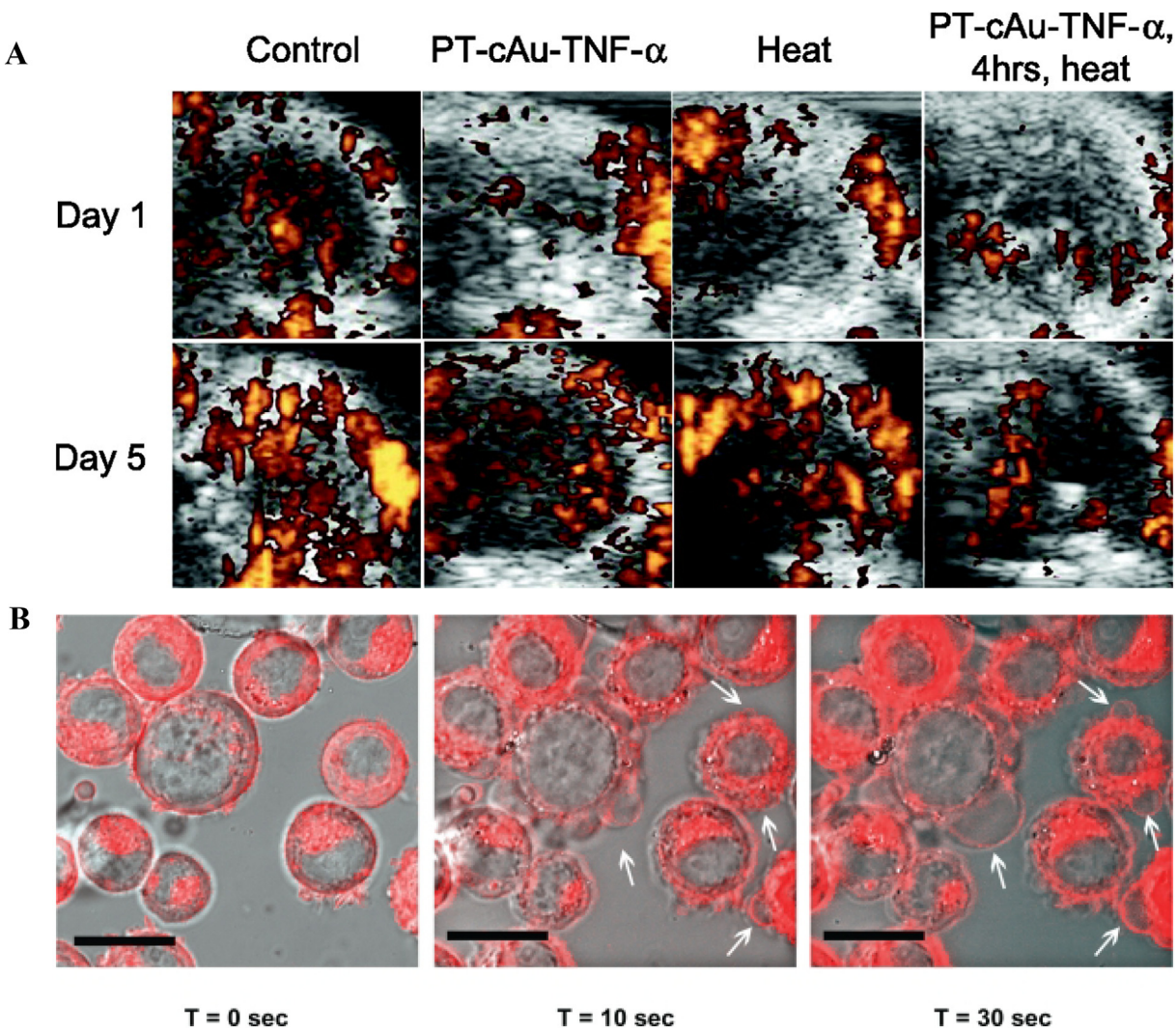

Fig. 6. Hyperthermia and PTT therapy by AuNPs. (A): SCK murine mammary carcinoma model: perfusion defects imaged employing contrast-enhanced ultrasonography after 1 day (*top*) and 5 days (*bottom*) [297]. (B): SK-BR-3 cells incubated with bioconjugated AuNPs and 50 mW laser power over time. White arrows pointed the membrane blebbing [301]. Reproduced under the terms of the Creative Commons Attribution License (CC BY).

5.2.2.5. Dual contrast and therapeutic materials. In this field, Day et al. [301] developed NIR resonant Au-Au sulfide NPs (AuAuS-NPs) as a dual nanoconjugate to simultaneously act as a contrast agent as well as a therapeutic nanodrug for cancer treatment. They showed that AuAuS-NPs in the presence of a pulsed NIR laser emit photoluminescence employed to visualize tumorous tissue *in vitro*. Upon conjugation with antibodies, AuAuS-NPs selectively accumulate in the vicinity of breast carcinoma cells. Afterward, cancer cells can be visualized and damaged (membrane leakage) by laser power of 1 mW and 50 mW, respectively (Fig. 6B).

5.2.3. Gold nanorods

AuNRs are nanometer-sized Au particles with a rod-shaped morphology. These cylindrical NPs show uniform diameters ranging from 1 to 100 nm, with aspect ratios between 1 and 10. Owing to their well-documented physical properties, AuNRs have many potential applications in different areas such as medical, biological, and biotechnological sciences [302]. In the field of nanomedicine, the typical sizes studied for AuNRs are the nanometer-sized diameter and micrometer-sized length [302].

5.2.3.1. Computational therapy design. The crystalline structures of AuNRs can be changed following the polycrystals or single crystals, depending on the synthesis methods and conditions. Hence, Von Maltzahn et al. [302] described an integrated route to improve plasmonic therapy comprised of NPs as well as radiation. They fabricated PEG-AuNRs to develop a high rate of heat generation, high circulation half-life, and higher X-ray oscillation. In computationally mediated pilot therapeutic investigations, they showed that a single injection of PEG-AuNRs resulted in ablation of all irradiated human xenograft cancer cells *in vivo* (Fig. 7A).

5.2.3.2. Simultaneously control heat and deliver anticancer drugs. Zhang et al. [303] produced polymer encapsulated AuNRs-DOX nanocomposite to combine the photothermal features of AuNRs with the thermal and pH-susceptible characteristics of polymers. The polymer-encapsulated AuNRs- DOX nanocomposite accumulation in the tumor can be remarkably increased by irradiation; inducing a condition for their medicinal demands which entirely blocked cancer cell division. In this system irradiation can be controlled accurately and with flexibility, the nanocomposite can be employed as a versatile agent to control heat and additionally carry anticancer agents [303]. In the following, Larson et al. [304] suggested synergistic intensification of tumor ablation by a combination of heat shock protein targeted copolymer–drug nanoconjugates and AuNRs-triggered PPT. Whereas, Frazier et al. [305] discussed on the impacts of temperature and time by

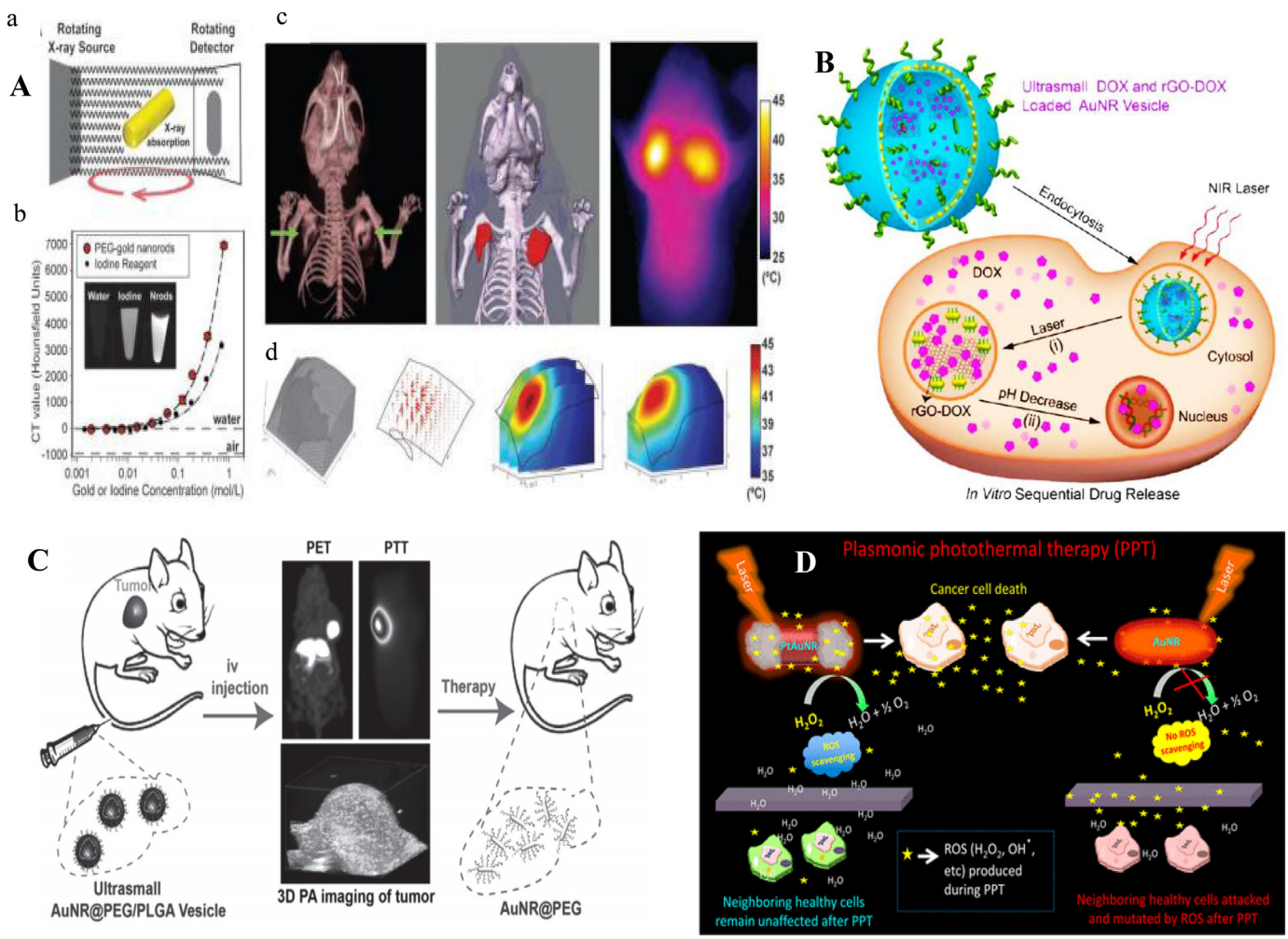

Fig. 7. Phototehramal therapy and imaging. (A): X-ray CT, quantitative PTT, and NIR photothermal activity of AuNRs. (a) illustration of X-ray attenuating; (b) X-ray CT number of PEG-AuNRs; (c) PEG-AuNRs were injected into mice and imaged (left). Image processing for utilization with computational photothermal modeling (middle). Red, PEG-AuNRs. Thermographic observation of NIR irradiation; (d) geometry of the left tumor (left). Schematic illustration of theoretical heat flux variation inside the tumor (middle left). The temperature of the tumor (middle right) along with surface temperature map (right) [302]. (B): Schematic presentation of DOX release mediated by (i) NIR laser and (ii) acidic environment inside the cancer cell [309]. (C): PET and PA imaging mediated PTT of tumor tissue were applied after intravenous injection of the synthesized agents [314]. (D): Higher photothermal potential and antioxidant activity of PtAuNRs compared to bare AuNRs [316]. Reproduced under the terms of the Creative Commons Attribution License (CC BY).

AuNRs-induced PTT on copolymer targeting in tumor cells. Likewise, Ali et al. [284] showed that targeting heat shock protein 70 by AuNRs increases cancer cell mortality in PTT. Also, Parida [306] demonstrated that AuNRs embedded micelle-mediated drug delivery combined with PTT can act as a potential system for targeted cancer therapy. Recently, in a cancerous cells model, Sharifi et al. [307] with the development of the acid-sensitive AuNRs platform containing DOX drug, were able to improve the activity of phototherapy chemotherapy in addition to increasing the targeting of breast cancer treatment activities based on drug release in the acidic condition. Analogously, Wu et al. [308] using AuNRs coverd with hexadecyltrimethylammonium bromide, polyacrylic acid, and PEGylated anisamide containing Epirubicin, performed successful chemophototherapy in human prostate cancer PC-3 cells.

5.2.3.3. Photothermal, chemical therapy and photoacoustic effect. In this regard, Song et al. [309] indicated continuous drug release and an increased PTT and PA consequence of GO-loaded AuNRs-DOX nanoconjugate for tumor ablation. The loaded DOX showed a potent tumor accumulation and sequential release after NIR irradiation and intracellular acidic environment. Intravenous injection of nanohybrid in the presence of laser irradiation (0.25 W/cm^2) showed the tumor ablation due to the synergy between chemotherapy and PTT (Fig. 7B). Paclitaxel is also known as a chemotherapy drug implemented to treat several kinds of cancers. However, due to its poorly-water soluble properties, it can induce some adverse effects. AuNR-albumin NPs were loaded with paclitaxel and employed as a potent candidate for synergic chemotherapeutic and PTT on 4 T1 breast cancer cells [310]. More recently, Manivasagan et al. [311] with the development of the AuNRs platform containing the DOX drug and folic acids (FA), and the photothermal agent (FA–COS–TGA–AuNRs–DOX), provided multiple activities of chemotherapy, PTT, and the PA imaging with high targeting and photostabiliy, fast drug release by NIR, high performance in the conversion of light to heat, and high efficiency in killing cancerous cells.

5.2.3.4. Dual-modality PDT and PTT of tumors. Bimodal application of PDT and PTT treatment of cancer cells appears as a promising method for cancer treatment in clinical applications. AuNRs with a hematoporphyrin-loaded SiO_2 layer were applied for *in vivo* bimodality PDT and PTT of cancer cells [312]. Bioinspired- AuNRs were also applied for *in vivo* PTT/ PDT [313]. AuNRs carriers with increased ability to accumulate in the vicinity of tumor cells and fast clearance from the body were studied for tumor ablation [314]

(Fig. 7C). AuNR-photosensitizer conjugates with extracellular pH-mediated cancer cell targeting were showed to be an excellent candidate in PTT/PDT [315]. A functionalized AuNR-photosensitizer hybrid with a pH (low) insertion peptide (pHLIP) and a disulfide bond which induces extracellular pH (pHe)-mediated cancer cell targeting characteristic, was affluently designed for simultaneous PDT and PTT therapy. Therefore, chlorin e6 (Ce6), as a photosensitizer, was employed for PDT. AuNRs were implemented as hyperthermia material and additionally as a nanocarrier and quencher. The results showed that Ce6-pHLIPss-AuNRs, when exposed to acidic pH, can induce bimodal PTT/PDT therapy [315].

5.2.3.5. Reactive oxygen scavengers. Very recently, Aioub et al. [316] demonstrated that titanium-coated AuNRs could be employed as an antioxidant to avoid oxidative stress to normal cells during PTT therapy. AuNR-mediated PPT has demonstrated intensive attraction for the selective destruction of tumor cells. Nevertheless, the hyperthermia induced by AuNRs during the PPT therapy produces an elevated level of reactive oxygen species (ROS) leading to adverse effects against normal and untreated tissues by causing irreversible damage to biomacromolecules, potentially inducing cellular toxicity or mutation. As well, Aioub et al. [316] fabricated Pt-coated AuNRs (PtAuNRs) with varying Pt layer diameters as a replacement for AuNRs frequently utilized for the tumor ablation. They showed that the PtAuNRs provide the potential results like classical AuNRs for cancer ablation while acting as an antioxidant generated during PPT therapy, by that preserving healthy tissues from ROS-induced stress (Fig. 7D). The bimodal behavior PtAuNRs in the ablation of tumor cells and antioxidant activity was further investigated *in vitro* by cellular approaches [316].

5.2.4. Gold nanocage

AuNC is defined as an advanced set of nanomaterials having hollow interiors and porous structure. These nanosystems are prepared using a simple reaction between solutions containing Au salt salts and Ag NPs in boiling water. AuNC as safe materials are considered as great candidates for imaging to monitor cancers at an early stage [317]. In this field, Xia et al. [318] by designing an enzyme-sensitive probe loaded on Au nanocage, were able to provide potential imaging activity from living cells with the lowest concentration level and enzyme activity. This multimode probe was able to treat cancer through PTT in addition to PA imaging and detecting cancer [318]. Likewise, Hajfathalian et al. [319] in a cellular model using Au Wulff-shaped seeds into Au–Ag core–shell nanostructures generated by the galvanic replacement reactions [320], showed that in addition to improving the imaging capability of living cells, the NPs had no negative effect on the viabilities of J774A.1, Renca, and HepG2 cells at any of the concentrations tested.

5.2.4.1. Photothermal transducers. In this field, Chen et al. [321] reported that AuNCs can act as potential candidates for tumor ablation. They employed PEGylated AuNC for PTT therapy *in vivo*. The compact AuNC showed strong electron vibration in the NIR region with a localized SPR peak. PEG modification induced the AuNC to selectively reach the outer surface of cancerous cells. The short-term outcome indicated that the AuNC is an ideal transducer for PTT therapy of cancerous cells.

5.2.4.2. Targeted drug release. The development of safe and selective drug delivery that can be activated against multiple stimuli is still so challenging for cancer treatment. Thus, Wang et al. [322] fabricated multi-purpose guided nanohybrids by (HA)-dopamine hydrochloride (DA)-DOX loaded AuNCs for targeted drug release inside the cell. Generally, fabricated nanohybrids could selectively bind tumor cells via HA and could release the loaded DOX in lysosomes (Fig. 8A). In addition, by considering the pronounced photothermal features, the AuNCs can control the release of loaded drug and cause a higher therapeutic index subsequent to NIR irradiation. *In vitro* studies have indicated that the loaded drug could only be selectively released inside the cells, which result in targeted cancer cell ablation and reduced adverse effects. Importantly, a complete ablation of tumor cell was seen by the combination of both chemotherapy and PTT, as opposed to the partial blockage of tumor growth when the two therapy methods are applied independently [322].

Srivatsan et al. [323] showed PEG-AuNC-photosensitizer nanohybrid can enable dual image/controlled delivery of photosensitizer [3-devinyl-3-(1′-hexyloxyethyl) pyropheophorbide (HPPH)] and remarkably enhance the potency of PDT in a murine model. The slow rate of the drug release led to the localization of the drug within the tumors and induced greater mortality than that of the free drug. Therefore, the hybrid revealed potential ablation of tumor cells, which is apparently comparable with what is observed when the free drug is used. Additionally, Chen et al. reported bioconjugated AuNCs with tailored optical features can be applied for selective PTT ablation of breast cancer cells [324]. While, Gao et al. [325] suggested that hypocrellin-loaded AuNCs with high two-photon efficiency can be applied for *in vitro* bimodal PTT/PDT therapy. Another investigation indicated the safety of therapeutic dose of the AuNCs nanohybrids.

5.2.4.3. Light-induced generation of free radicals. Tumor hypoxia greatly limits the medicinal potency of PDT, mostly since the production of ROS in PDT is achieved in the presence of a high level of oxygen. However, the generation of other toxic oxidant is oxygen independent. Wang et al. suggested a brand new therapeutic strategy for cancer therapy by the light-mediated production of oxidants [326]. Initiator loaded AuNCs as the free radical generator under NIR irradiation can produce alkyl radicals, with the possibility of enhancing the level of oxidative stress leading to DNA damages in cancer cells. It can also cause apoptotic cell death under different oxygen concentrations.

5.2.5. Gold nanoshells

Au nanoshells have demonstrated potential interest in medical fields. The seed-induced growth method by means of SiO_2 route is considered as the most used method for synthesizing Au nanoshells.

5.2.5.1. Sensitive and non-invasive methods for cancer treatment. Formerly, Loo et al. [327] explored the incubation of human breast cancer cell line (SKBr3) with bioconjugated Au nanoshells- SiO_2-AuNPs with a thin layer of Au followed by laser irradiation for bimodal imaging and therapy. Only the cells incubated with bioconjugated Au nanoshells- SiO_2-AuNPs were destructed by the laser (Fig. 9A). Moreover, O'Neal et al. [328] investigated the possibility of Au nanoshell-assisted PTT (NAPT) which exhibits strong absorption in the NIR region. Mice-bearing murine colon carcinoma cells were injected with PEG-Au nanoshell followed by laser irradiation for 3 min. All such treated mice showed a normal condition without any tumor after 90 days. This simple, sensitive, and non-invasive method can be considered as a potential candidate for selective photothermal tumor destruction [328]. Likewise, Hirsch et al. [329] studied the nanoshell-mediated NIR (820 nm, 35 W/cm^2) thermal therapy of human breast carcinoma cells under magnetic resonance guidance *in vitro* and *in vivo*.It was shown that cells received high dosages of NIR laser or nanoshells did not show mortality, suggesting that neither NIR nor nanoshell by itself is toxic. Bimodal application, nevertheless, induced localized cell ablation restricted to the incubated section. Similar outcomes were also observed *in vivo* (Fig. 9B). Bimodal imaging and NIR radiation caused the pronounced irreversible thermal ablation restricted to the tumor area.

5.2.5.2. Synergistic chemotherapy and PTT. Ma et al. [330] designed a cholesteryl succinylsilane (CSS) nanomicelles loaded with DOX, iron NPs, and Au nanoshells nanohybrid for potential MRI, light (808 nm)-mediated drug delivery, and PTT therapy.The nanohybrid

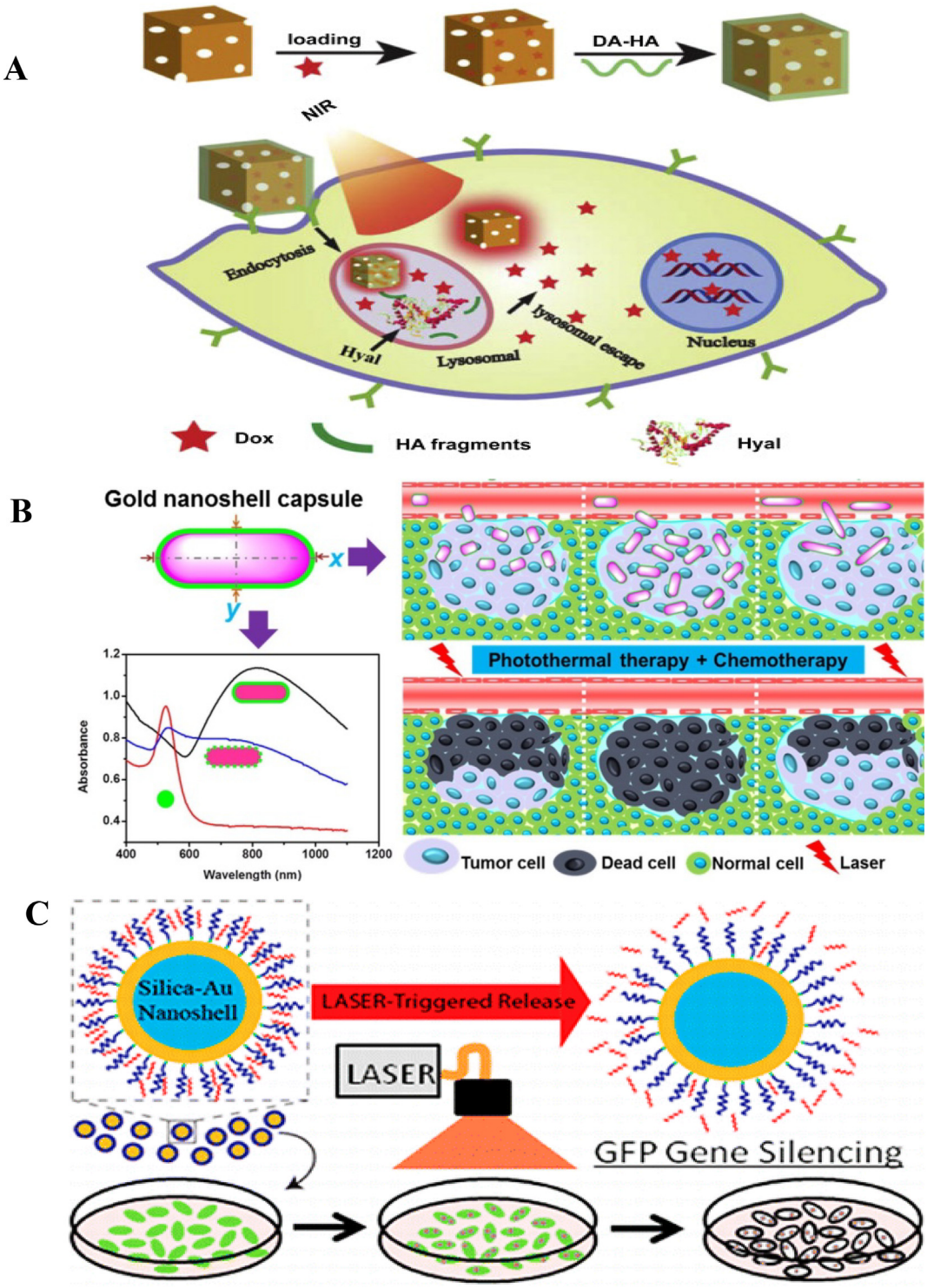

Fig. 8. Synergistic chemotherapy and PTT. (A): Schematic illustration of a multi-purpose guided nanohybrid with DOX loaded (HA)-dopamine hydrochloride (DA)-DOX loaded AuNCs for targeted drug release inside the cell and synergistic treatment [322]. (B): Controllable NIR plasmonic Au nanoshell capsules with varying dimension were prepared and employed with the features of both PTT and chemotherapy. The Au nanoshell capsules with moderate aspect ratio are potentially absorbed by melanoma cells and can infiltrate into tumor cells, leading to a highly successful destruction of malignant melanomas when employed along with irradiation and a single irradiation [332]. (C): Designed Au nanoshell-mediated medicinal oligonucleotide targeted delivery carrier, was fabricated to release its cargo selectively upon activating with a NIR laser [336]. Reproduced under the terms of the Creative Commons Attribution License (CC BY).

demonstrated potential drug-loading and potency, and an excellent reaction to magnetic fields. Amplification of T_2-weighted MR imaging was detected for the nanohybrid. Photothermal-driven cytotoxicity *in vitro* revealed that the nanohybrid resulted in cell mortality through photothermal consequence only in the presence of irradiation. Cancer cells in the presence of nanohybrid, irradiation and magnetic fields demonstrated a remarkable enhancement in cell mortality which may suggest the bimodal impacts of the magnetic-field-mediated drug release and the PTT [330]. Besides, Liu et al. [331] suggested a multi-purposes smart nanodrug delivery system by Au nanoshell-

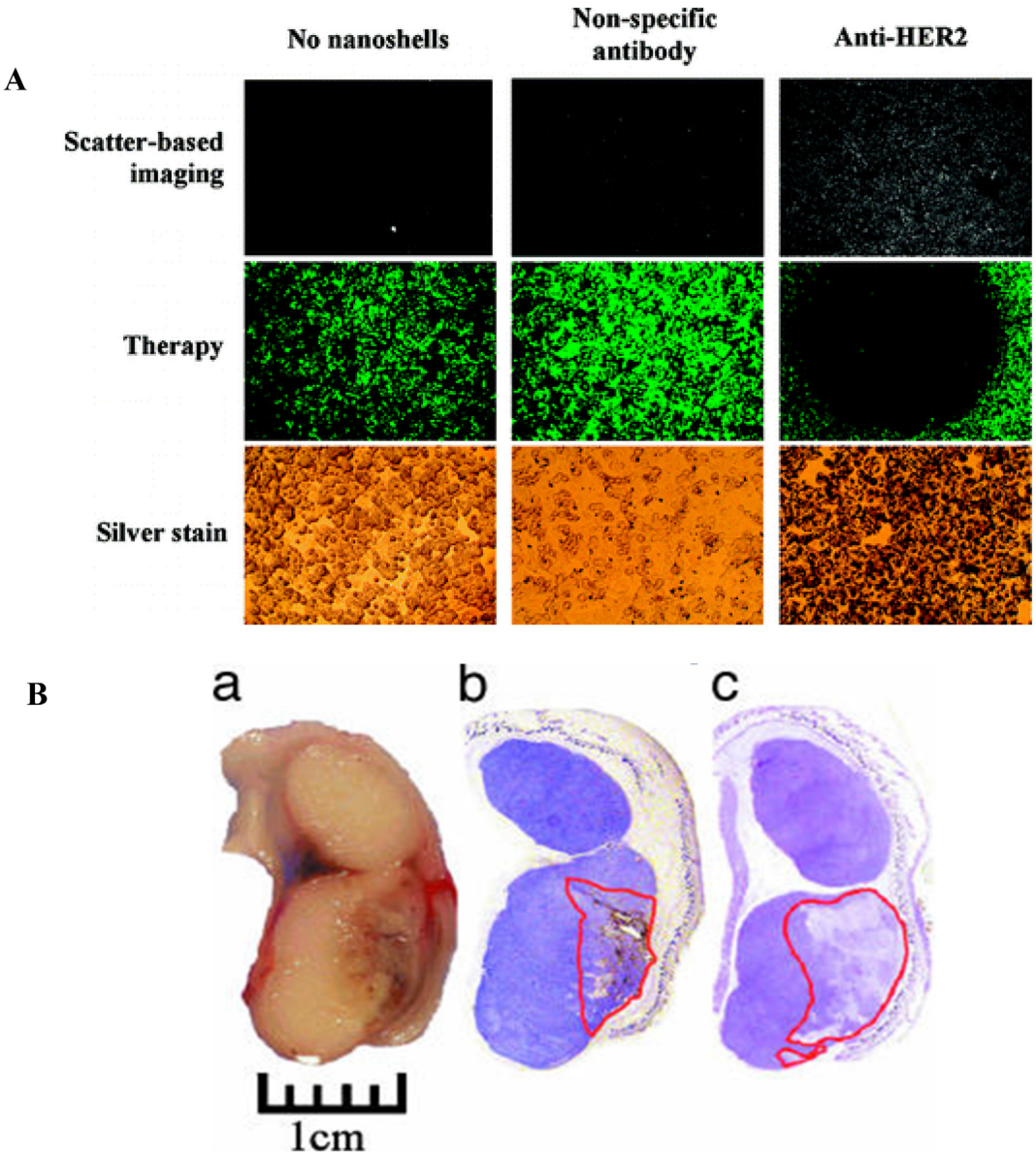

Fig. 9. Sensitive and non-invasive methods for cancer treatment (A): Bimodal imaging/therapy bioconjugated Au nanoshells-SiO_2-AuNPs were employed to image and damage breast carcinoma tumor cells [327]. (B): (*a*) Application of Au nanoshells along with NIR laser show hemorrhaging and defect of tissue. (*b*) Staining of a tissue section demonstrates the accumulated Au nanoshells. (*c*) Staining method distinctly depicts tissue [329]. Reproduced under the terms of the Creative Commons Attribution License (CC BY).

coated betulinic acid liposomes (AuNS-BA-Lips) mediated by a glutathione for synergistic chemo-PTT. The AuNS-BA-Lips revealed narrow size distribution (149.4 ± 2.4 nm), potential photothermal conversion characteristic and dual chemo-PTT. In the presence of NIR irradiation, the AuNS-BA-Lips exhibited highly potent antitumor activity on tumor-bearing mice with an inhibition rate of 83.02%, thus showing a significant synergistic therapeutic outcome of chemotherapy and thermotherapy [331]. Whereas, Wang et al. [332] considered the aspect ratios of Au nanoshell capsules that can mediate the melanoma ablation by synergistic PTT and chemotherapy. They concluded that controllable NIR plasmonic Au nanoshell capsules (GNSCs) with moderate aspect ratio can potentially be penetrated into the melanoma cells and tumor tissues, leading to highly pronounced mortality of advanced malignant melanomas when applied along with irradiation and a single dose (Fig. 8B). Also, Wang et al. [333] designed a system by loading resveratrol (Res) in chitosan (CTS)-modified liposomes, and coated by Au nanoshells (GNS@CTS@Res-lips) for bimodal carriage of drug and chemo-PTT therapy. The fabricated GNS@CTS@Res-lips exhibited high photothermal efficiency for potential PTT therapy. In addition, the GNS@CTS@Res-lips showed the descent pH/photothermal-driven drug release. NIR laser irradiation could markedly increase the cellular uptake of drugs based on a drug delivery system. More considerably, relative to chemotherapy or PTT, the vehicle with NIR irradiation demonstrated a pronounced therapeutic impact in HeLa cells. Therefore, the Au nanoshells conjugates with a bimodal application can be used as an effective nanosystem for application in cancer therapy [333,334]. Previously, Luo et al. [335] indicated that lung cancer (A549) cellular mortality was triggered by using recombinant human endostatin Au nanoshell-induced PTT therapy.

5.2.5.3. Gene delivery. RNA interference (RNAi)—utilizing antisense nucleic acid oligonucleotides to downregulate the pathogenic gene expression and subsequent encoded protein—plays a pivotal role in analyzing the genetic function and can be applied as a potential candidate for molecular therapeutic. A crucial barrier in the

application of gene silencing with RNAi technology is the systemic loading of medicinal oligonucleotides. In this regard, engineered Au nanoshell-mediated medicinal oligonucleotide delivery carrier was developed to release its drug selectively upon activating with radiation. A specified peptide epilayer covalently bound to the Au nanoshell surface was employed to determine siRNA molecules [336] (Fig. 8C). Also, Ding et al. [337] suggested the Rap2b double-stranded short-interfering RNA (siRNA) can significantly increase the *in vitro* and *in vivo* anticancer medicinal potencies of Adriamycin in an Au nanoshell-mediated drug/gene co-delivery carrier. In addition, they claimed that laser irradiation of the NPs might induce an additional thermal killing effect on cancer cells and further anticancer efficacy of Adriamycin [337]. More recently, Morgan et al. [338] revealed that Au nanoshell provide potential loading and transfer of siRNA into HeLa cells more efficient that Au nanocages.

5.2.5.4. Gold nanoshell loaded macrophage. Targeted delivery of NPs holds a significant problem, mainly in the CNS where the blood–brain barrier blocks the internalization of most medicinal drugs. In this regards, the utilization of macrophages as carriers for the targeted delivery of Au nanoshells to permeating glioma will lead to the development of new drugs and therapeutic approaches [339]. Au–SiO_2 nanoshells were easily phagocytosed by macrophages, and the outcomes have exhibited the migratory prospective of Au nanoshell-loaded macrophages in glioma spheroids (Fig. 10). In particular, after NIR irradiation of spheroids having Au nanoshell-loaded macrophages, produced heat was strong enough to induce spheroid ablation. Trinidad et al. [340] developed a combined concurrent photodynamic ($\lambda = 670$ nm) and Au nanoshell loaded macrophage-mediated PTT (14 or 28 W/cm^2, $\lambda = 810$ nm) therapies for the treatment of head and neck squamous cell carcinoma (HNSCC). Collectively, these data hold a great promise of macrophages utilization as nanoshell delivery platform for PTT of cancerous cells.

6. Impending clinical impact of AuNPs

Much of the ongoing anticipation all round nanoscience is straightly associated with the potential of modern nanotechnology implementations in cancer diagnostics and therapy. SPR features of AuNPs are controlled by physicochemical parameters of NPs such as shape and size, NPs can be utilized to design and develop new and distinguished tools for innovative light-based applications.

AuNPs with different shapes have potentials for the development of PTT and PDT therapy of tumor tissue as well as diagnosis [341–343]. By engineering NP morphology, scientists can optimize the SPR features of NPs to any wavelength of concern. Blood and tissue do not absorb light in the NIR region [344]. When AuNPs resonances are tuned to NIR region, these NPs can be utilized as potential contrast candidates in the diagnostic imaging of cancerous cells. When irradiated, photothermally triggering cell death and tumor ablation can be achieved by AuNPs as a source of thermal induction. AuNP-mediated diagnostics and therapeutics may be employed from basic research to medicinal applications; this review investigated the potential attainment of this outlook in the context of the trial of complex diseases like cancer. Indeed, AuNPs exhibit a decent model of a highly propitious demand of nanochemistry to biomedical challenges.

We outlined the characteristics of AuNPs that are associated with their physicochemical features and their applications in cancer diagnostics and therapy. Distinctive surface modification can play a pivotal role in the passive internalization of AuNPs into tumors and for targeted drug delivery by bioconjugate approaches. We also reviewed that PTT can be performed for the photothermal destruction of tumor cells by the aid of AuNPs. AuNP-based PTT in several *in vivo* and human models have exhibited highly promising trends, and it can be concluded that NP concentration, thermal response, and tumor location can be considered as critical factors for the NP-induced thermal ablation of tumor cells [345,346]. Finally, we can go beyond this review and discuss the next questions as AuNPs-based cancer diagnosis and therapy in clinical trials [347,348].

7. Future applications of gold NPs

AuNPs are flexible elements for a wide range of implementations which can be achieved only by interdisciplinary studies, jointly driven by the scientists from chemistry, biology, and medicine. For instance, plasmonic NPs exhibit high refractive index sensitivities, which is

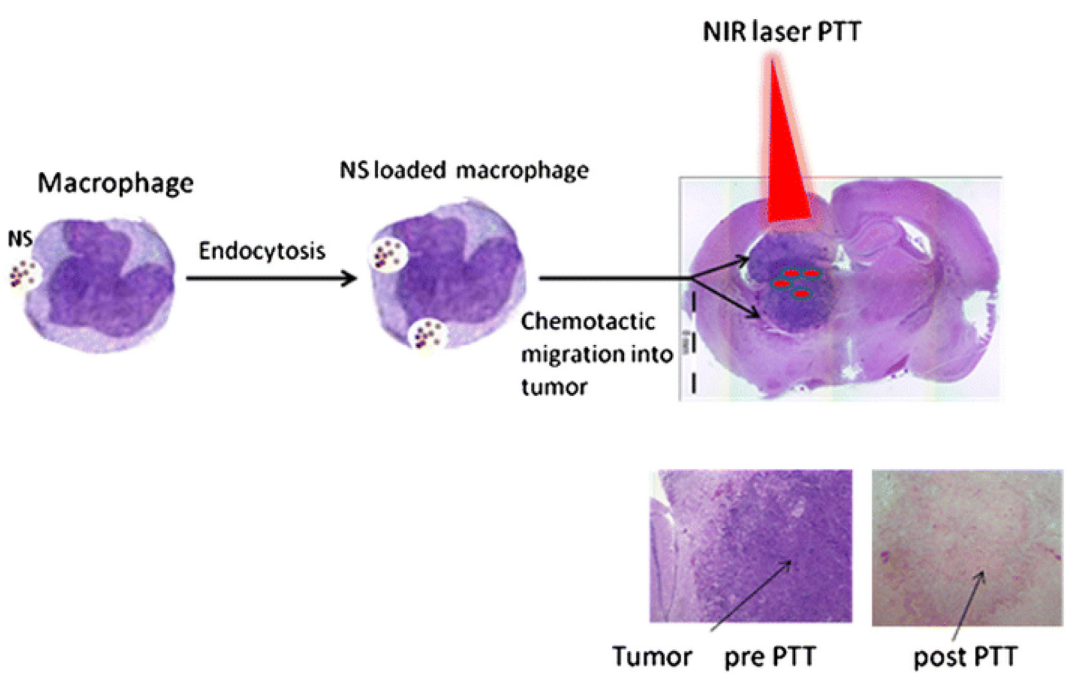

Fig. 10. Basic abstraction of nanoshell-mediated PPT using macrophages as nanoshell delivery carriers. Reproduced under the terms of the Creative Commons Attribution License (CC BY) from Ref. [339].

useful in developing powerful sensing devices. One-dimensional plasmonic NP arrays have intriguing optical properties that can be utilized in a number of applications [40]. It has been shown that well-engineered chains of plasmonic NPs can provide a significant increase in sensitivity relative to the conventional plasmonic sensors consisting of isolated or randomly placed NPs. Hooshmand et al. [55] found that an increase in the sensitivity factor was observed when the number of nanocubes and their orientation were controlled in the chain. In comparison to the face-to-face (FF) orientation, the changes in optical properties were more prominent in the edge-to-edge (EE) configuration. These results suggested that plasmonic coupling in linearly assembled NPs becomes extremely important at sub-nm distances [45].

In analytical chemistry, AuNPs play two main roles - as target analytes in the realm of the analysis of the nanoworld and as analytical tools to improve physicochemical processes, such as the use of AuNPs as components of electrodes, in spectroscopic techniques and chemical sensors (sensors based on colorimetric sensing, on fluorescence-related phenomena, electrical and electrochemical sensing) [307]. Furthermore, AuNPs show several potential characteristics for application in electrochemistry including electroanalysis, their employment as probes in electrochemical sensors, and their deposition on the surface and in the bulk material of electrodes for electrochemical applications. One of the most propitious areas of AuNPs implementation is physical chemistry including spectroscopic techniques, e.g. spectrophotometric methods of determination, colorimetric detection, imaging, fluorescence-based methodologies, phosphorescence processes, chemiluminiscence reactions [40]. Another development is that AuNPs are being investigated extensively for application in high technology devises such as sensory probes for detection of heavy metal cations, small organic compounds, nucleic acids, proteins, as electronic conductors, organic photovoltaics, and nanowires [56].

AuNPs are ideal candidates for catalysis in several chemical reactions because their physicochemical properties can be tuned by adjusting their structural dimensions and especially supported systems are already proven catalysts. The future of Au catalysis should grow further for a range of catalytic applications not yet explored to result in a better understanding of the fundamental underlying phenomena that give rise to the exceptional catalytic activity of Au [349]. The ability to prepare robust AuNPs and multimetallic alloys with homogeneous and controlled morphologies and properties has already demonstrated to be fundamental for the advance of catalysis. In the future, it is expected that thermal and photocatalysis will continue to thrive. In photocatalysis, the direct plasmon absorption-light excitation relationship and its tuneability offer a myriad of options for new exciting catalysis [45]. Specifically, a plethora of anisotropic shapes and the development of their synthetic procedures should enable the rapid expansion of studies showing morphologies sensitive to specific light wavelengths, also closely related to sensing, such as SERRS. Moreover, the addition of a second metal was already shown to enhance the light response and can further expand the selection of catalysts. This opens the possibilities for Au, along with its resistance to oxidation, as perfect systems for many types of reactions, such as oxidation, and reduction/hydrogenation.

AuNPs have gained potential interest in biomedical implementations due to the presence of unique physicochemical features, ease of fabrication and surface modification in the nanoscale range, biocompatibility, and several other advantages. For example, AuNPs can be conjugated with specific antibodies or functional groups to develop platforms to simultaneously control heat and deliver anticancer drug for the targeted destruction of cancerous tissue, synergistic chemotherapy and PTT and dual contrast and therapeutic system [40]. Although, Au is biologically inert and thus does not exhibit substantial adverse effects; the moderately low rate of clearance from the body can result in some serious health adverse effects [3]. Therefore, targeted AuNPs delivering to cancerous cells must be addressed before AuNPs find their implementation for the ordinary biomedical application.

8. Opportunities and challenges

Au materials manufactured at the nanoscale level have unique and beneficial properties for the medical sector in the area of implants, tissue engineering, organs, detection, biosensors, immunoanalysis, diagnosis, PTT of cancer cells, − specific drug delivery, optical bioimaging or monitoring of cells and tissues. Therefore it may be concluded that AuNPs could be applied in almost all medical systems: diagnostics, therapy, prevention, and hygiene. We believe that the next decade will witness the commencement of additional clinical trials of recently designed AuNPs, the expansion into employment beyond cancer, and the assay of multimodal approaches.

However, there are a number of crucial opportunities and challenges that should be addressed as AuNPs continue to be developed as standalone nanomaterials and as a component of a multifunctional platform for a number of applications. For example, detailed studies should be done to realize how adjusting nanomaterial conditions such as size, shape, moieties, and conjugated bodies influence the underlying impacts in the AuNPs-based system, including the mechanism of detection, catalyst, diagnosis and cell death. Also, there are some adverse effects that should be examined before the NPs formulation can be successfully translated into chemical and biological applications. This includes the reproducibility [350], reliability [351], scalability [352], safety [353–357], biodegradability [358], and biocompatibility [358] in manufacturing NP-based sensing/medical tools.

9. Conclusions

AuNPs show exclusive colloidal stability and can be fabricated in several routes for the controlling of their dimension and morphology. AuNP-mediated applications have been thoroughly investigated as standalone analytical tools for their specific utilizations such as detection, catalyst, diagnosis, and therapy. AuNPs are ideal candidates for colorimetric detection, catalysis, imaging, and photothermal transducers, because their physicochemical properties can be tuned by adjusting their structural dimensions. Furthermore, AuNPs show several potential characteristics for utilization in multimodal applications including simple Au-functionalization, bioconjugation, efficient activity and target accumulation. In general, it is critical to reveal the mechanism of activity and therapeutic of NPs to optimally design and develop multimodal NP-based sensing and diagnostic tools.

Acknowledgements

The financial support of Tehran Medical Sciences, Islamic Azad University, Tehran, Iran is greatly acknowledged.

References

[1] K.A. Willets, R.P. Van Duyne, Localized surface plasmon resonance spectroscopy and sensing, Annu. Rev. Phys. Chem. 58 (2007) 267–297.
[2] Y. Zhuang, L. Liu, X. Wu, Y. Tian, X. Zhou, S. Xu, Z. Xie, Y. Ma, Size and shape effect of gold nanoparticles in “far-field” surface plasmon resonance, Part. Part. Syst. Charact. 36 (2019) 1800077.
[3] Y. Wu, M.R. Ali, K. Chen, N. Fang, M.A. El-Sayed, Gold nanoparticles in biological optical imaging, Nano Today 24 (2019) 120–140.
[4] K. Pathakoti, M. Manubolu, H.-M. Hwang, Nanostructures: current uses and future applications in food science, J. Food Drug Anal. 25 (2017) 245–253.
[5] M.-C. Daniel, D. Astruc, Gold nanoparticles: assembly, supramolecular chemistry, quantum-size-related properties, and applications toward biology, catalysis, and nanotechnology, Chem. Rev. 104 (2004) 293–346.
[6] Y. Hernández, B.C. Galarreta, Noble metal-based plasmonic nanoparticles for SERS imaging and photothermal therapy, Nanomaterials for Magnetic and Optical Hyperthermia Applications, Elsevier, 2019, pp. 83–109.
[7] W. Zhao, M.A. Brook, Y. Li, Design of gold nanoparticle-based colorimetric biosensing assays, ChemBioChem 9 (2008) 2363–2371.
[8] D.D. Gurav, Y.A. Jia, J. Ye, K. Qian, Design of plasmonic nanomaterials for diagnostic spectrometry, Nanoscale Adv. 1 (2019) 459–469.
[9] K.L. Kelly, E. Coronado, L.L. Zhao, G.C. Schatz, The Optical Properties of Metal Nanoparticles: the Influence of Size, Shape, and Dielectric Environment, ACS Publications, 2003.

[10] J. Pérez-Juste, I. Pastoriza-Santos, L.M. Liz-Marzán, P. Mulvaney, Gold nanorods: synthesis, characterization and applications, Coord. Chem. Rev. 249 (2005) 1870–1901.
[11] B. Hvolbæk, T.V. Janssens, B.S. Clausen, H. Falsig, C.H. Christensen, J.K. Nørskov, Catalytic activity of au nanoparticles, Nano Today 2 (2007) 14–18.
[12] D.T. Thompson, Using gold nanoparticles for catalysis, Nano Today 2 (2007) 40–43.
[13] M.B. Cortie, The weird world of nanoscale gold, Gold Bull. 37 (2004) 12–19.
[14] P. Pyykkö, Theoretical chemistry of gold, Angew. Chem. Int. Ed. 43 (2004) 4412–4456.
[15] M. Chen, D.W. Goodman, Catalytically active gold: from nanoparticles to ultrathin films, Acc. Chem. Res. 39 (2006) 739–746.
[16] R. Meyer, C. Lemire, S.K. Shaikhutdinov, H.-J. Freund, Surface chemistry of catalysis by gold, Gold Bull. 37 (2004) 72–124.
[17] I. Kostova, Gold coordination complexes as anticancer agents, Anti Cancer Agents Med. Chem. 6 (2006) 19–32.
[18] G. Yilmaz, E. Guler, C. Geyik, B. Demir, M. Ozkan, D.O. Demirkol, S. Ozcelik, S. Timur, C.R. Becer, pH responsive glycopolymer nanoparticles for targeted delivery of anti-cancer drugs, Mol. Syst. Des. Eng. 3 (2018) 150–158.
[19] R. García-Álvarez, M. Hadjidemetriou, A. Sánchez-Iglesias, L.M. Liz-Marzán, K. Kostarelos, In vivo formation of protein corona on gold nanoparticles. the effect of their size and shape, Nanoscale 10 (2018) 1256–1264.
[20] J. Turkevich, P.C. Stevenson, J. Hillier, A study of the nucleation and growth processes in the synthesis of colloidal gold Discuss, Faraday Soc. 11 (1951) 55–75.
[21] A. Clemente, N. Moreno, M.P. Lobera, F. Balas, J. Santamaria, Versatile hollow fluorescent metal-silica nanohybrids through a modified microemulsion synthesis route, J. Colloid Interface Sci. 513 (2018) 497–504.
[22] G. Carrot, J. Valmalette, C. Plummer, S. Scholz, J. Dutta, H. Hofmann, J. Hilborn, Gold nanoparticle synthesis in graft copolymer micelles, Colloid Polym. Sci. 276 (1998) 853–859.
[23] C.-H. Kuo, M.H. Huang, Synthesis of branched gold nanocrystals by a seeding growth approach, Langmuir 21 (2005) 2012–2016.
[24] A. Laguna, Modern Supramolecular Gold Chemistry: Gold-Metal Interactions and Applications, John Wiley & Sons, 2008.
[25] Y. Tan, X. Dai, Y. Li, D. Zhu, Preparation of gold, platinum, palladium and silver nanoparticles by the reduction of their salts with a weak reductant–potassium bitartrate, J. Mater. Chem. 13 (2003) 1069–1075.
[26] X. Gao, Y. Zhang, Y. Zhao, Biosorption and reduction of Au (III) to gold nanoparticles by thiourea modified alginate, Carbohydr. Polym. 159 (2017) 108–115.
[27] J. Zhou, J. Ralston, R. Sedev, D.A. Beattie, Functionalized gold nanoparticles: synthesis, structure and colloid stability, J. Colloid Interface Sci. 331 (2009) 251–262.
[28] M. Grzelczak, J. Pérez-Juste, P. Mulvaney, L.M. Liz-Marzán, Shape control in gold nanoparticle synthesis, Chem. Soc. Rev. 37 (2008) 1783–1791.
[29] H. Kang, J.T. Buchman, R.S. Rodriguez, H.L. Ring, J. He, K.C. Bantz, C.L. Haynes, Stabilization of silver and gold nanoparticles: preservation and improvement of plasmonic functionalities, Chem. Rev. 119 (2018) 664–699.
[30] M.F. Zayed, W.H. Eisa, S.M. El-kousy, W.K. Mleha, N. Kamal, Ficus retusa-stabilized gold and silver nanoparticles: controlled synthesis, spectroscopic characterization, and sensing properties, Spectrochim. Acta A 214 (2019) 496–512.
[31] M. Dasog, W. Hou, R.W. Scott, Controlled growth and catalytic activity of gold monolayer protected clusters in presence of borohydride salts, Chem. Commun. 47 (2011) 8569–8571.
[32] L. Wallenberg, J.-O. Bovin, G. Schmid, On the crystal structure of small gold crystals and large gold clusters, Surf. Sci. 156 (1985) 256–264.
[33] J. Li, X. Li, H.-J. Zhai, L.-S. Wang, Au20: a tetrahedral cluster, Science 299 (2003) 864–867.
[34] D. Vollath, D. Holec, F.D. Fischer, Au55, a stable glassy cluster: results of ab initio calculations, Beilstein J. Nanotechnol. 8 (2017) 2221.
[35] L.F. Hartje, B. Munsky, T.W. Ni, C.J. Ackerson, C.D. Snow, Adsorption-coupled diffusion of gold nanoclusters within a large-pore protein crystal scaffold, J. Phys. Chem. B 121 (2017) 7652–7659.
[36] A. Dass, T.C. Jones, S. Theivendran, L. Sementa, A. Fortunelli, Core Size Interconversions of Au30 (S-t Bu) 18 and Au36 (SPhX) 24, J. Phys. Chem. C 121 (2017) 14914–14919.
[37] W.W. Xu, Y. Li, Y. Gao, X.C. Zeng, Medium-sized Au 40 (SR) 24 and Au 52 (SR) 32 nanoclusters with distinct gold-kernel structures and spectroscopic features, Nanoscale 8 (2016) 1299–1304.
[38] T. Higaki, C. Liu, M. Zhou, T.-Y. Luo, N.L. Rosi, R. Jin, Tailoring the structure of 58-electron gold nanoclusters: au103s2 (S-Nap) 41 and its implications, J. Am. Chem. Soc. 139 (2017) 9994–10001.
[39] H. Schmidbaur, Gold Chemistry: Applications and Future Directions in the Life Sciences, John Wiley & Sons, 2009.
[40] M. Sharifi, F. Attar, A.A. Saboury, K. Akhtari, N. Hooshmand, A. Hasan, M. El-Sayed, M. Falahati, Plasmonic gold nanoparticles: optical manipulation, imaging, drug delivery and therapy, J. Control. Release 311-312 (2019) 170–189.
[41] P. Sajanlal, T. Sreeprasad, A.S. Nair, T. Pradeep, Wires, plates, flowers, needles, and core− shells: diverse nanostructures of gold using polyaniline templates, Langmuir 24 (2008) 4607–4614.
[42] M.U.-B. Christiansen, N. Seselj, C. Engelbrekt, M. Wagner, F.N. Stappen, J. Zhang, Chemically controlled interfacial nanoparticle assembly into nanoporous gold films for electrochemical applications, J. Mater. Chem. A 6 (2018) 556–564.
[43] E. Torres-Chavolla, R.J. Ranasinghe, E.C. Alocilja, Characterization and functionalization of biogenic gold nanoparticles for biosensing enhancement, IEEE Trans. Nanotechnol. 9 (2010) 533–538.
[44] M. Borzenkov, G. Chirico, L. D'Alfonso, L. Sironi, M. Collini, E. Cabrini, G. Dacarro, C. Milanese, P. Pallavicini, A. Taglietti, C. Bernhard, F. Denat, Thermal and chemical stability of thiol bonding on gold nanostars, Langmuir 31 (2015) 8081–8091.
[45] V. Amendola, R. Pilot, M. Frasconi, O.M. Marago, M.A. Iati, Surface plasmon resonance in gold nanoparticles: a review, J. Phys. 29 (2017) 203002.
[46] H. Grönbeck, A. Curioni, W. Andreoni, Thiols and disulfides on the Au (111) surface: the headgroup− gold interaction, J. Am. Chem. Soc. 122 (2000) 3839–3842.
[47] B. Kim, S.H. Choi, X.-Y. Zhu, C.D. Frisbie, Molecular tunnel junctions based on π-conjugated oligoacene thiols and dithiols between Ag, Au, and Pt contacts: effect of surface linking group and metal work function, J. Am. Chem. Soc. 133 (2011) 19864–19877.
[48] H.A. Bent, Structural chemistry of donor-acceptor interactions, Chem. Rev. 68 (1968) 587–648.
[49] H.E. Toma, V.M. Zamarion, S.H. Toma, K. Araki, The coordination chemistry at gold nanoparticles, J. Braz. Chem. Soc. 21 (2010) 1158–1176.
[50] H. Jeong, S. Yoon, J.H. Kim, D.-H. Kwak, D.H. Gu, S.H. Heo, H. Kim, S. Park, H.W. Ban, J. Park, Transition metal-based thiometallates as surface ligands for functionalization of all-inorganic nanocrystals, Chem. Mater. 29 (2017) 10510–10517.
[51] Y. Chen, Y. Xianyu, X. Jiang, Surface modification of gold nanoparticles with small molecules for biochemical analysis, Acc. Chem. Res. 50 (2017) 310–319.
[52] P. Miao, Y. Tang, L. Wang, DNA modified Fe3O4@ Au magnetic nanoparticles as selective probes for simultaneous detection of heavy metal ions, ACS Appl. Mater. Interfaces 9 (2017) 3940–3947.
[53] E.K. Beloglazkina, A.G. Majouga, R.B. Romashkina, N.V. Zyk, N.S. Zefirov, Gold nanoparticles modified with coordination compounds of metals: synthesis and application, Russ. Chem. Rev. 81 (2012) 65.
[54] L. Pérez-Mirabet, S. Surinyach, J. Ros, J. Suades, R. Yáñez, Gold and silver nanoparticles surface functionalized with rhenium carbonyl complexes, Mater. Chem. Phys. 137 (2012) 439–447.
[55] N. Hooshmand, J.A. Bordley, M.A. El-Sayed, Are hot spots between two plasmonic nanocubes of silver or gold formed between adjacent corners or adjacent facets? a DDA examination, J. Phys. Chem. Lett. 5 (2014) 2229–2234.
[56] N. Elahi, M. Kamali, M.H. Baghersad, Recent biomedical applications of gold nanoparticles: a review, Talanta 184 (2018) 537–556.
[57] M. Lu, H. Zhu, C.G. Bazuin, W. Peng, J.-F. Masson, Polymer-templated gold nanoparticles on optical fibers for enhanced-sensitivity localized surface plasmon resonance biosensors, ACS Sensors 4 (2019) 613–622.
[58] P.J. Rivero, E. Ibañez, J. Goicoechea, A. Urrutia, I.R. Matias, F.J. Arregui, A self-referenced optical colorimetric sensor based on silver and gold nanoparticles for quantitative determination of hydrogen peroxide, Sensors Actuators B 251 (2017) 624–631.
[59] A. Mohamad, H. Teo, N.A. Keasberry, M.U. Ahmed, Recent developments in colorimetric immunoassays using nanozymes and plasmonic nanoparticles, Crit. Rev. Biotechnol. 39 (2019) 50–66.
[60] K. Gilroy, A. Sundar, M. Hajfathalian, A. Yaghoubzade, T. Tan, D. Sil, E. Borguet, R. Hughes, S. Neretina, Transformation of truncated gold octahedrons into triangular nanoprisms through the heterogeneous nucleation of silver, Nanoscale 7 (2015) 6827–6835.
[61] J. Yang, Y. Zhang, L. Zhang, H. Wang, J. Nie, Z. Qin, J. Li, W. Xiao, Analyte-triggered autocatalytic amplification combined with gold nanoparticle probes for colorimetric detection of heavy-metal ions, Chem. Commun. 53 (2017) 7477–7480.
[62] K.N. Han, J.-S. Choi, J. Kwon, Gold nanozyme-based paper chip for colorimetric detection of mercury ions, Sci. Rep. 7 (2017) 2806.
[63] K. Sadani, P. Nag, S. Mukherji, LSPR based optical fiber sensor with chitosan capped gold nanoparticles on BSA for trace detection of Hg (II) in water, soil and food samples, Biosens. Bioelectron. 134 (2019) 90–96.
[64] E. Priyadarshini, N. Pradhan, Gold nanoparticles as efficient sensors in colorimetric detection of toxic metal ions: a review, Sensors Actuators B 238 (2017) 888–902.
[65] S. Thatai, P. Khurana, S. Prasad, S.K. Soni, D. Kumar, Trace colorimetric detection of Pb2+ using plasmonic gold nanoparticles and silica–gold nanocomposites, Microchem. J. 124 (2016) 104–110.
[66] B.S. Boruah, R. Biswas, Localized surface plasmon resonance based U-shaped optical fiber probe for the detection of Pb2+ in aqueous medium, Sensors Actuators B 276 (2018) 89–94.
[67] Y. Zhang, J. Jiang, M. Li, P. Gao, G. Zhang, L. Shi, C. Dong, S. Shuang, Green synthesis of gold nanoparticles with pectinase: a highly selective and ultra-sensitive colorimetric assay for Mg2+, Plasmonics 12 (2017) 717–727.
[68] S. Xu, W. Ouyang, P. Xie, Y. Lin, B. Qiu, Z. Lin, G. Chen, L. Guo, Highly uniform gold nanobipyramids for ultrasensitive colorimetric detection of influenza virus, Anal. Chem. 89 (2017) 1617–1623.
[69] P. Weerathunge, R. Ramanathan, V.A. Torok, K. Hodgson, Y. Xu, R. Goodacre, B.K. Behera, V. Bansal, Ultrasensitive colorimetric detection of murine norovirus using nanozyme aptasensor, Anal. Chem. 91 (2019) 3270–3276.
[70] X. Wei, Z. Chen, L. Tan, T. Lou, Y. Zhao, DNA-catalytically active gold nanoparticle conjugates-based colorimetric multidimensional sensor array for protein discrimination, Anal. Chem. 89 (2016) 556–559.
[71] C.-C. Chang, G. Wang, T. Takarada, M. Maeda, Target-recycling-amplified colorimetric detection of pollen allergen using non-cross-linking aggregation of dna-modified gold Nanoparticles, ACS Sensors 4 (2019) 363–369.
[72] E. Shokri, M. Hosseini, M.D. Davari, M.R. Ganjali, M.P. Peppelenbosch, F. Rezaee, Disulfide-induced self-assembled targets: a novel strategy for the label free colorimetric detection of DNAs/RNAs via unmodified gold Nanoparticles, Sci. Rep. 7

(2017) 45837.
[73] M. Haruta, Size- and support-dependency in the catalysis of gold, Catal. Today 36 (1997) 153–166.
[74] G.C. Bond, Gold: a relatively new catalyst, Catal. Today 72 (2002) 5–9.
[75] G.J. Hutchings, Gold catalysis in chemical processing, Catal. Today 72 (2002) 11–17.
[76] M. Haruta, Gold as a novel catalyst in the 21st century: preparation, working mechanism and applications, Gold Bull. 37 (2004) 27–36.
[77] A.S.K. Hashmi, G.J. Hutchings, Gold catalysis, Angew. Chem. Int. Ed. 45 (2006) 7896–7936.
[78] S. Eustis, M.A. El-Sayed, Why gold nanoparticles are more precious than pretty gold: Noble metal surface plasmon resonance and its enhancement of the radiative and nonradiative properties of nanocrystals of different shapes, Chem. Soc. Rev. 35 (2006) 209–217.
[79] A.S.K. Hashmi, M. Rudolph, Gold catalysis in total synthesis, Chem. Soc. Rev. 37 (2008) 1766–1775.
[80] A. Corma, H. Garcia, Supported gold nanoparticles as catalysts for organic reactions, Chem. Soc. Rev. 37 (2008) 2096–2126.
[81] R. Sardar, A.M. Funston, P. Mulvaney, R.W. Murray, Gold Nanoparticles: past, present, and future, Langmuir 25 (2009) 13840–13851.
[82] A.I. Kozlov, A.P. Kozlova, H. Liu, Y. Iwasawa, A new approach to active supported Au catalysts, Appl. Catal. A. 182 (1999) 9–28.
[83] T.V. Choudhary, D.W. Goodman, Oxidation catalysis by supported gold Nano-Clusters, Top. Catal. 21 (2002) 25–34.
[84] M. Stratakis, H. Garcia, Catalysis by supported gold Nanoparticles: beyond aerobic oxidative processes, Chem. Rev. 112 (2012) 4469–4506.
[85] Z. Li, C. Brouwer, C. He, Gold-catalyzed organic transformations, Chem. Rev. 108 (2008) 3239–3265.
[86] A. Corma, A. Leyva-Pérez, M.J. Sabater, Gold-catalyzed carbon – heteroatom bond-forming reactions, Chem. Rev. 111 (2011) 1657–1712.
[87] M. Haruta, Catalysis: gold rush, Nature 437 (2005) 1098–1099.
[88] A.S.K. Hashmi, Gold-catalyzed organic reactions, Chem. Rev. 107 (2007) 3180–3211.
[89] X. Chen, H. Zhu, R.J. Groarke, Catalysis by supported gold Nanoparticles, Reference Module in Materials Science and Materials Engineering, Elsevier, 2016.
[90] T.A. Baker, X. Liu, C.M. Friend, The mystery of gold's chemical activity: local bonding, morphology and reactivity of atomic oxygen, Phys. Chem. Chem. Phys. 13 (2011) 34–46.
[91] N. Dimitratos, C. Hammond, C.J. Kiely, G.J. Hutchings, Catalysis using colloidal-supported gold-based nanoparticles, Appl. Petrochem. Res. 4 (2014) 85–94.
[92] N. Dimitratos, J.K. Edwards, C.J. Kiely, G.J. Hutchings, Gold catalysis: helping create a sustainable future, Appl. Petrochem. Res. 2 (2012) 7–14.
[93] A. Stephen, K. Hashmi, Homogeneous catalysis by gold, Gold Bull. 37 (2004) 51–65.
[94] A. Primo, A. Corma, H. Garcia, Titania supported gold nanoparticles as photocatalyst, Phys. Chem. Chem. Phys. 13 (2011) 886–910.
[95] C.D. Pina, E. Falletta, M. Rossi, Update on selective oxidation using gold, Chem. Soc. Rev. 41 (2012) 350–369.
[96] C. Della Pina, E. Falletta, L. Prati, M. Rossi, Selective oxidation using gold, Chem. Soc. Rev. 37 (2008) 2077–2095.
[97] N. Dimitratos, J.A. Lopez-Sanchez, G.J. Hutchings, Slective liquid phase oxidation with supported metal Nanoparticles, Chem. Sci. 3 (2012) 20–44.
[98] M. Hajfathalian, K.D. Gilroy, A. Yaghoubzade, A. Sundar, T. Tan, R.A. Hughes, S. Neretina, Photocatalytic enhancements to the reduction of 4-nitrophenol by resonantly excited triangular gold–copper nanostructures, J. Phys. Chem. C 119 (2015) 17308–17315.
[99] S. Najafishirtari, R. Brescia, P. Guardia, S. Marras, L. Manna, M. Colombo, Nanoscale transformations of alumina-supported AuCu ordered phase Nanocrystals and their activity in CO oxidation, ACS Catal. 5 (2015) 2154–2163.
[100] L. Kesavan, R. Tiruvalam, M.H.A. Rahim, M.I. bin Saiman, D.I. Enache, R.L. Jenkins, N. Dimitratos, J.A. Lopez-Sanchez, S.H. Taylor, D.W. Knight, C.J. Kiely, G.J. Hutchings, Solvent-free oxidation of primary carbon-hydrogen bonds in toluene using Au-Pd alloy Nanoparticles, Science 331 (2011) 195–199.
[101] J.A. Lopez-Sanchez, N. Dimitratos, C. Hammond, G.L. Brett, L. Kesavan, S. White, P. Miedziak, R. Tiruvalam, R.L. Jenkins, A.F. Carley, D. Knight, C.J. Kiely, G.J. Hutchings, Facile removal of stabilizer-ligands from supported gold nanoparticles, Nat. Chem. 3 (2011) 551–556.
[102] J.A. Lopez-Sanchez, N. Dimitratos, P. Miedziak, E. Ntainjua, J.K. Edwards, D. Morgan, A.F. Carley, R. Tiruvalam, C.J. Kiely, G.J. Hutchings, Au-Pd supported nanocrystals prepared by a sol immobilisation technique as catalysts for selective chemical synthesis, Phys. Chem. Chem. Phys. 10 (2008) 1921–1930.
[103] C.E. Chan-Thaw, A. Villa, L. Prati, Immobilization of Preformed Gold Nanoparticles, in: L. Prati, A. Villa (Eds.), Gold Catalysis: Preparation, Characterization, and Applications, 2016, p. 39.
[104] C. Lofton, W. Sigmund, Mechanisms controlling crystal habits of gold and silver colloids, Adv. Funct. Mater. 15 (2005) 1197–1208.
[105] C.J. Murphy, T.K. Sau, A.M. Gole, C.J. Orendorff, J. Gao, L. Gou, S.E. Hunyadi, T. Li, Anisotropic metal nanoparticles: synthesis, assembly, and optical applications, J. Phys. Chem. B 109 (2005) 13857–13870.
[106] Y. Xia, N.J. Halas, Shape-controlled synthesis and surface plasmonic properties of metallic Nanostructures, MRS Bull. 30 (2005) 338–348.
[107] A.R. Tao, S. Habas, P. Yang, Shape control of colloidal metal Nanocrystals, Small 4 (2008) 310–325.
[108] T.K. Sau, A.L. Rogach, Nonspherical noble metal nanoparticles: colloid-chemical synthesis and Morphology control, Adv. Mater. 22 (2010) 1781–1804.
[109] A. Guerrero-Martínez, S. Barbosa, I. Pastoriza-Santos, L.M. Liz-Marzán, Nanostars shine bright for you: colloidal synthesis, properties and applications of branched metallic nanoparticles, Curr. Opin. Colloid Interface Sci. 16 (2011) 118–127.
[110] S.E. Lohse, C.J. Murphy, The quest for shape control: a history of gold nanorod synthesis, Chem. Mater. 25 (2013) 1250–1261.
[111] X. Hong, C. Tan, J. Chen, Z. Xu, H. Zhang, Synthesis, properties and applications of one- and two-dimensional gold nanostructures, Nano Res. 8 (2014) 40–55.
[112] N. Li, P. Zhao, D. Astruc, Anisotropic gold Nanoparticles: synthesis, properties, applications, and toxicity, Angew. Chem. Int. Ed. 53 (2014) 1756–1789.
[113] S.E. Lohse, N.D. Burrows, L. Scarabelli, L.M. Liz-Marzán, C.J. Murphy, Anisotropic noble metal nanocrystal growth: the role of halides, Chem. Mater. 26 (2014) 34–43.
[114] H. Hu, J. Zhou, Q. Kong, C. Li, Two-dimensional Au Nanocrystals: shape/size controlling synthesis, morphologies, and applications, Part. Part. Syst. Charact. 32 (2015) 796–808.
[115] J. Lai, W. Niu, R. Luque, G. Xu, Solvothermal synthesis of metal nanocrystals and their applications, Nano Today 10 (2015) 240–267.
[116] C. Xue, Q. Li, Anisotropic gold Nanoparticles: preparation, properties, and applications, in: Q. Li (Ed.), Anisotropic Nanomaterials: Preparation, Properties, and Applications, Springer International Publishing, Cham, 2015, pp. 69–118.
[117] N.D. Burrows, A.M. Vartanian, N.S. Abadeer, E.M. Grzincic, L.M. Jacob, W. Lin, J. Li, J.M. Dennison, J.G. Hinman, C.J. Murphy, Anisotropic nanoparticles and anisotropic surface chemistry, J. Phys. Chem. Lett. 7 (2016) 632–641.
[118] P. Zhao, N. Li, D. Astruc, State of the art in gold nanoparticle synthesis, Coord. Chem. Rev. 257 (2013) 638–665.
[119] P.R. Sajanlal, T.S. Sreeprasad, A.K. Samal, T. Pradeep, Anisotropic Nanomaterials: Structure, Growth, Assembly, and Functions, 2011 (2011).
[120] T.K. Sau, A.L. Rogach, Colloidal synthesis of noble metal nanoparticles of complex Morphologies, Complex-Shaped Metal Nanoparticles, Wiley-VCH Verlag GmbH & Co. KGaA, 2012, pp. 7–90.
[121] C. Burda, X. Chen, R. Narayanan, M.A. El-Sayed, Chemistry and properties of nanocrystals of different shapes, Chem. Rev. 105 (2005) 1025–1102.
[122] H.A. Al-Zubaidi, C.D.J. Bonner, M. Liu, S.O. Obare, Strategies for the synthesis of anisotropic catalytic Nanoparticles, in: S.E. Hunyadi Murph, G.K. Larsen, K.J. Coopersmith (Eds.), Anisotropic and Shape-Selective Nanomaterials: Structure-Property Relationships, Springer International Publishing, Cham, 2017, pp. 375–398.
[123] A. Liu, G. Wang, F. Wang, Y. Zhang, Gold nanostructures with near-infrared plasmonic resonance: synthesis and surface functionalization, Coord. Chem. Rev. 336 (2017) 28–42.
[124] S. Link, M.A. El-Sayed, Shape and size dependence of radiative, non-radiative and photothermal properties of gold nanocrystals, Int. Rev. Phys. Chem. 19 (2000) 409–453.
[125] M.A. El-Sayed, Some interesting properties of metals confined in time and nanometer space of different shapes, Acc. Chem. Res. 34 (2001) 257–264.
[126] H. Jing, L. Zhang, H. Wang, Geometrically tunable optical properties of metal Nanoparticles, in: C. Kumar (Ed.), UV-VIS and Photoluminescence Spectroscopy for Nanomaterials Characterization, Springer Berlin Heidelberg, Berlin, Heidelberg, 2013, pp. 1–74.
[127] L. Judith, M.N. Sergey, M.L.-M. Luis, Sensing using plasmonic nanostructures and nanoparticles, Nanotechnology 26 (2015) 322001.
[128] Y. Peng, B. Xiong, L. Peng, H. Li, Y. He, E.S. Yeung, Recent advances in optical imaging with anisotropic plasmonic Nanoparticles, Anal. Chem. 87 (2015) 200–215.
[129] L.D. Marks, L. Peng, Nanoparticle shape, thermodynamics and kinetics, J. Phys. 28 (2016) 053001.
[130] C.J. Murphy, L.B. Thompson, A.M. Alkilany, P.N. Sisco, S.P. Boulos, S.T. Sivapalan, J.A. Yang, D.J. Chernak, J. Huang, The many faces of gold nanorods, J. Phys. Chem. Lett. 1 (2010) 2867–2875.
[131] H. Chen, L. Shao, Q. Li, J. Wang, Gold nanorods and their plasmonic properties, Chem. Soc. Rev. 42 (2013) 2679–2724.
[132] E. Carbó-Argibay, S. Mourdikoudis, I. Pastoriza-Santos, J. Pérez-Juste, Chapter 2 - nanocolloids of noble metals, in: C.R. Abreu (Ed.), Nanocolloids, Elsevier, Amsterdam, 2016, pp. 37–73.
[133] C.L. Nehl, J.H. Hafner, Shape-dependent plasmon resonances of gold nanoparticles, J. Mater. Chem. 18 (2008) 2415–2419.
[134] K. Thorkelsson, P. Bai, T. Xu, Self-assembly and applications of anisotropic nanomaterials: a review, Nano Today 10 (2015) 48–66.
[135] C.J. Murphy, A.M. Gole, S.E. Hunyadi, J.W. Stone, P.N. Sisco, A. Alkilany, B.E. Kinard, P. Hankins, Chemical sensing and imaging with metallic nanorods, Chem. Commun. (2008) 544–557.
[136] L.A. Bauer, N.S. Birenbaum, G.J. Meyer, Biological applications of high aspect ratio nanoparticles, J. Mater. Chem. 14 (2004) 517–526.
[137] M. Wirtz, M. Parker, Y. Kobayashi, C.R. Martin, molecular sieving and sensing with gold nanotube membranes, Chem. Rec. 2 (2002) 259–267.
[138] M. Wirtz, S. Yu, C.R. Martin, Template synthesized gold nanotube membranes for chemical separations and sensing, Analyst 127 (2002) 871–879.
[139] P. Priecel, H.A. Salami, R.H. Padilla, Z.Y. Zhong, J.A. Lopez-Sanchez, Anisotropic gold nanoparticles: preparation and applications in catalysis, Chin. J. Catal. 37 (2016) 1619–1650.
[140] Y. Khalavka, J. Becker, C. Sönnichsen, Synthesis of rod-shaped gold nanorattles with improved plasmon sensitivity and catalytic activity, J. Am. Chem. Soc. 131 (2009) 1871–1875.
[141] X. Li, Y. Yang, G. Zhou, S. Han, W. Wang, L. Zhang, W. Chen, C. Zou, S. Huang, The unusual effect of AgNO3 on the growth of Au nanostructures and their catalytic performance, Nanoscale 5 (2013) 4976–4985.
[142] E. Martinsson, M.M. Shahjamali, N. Large, N. Zaraee, Y. Zhou, G.C. Schatz,

C.A. Mirkin, D. Aili, Influence of surfactant bilayers on the refractive index sensitivity and catalytic properties of anisotropic gold Nanoparticles, Small 12 (2016) 330–342.
[143] M.H. Rashid, T.K. Mandal, Templateless synthesis of polygonal gold nanoparticles: an unsupported and reusable catalyst with superior activity, Adv. Funct. Mater. 18 (2008) 2261–2271.
[144] C. Novo, A.M. Funston, P. Mulvaney, Direct observation of chemical reactions on single gold nanocrystals using surface plasmon spectroscopy, Nat. Nanotechnol. 3 (2008) 598–602.
[145] S. Kundu, S. Lau, H. Liang, Shape-controlled catalysis by cetyltrimethylammonium bromide terminated gold nanospheres, nanorods, and nanoprisms, J. Phys. Chem. C 113 (2009) 5150–5156.
[146] Q. Zhang, H. Wang, Facet-dependent catalytic activities of Au Nanoparticles enclosed by high-index facets, ACS Catal. 4 (2014) 4027–4033.
[147] H.F. Zarick, W.R. Erwin, J. Aufrecht, A. Coppola, B.R. Rogers, C.L. Pint, R. Bardhan, Morphological modulation of bimetallic nanostructures for accelerated catalysis, J. Mater. Chem. A 2 (2014) 7088–7098.
[148] J. Zeng, Q. Zhang, J. Chen, Y. Xia, A comparison study of the catalytic properties of Au-based nanocages, nanoboxes, and nanoparticles, Nano Lett. 10 (2010) 30–35.
[149] Y.-C. Tsao, S. Rej, C.-Y. Chiu, M.H. Huang, Aqueous phase synthesis of Au–Ag core–shell nanocrystals with tunable shapes and their optical and Catalytic properties, J. Am. Chem. Soc. 136 (2014) 396–404.
[150] Z.W. Seh, S. Liu, S.-Y. Zhang, M.S. Bharathi, H. Ramanarayan, M. Low, K.W. Shah, Y.-W. Zhang, M.-Y. Han, Anisotropic growth of titania onto various gold nanostructures: synthesis, theoretical understanding, and optimization for Catalysis, Angew. Chem. 123 (2011) 10322–10325.
[151] Z.W. Seh, S. Liu, S.-Y. Zhang, K.W. Shah, M.-Y. Han, Synthesis and multiple reuse of eccentric Au@ TiO 2 nanostructures as catalysts, Chem. Commun. 47 (2011) 6689–6691.
[152] B. Wu, D. Liu, S. Mubeen, T.T. Chuong, M. Moskovits, G.D. Stucky, Anisotropic growth of TiO2 onto gold nanorods for plasmon-enhanced hydrogen production from water reduction, J. Am. Chem. Soc. 138 (2016) 1114–1117.
[153] J. Zhao, P. Xu, Y. Li, J. Wu, J. Xue, Q. Zhu, X. Lu, W. Ni, Direct coating of mesoporous titania on CTAB-capped gold nanorods, Nanoscale 8 (2016) 5417–5421.
[154] N. Zhou, L. Polavarapu, N. Gao, Y. Pan, P. Yuan, Q. Wang, Q.-H. Xu, TiO2 coated Au/Ag nanorods with enhanced photocatalytic activity under visible light irradiation, Nanoscale 5 (2013) 4236–4241.
[155] A. Li, P. Zhang, X. Chang, W. Cai, T. Wang, J. Gong, Nanostructures: gold nanorod@ TiO2 yolk-shell nanostructures for visible-light-driven Photocatalytic oxidation of Benzyl alcohol, Small 11 (2015) 1861–1899.
[156] L. Liu, T.D. Dao, R. Kodiyath, Q. Kang, H. Abe, T. Nagao, J. Ye, Plasmonic janus-composite photocatalyst comprising Au and C–TiO2 for enhanced Aerobic oxidation over a broad visible-light range, Adv. Funct. Mater. 24 (2014) 7754–7762.
[157] A.J. van de Glind, P.E. de Jongh, A. Imhof, A. van Blaaderen, K.P. de Jong, Gold Nanorods, Stabilized by a mesoporous silica layer used as catalyst for the selective hydrogenation of cinnamaldehyde, 23rd North American Catalysis Society Meeting, Nam, 2013.
[158] J. Mohanta, S. Satapathy, S. Si, Porous silica-coated gold nanorods: a highly active catalyst for the reduction of 4-nitrophenol, ChemPhysChem 17 (2016) 364–368.
[159] X. Wu, L. Tan, D. Chen, X. Meng, F. Tang, Icosahedral gold-platinum alloy nanocrystals in hollow silica: a highly active and stable catalyst for Ullmann reactions, Chem. Commun. 50 (2014) 539–541.
[160] B. Li, T. Gu, T. Ming, J. Wang, P. Wang, J. Wang, J.C. Yu, (Gold Core)@(Ceria Shell) Nanostructures for plasmon-enhanced catalytic reactions under visible light, ACS Nano 8 (2014) 8152–8162.
[161] J.-H. Wang, M. Chen, Z.-J. Luo, L. Ma, Y.-F. Zhang, K. Chen, L. Zhou, Q.-Q. Wang, Ceria-coated gold nanorods for plasmon-enhanced near-infrared photocatalytic and photoelectrochemical performances, J. Phys. Chem. C 120 (2016) 14805–14812.
[162] M.V. Landau, Sol–Gel Process, Handbook of Heterogeneous Catalysis, Wiley-VCH Verlag GmbH & Co, KGaA, 2008.
[163] F. Schüth, M. Hesse, K.K. Unger, Precipitation and coprecipitation, Handbook of Heterogeneous Catalysis, Wiley-VCH Verlag GmbH & Co, KGaA, 2008.
[164] A. Trovarelli, Catalysis by Ceria and Related Materials, Imperial College Press, 2002.
[165] A. Trovarelli, Catalytic properties of ceria and CeO2-containing materials, Catal. Rev. 38 (1996) 439–520.
[166] S. Matsuda, A. Kato, Titanium oxide based catalysts - a review, Appl. Catal. 8 (1983) 149–165.
[167] L. Kong, W. Chen, D. Ma, Y. Yang, S. Liu, S. Huang, Size control of Au@Cu2O octahedra for excellent photocatalytic performance, J. Mater. Chem. 22 (2012) 719–724.
[168] Y. Li, J. Zhao, W. You, D. Cheng, W. Ni, Gold nanorod@iron oxide core–shell heterostructures: synthesis, characterization, and photocatalytic performance, Nanoscale 9 (2017) 3925–3933.
[169] L. Liu, S. Ouyang, J. Ye, Gold-nanorod-photosensitized titanium dioxide with wide-range visible-light harvesting based on localized surface plasmon resonance, Angew. Chem. Int. Ed. 125 (2013) 6821–6825.
[170] M. Boronat, A. Corma, Oxygen activation on gold nanoparticles: separating the influence of particle size, particle shape and support interaction, Dalton Trans. 39 (2010) 8538–8546.
[171] Y.-C. Pu, G. Wang, K.-D. Chang, Y. Ling, Y.-K. Lin, B.C. Fitzmorris, C.-M. Liu, X. Lu, Y. Tong, J.Z. Zhang, Au nanostructure-decorated TiO2 nanowires exhibiting photoactivity across entire UV-visible region for photoelectrochemical water splitting, Nano Lett. 13 (2013) 3817–3823.
[172] O. Elbanna, S. Kim, M. Fujitsuka, T. Majima, TiO2 mesocrystals composited with gold nanorods for highly efficient visible-NIR-photocatalytic hydrogen production, Nano Energy 35 (2017) 1–8.
[173] I. Levchuk, M. Sillanpää, C. Guillard, D. Gregori, D. Chateau, F. Chaput, F. Lerouge, S. Parola, Enhanced photocatalytic activity through insertion of plasmonic nanostructures into porous TiO2/SiO2 hybrid composite films, J. Catal. 342 (2016) 117–124.
[174] A. Gołąbiewska, A. Malankowska, M. Jarek, W. Lisowski, G. Nowaczyk, S. Jurga, A. Zaleska-Medynska, The effect of gold shape and size on the properties and visible light-induced photoactivity of Au-TiO2, Appl. Catal. B 196 (2016) 27–40.
[175] A. Sousa-Castillo, M. Comesaña-Hermo, B. Rodríguez-González, M. Pérez-Lorenzo, Z. Wang, X.-T. Kong, A.O. Govorov, M.A. Correa-Duarte, Boosting hot electron-driven photocatalysis through anisotropic plasmonic Nanoparticles with hot spots in Au–TiO2 Nanoarchitectures, J. Phys. Chem. C 120 (2016) 11690–11699.
[176] Z. Lou, M. Fujitsuka, T. Majima, Two-dimensional Au-nanoprism/reduced graphene oxide/Pt-nanoframe as plasmonic photocatalysts with multiplasmon modes boosting hot electron transfer for hydrogen generation, J. Phys. Chem. Lett. 8 (2017) 844–849.
[177] W. Ye, J. Yu, Y. Zhou, D. Gao, D. Wang, C. Wang, D. Xue, Green synthesis of Pt–Au dendrimer-like nanoparticles supported on polydopamine-functionalized graphene and their high performance toward 4- nitrophenol reduction, Appl. Catal. B 181 (2016) 371–378.
[178] A. Sanchez-Iglesias, J. Barroso, D.M. Solis, J.M. Taboada, F. Obelleiro, V. Pavlov, A. Chuvilin, M. Grzelczak, Plasmonic substrates comprising gold nanostars efficiently regenerate cofactor molecules, J. Mater. Chem. A 4 (2016) 7045–7052.
[179] W. Wang, J. Zhang, S. Yang, B. Ding, X. Song, Au@Pd core–shell nanobricks with concave structures and their catalysis of ethanol oxidation, ChemSusChem 6 (2013) 1945–1951.
[180] G. Su, H. Jiang, H. Zhu, J.-J. Lv, G. Yang, B. Yan, J.-J. Zhu, Controlled deposition of palladium nanodendrites on the tips of gold nanorods and their enhanced catalytic activity, Nanoscale 9 (2017) 12494–12502.
[181] Y. Chen, Z. Fan, Z. Luo, X. Liu, Z. Lai, B. Li, Y. Zong, L. Gu, H. Zhang, High-yield synthesis of crystal-phase-heterostructured 4H/fcc Au@Pd core–shell nanorods for electrocatalytic ethanol oxidation, Adv. Mater. 29 (2017) 1701331(n/a).
[182] B.K. Jena, C.R. Raj, Synthesis of flower-like gold nanoparticles and their electrocatalytic activity towards the oxidation of methanol and the reduction of oxygen, Langmuir 23 (2007) 4064–4070.
[183] B.K. Jena, C.R. Raj, Shape-controlled synthesis of gold nanoprism and nanoperiwinkles with pronounced electrocatalytic activity, J. Phys. Chem. C 111 (2007) 15146–15153.
[184] B.K. Jena, C.R. Raj, Seedless, surfactantless room temperature synthesis of single crystalline fluorescent gold nanoflowers with pronounced sers and electrocatalytic activity, Chem. Mater. 20 (2008) 3546–3548.
[185] H. Jia, G. Chang, M. Lei, H. He, X. Liu, H. Shu, T. Xia, J. Su, Y. He, Platinum nanoparticles decorated dendrite-like gold nanostructure on glassy carbon electrodes for enhancing electrocatalysis performance to glucose oxidation, Appl. Surf. Sci. 384 (2016) 58–64.
[186] V. Kravets, F. Schedin, A. Grigorenko, Extremely narrow plasmon resonances based on diffraction coupling of localized plasmons in arrays of metallic nanoparticles, Phys. Rev. Lett. 101 (2008) 087403.
[187] A. Wittstock, V. Zielasek, J. Biener, C.M. Friend, M. Bäumer, Nanoporous gold catalysts for selective gas-phase oxidative coupling of methanol at low temperature, Science 327 (2010) 319–322.
[188] X. Bai, Y. Gao, H.-g. Liu, L. Zheng, Synthesis of amphiphilic ionic liquids terminated gold nanorods and their superior catalytic activity for the reduction of nitro compounds, J. Phys. Chem. C 113 (2009) 17730–17736.
[189] R. Kaur, B. Pal, Improved surface properties and catalytic activity of anisotropic shapes of photoetched Au nanostructures formed by variable energy laser exposure, J. Mol. Catal. A 395 (2014) 7–15.
[190] R. Kaur, B. Pal, Physicochemical and catalytic properties of Au nanorods micro-assembled in solvents of varying dipole moment and refractive index, Mater. Res. Bull. 62 (2015) 11–18.
[191] W. Xiong, D. Sikdar, L.W. Yap, P. Guo, M. Premaratne, X. Li, W. Cheng, Matryoshka-caged gold nanorods: Synthesis, plasmonic properties, and catalytic activity, Nano Res. 9 (2016) 415–423.
[192] M.A. Mahmoud, M.A. El-Sayed, Time dependence and signs of the shift of the surface plasmon resonance frequency in nanocages elucidate the nanocatalysis mechanism in hollow nanoparticles, Nano Lett. 11 (2011) 946–953.
[193] M.A. Bhosale, D.R. Chenna, J.P. Ahire, B.M. Bhanage, Morphological study of microwave-assisted facile synthesis of gold nanoflowers/nanoparticles in aqueous medium and their catalytic application for reduction of p-nitrophenol to p-aminophenol, RSC Adv. 5 (2015) 52817–52823.
[194] M.A. Bhosale, S.R. Gupta, B.M. Bhanage, Size controlled synthesis of gold nanostructures using ketones and their catalytic activity towards reduction of p-nitrophenol, Polyhedron 120 (2016) 96–102.
[195] M. Guo, J. He, Y. Li, S. Ma, X. Sun, One-step synthesis of hollow porous gold nanoparticles with tunable particle size for the reduction of 4-nitrophenol, J. Hazard. Mater. 310 (2016) 89–97.
[196] T. Ma, F. Liang, R. Chen, S. Liu, H. Zhang, Synthesis of Au-Pd bimetallic nanoflowers for catalytic reduction of 4-nitrophenol, Nanomaterials 7 (2017) 239.
[197] F. de Oliveira, L. Nascimento, C. Calado, M. Meneghetti, M. da Silva, Aqueous-phase catalytic chemical reduction of p-nitrophenol employing soluble gold nanoparticles with different shapes, Catalysts 6 (2016) 215.
[198] Z. Zheng, T. Tachikawa, T. Majima, Plasmon-enhanced formic acid dehydrogenation using anisotropic Pd–Au nanorods studied at the single-particle level, J. Am. Chem. Soc. 137 (2015) 948–957.

[199] W. Hu, H. Chen, C.M. Li, One-step synthesis of monodisperse gold dendrite@polypyrrole core-shell nanoparticles and their enhanced catalytic durability, Colloid Polym. Sci. 293 (2014) 505–512.
[200] R. Kodiyath, M. Manikandan, L. Liu, G.V. Ramesh, S. Koyasu, M. Miyauchi, Y. Sakuma, T. Tanabe, T. Gunji, T. Duy Dao, S. Ueda, T. Nagao, J. Ye, H. Abe, Visible-light photodecomposition of acetaldehyde by TiO2-coated gold nanocages: plasmon-mediated hot electron transport via defect states, Chem. Commun. 50 (2014) 15553–15556.
[201] S. Hebié, L. Cornu, T.W. Napporn, J. Rousseau, B.K. Kokoh, Insight on the surface structure effect of free gold nanorods on glucose electrooxidation, J. Phys. Chem. C 117 (2013) 9872–9880.
[202] Q. Zhang, X. Guo, Z. Liang, J. Zeng, J. Yang, S. Liao, Hybrid PdAg alloy-Au nanorods: controlled growth, optical properties and electrochemical catalysis, Nano Res. 6 (2013) 571–580.
[203] S. Karra, M. Wooten, W. Griffith, W. Gorski, Morphology of gold nanoparticles and electrocatalysis of glucose oxidation, Electrochim. Acta 218 (2016) 8–14.
[204] M. Shanmugam, K. Kim, Electrodeposited gold dendrites at reduced graphene oxide as an electrocatalyst for nitrite and glucose oxidation, J. Electroanal. Chem. 776 (2016) 82–92.
[205] A. Li, Y. Chen, W. Duan, C. Wang, K. Zhuo, Shape-controlled electrochemical synthesis of Au nanocrystals in reline: control conditions and electrocatalytic oxidation of ethylene glycol, RSC Adv. 7 (2017) 19694–19700.
[206] H. Xu, B. Yan, J. Wang, K. Zhang, S. Li, Z. Xiong, C. Wang, Y. Shiraishi, Y. Du, P. Yang, Self-supported porous 2D AuCu triangular nanoprisms as model electrocatalysts for ethylene glycol and glycerol oxidation, J. Mater. Chem. A 5 (2017) 15932–15939.
[207] S. Momeni, A. Safavi, R. Ahmadi, I. Nabipour, Gold nanosheets synthesized with red marine alga Actinotrichia fragilis as efficient electrocatalysts toward formic acid oxidation, RSC Adv. 6 (2016) 75152–75161.
[208] M. Xu, Y. Sui, G. Xiao, X. Yang, Y. Wei, B. Zou, Kinetically controlled synthesis of nanoporous Au and its enhanced electrocatalytic activity for glucose-based biofuel cells, Nanoscale 9 (2017) 2514–2520.
[209] Q.-L. Wang, R. Fang, L.-L. He, J.-J. Feng, J. Yuan, A.-J. Wang, Bimetallic PdAu alloyed nanowires: rapid synthesis via oriented attachment growth and their high electrocatalytic activity for methanol oxidation reaction, J. Alloys Compd. 684 (2016) 379–388.
[210] Z. Fan, Z. Luo, X. Huang, B. Li, Y. Chen, J. Wang, Y. Hu, H. Zhang, Synthesis of 4H/fcc Noble multimetallic nanoribbons for electrocatalytic hydrogen evolution reaction, J. Am. Chem. Soc. 138 (2016) 1414–1419.
[211] X. Yu, F. Liu, J. Bi, B. Wang, S. Yang, Improving the plasmonic efficiency of the Au nanorod-semiconductor photocatalysis toward water reduction by constructing a unique hot-dog nanostructure, Nano Energy 33 (2017) 469–475.
[212] C.Y. Chiu, P.J. Chung, K.U. Lao, C.W. Liao, M.H. Huang, Facet-dependent catalytic activity of gold nanocubes, octahedra, and rhombic dodecahedra toward 4-nitroaniline reduction, J. Phys. Chem. C 116 (2012) 23757–23763.
[213] J. Lin, H. Abroshan, C. Liu, M. Zhu, G. Li, M. Haruta, Sonogashira cross-coupling on the Au(1 1 1) and Au(1 0 0) facets of gold nanorod catalysts: experimental and computational investigation, J. Catal. 330 (2015) 354–361.
[214] Y. Qin, Y. Song, N. Sun, N. Zhao, M. Li, L. Qi, Ionic liquid-assisted growth of single-crystalline dendritic gold nanostructures with a three-fold symmetry, Chem. Mater. 20 (2008) 3965–3972.
[215] T. Huang, F. Meng, L. Qi, Controlled synthesis of dendritic gold nanostructures assisted by supramolecular complexes of surfactant with cyclodextrin, Langmuir 26 (2010) 7582–7589.
[216] X. Xu, J. Jia, X. Yang, S. Dong, A templateless, surfactantless, simple electrochemical route to a dendritic gold nanostructure and its application to oxygen reduction, Langmuir 26 (2010) 7627–7631.
[217] W. Ye, J. Yan, Q. Ye, F. Zhou, Template-free and direct electrochemical deposition of hierarchical dendritic gold microstructures: growth and their multiple applications, J. Phys. Chem. C 114 (2010) 15617–15624.
[218] S. Kumar-Krishnan, E. Prokhorov, O. Arias de Fuentes, M. Ramirez, N. Bogdanchikova, I.C. Sanchez, J.D. Mota-Morales, G. Luna-Barcenas, Temperature-induced Au nanostructure synthesis in a nonaqueous deep-eutectic solvent for high performance electrocatalysis, J. Mater. Chem. A 3 (2015) 15869–15875.
[219] H. Sun, S. Zeng, Q. He, P. She, K. Xu, Z. Liu, Spiky TiO 2 /Au nanorod plasmonic photocatalysts with enhanced visible-light photocatalytic activity, Dalton Trans. 46 (2017) 3887–3894.
[220] F. Han, X. Mao, Q.-H. Xu, Flower-like Au/Ag/TiO2 nanocomposites with enhanced photocatalytic efficiency under visible light irradiation, Sci.China Chem. 60 (2017) 521–527.
[221] M.C. Ortega-Liebana, J.L. Hueso, R. Arenal, J. Santamaria, Titania-coated gold nanorods with expanded photocatalytic response. enzyme-like glucose oxidation under near-infrared illumination, Nanoscale 9 (2017) 1787–1792.
[222] Y. Wang, L. Polavarapu, L.M. Liz-Marzán, Reduced graphene oxide-supported gold nanostars for improved sers sensing and drug delivery, ACS Appl. Mater. Interfaces 9 (2014) 21798–21805.
[223] P. Zhang, M. Fujitsuka, T. Majima, Hot electron-driven hydrogen evolution using anisotropic gold nanostructure assembled monolayer MoS2, Nanoscale 9 (2017) 1520–1526.
[224] K. Woan, G. Pyrgiotakis, W. Sigmund, Photocatalytic Carbon-Nanotube–TiO2 composites, Adv. Mater. 21 (2009) 2233–2239.
[225] X. Wang, S. Blechert, M. Antonietti, Polymeric graphitic carbon nitride for heterogeneous photocatalysis, ACS Catal. 2 (2012) 1596–1606.
[226] X. Li, J. Yu, S. Wageh, A.A. Al-Ghamdi, J. Xie, Graphene in photocatalysis: a review, Small 12 (2016) 6640–6696.
[227] W. Jian, H. Hengming, X. Zhongzi, K. Jiahui, L. Chunhua, The potential of Carbon-Based materials for photocatalytic application, Curr. Org. Chem. 18 (2014) 1346–1364.
[228] S. Cao, J. Low, J. Yu, M. Jaroniec, Polymeric photocatalysts based on graphitic Carbon Nitride, Adv. Mater. 27 (2015) 2150–2176.
[229] J. Liu, R. Liu, H. Li, W. Kong, H. Huang, Y. Liu, Z. Kang, Au nanoparticles in carbon nanotubes with high photocatalytic activity for hydrocarbon selective oxidation, Dalton Trans. 43 (2014) 12982–12988.
[230] S. Kaur, V. Bhalla, M. Kumar, Facile decoration of multiwalled carbon nanotubes with hetero-oligophenylene stabilized-gold nanoparticles: visible light photocatalytic degradation of rhodamine b dye, ACS Appl. Mater. Interfaces 7 (2015) 16617–16624.
[231] H.-C. Hsu, I. Shown, H.-Y. Wei, Y.-C. Chang, H.-Y. Du, Y.-G. Lin, C.-A. Tseng, C.-H. Wang, L.-C. Chen, Y.-C. Lin, K.-H. Chen, Graphene oxide as a promising photocatalyst for CO2 to methanol conversion, Nanoscale 5 (2013) 262–268.
[232] M. Rycenga, C.M. Cobley, J. Zeng, W. Li, C.H. Moran, Q. Zhang, D. Qin, Y. Xia, Controlling the synthesis and assembly of silver nanostructures for plasmonic applications, Chem. Rev. 111 (2011) 3669–3712.
[233] C. Noguez, Surface plasmons on metal nanoparticles: the influence of shape and physical environment, J. Phys. Chem. C 111 (2007) 3806–3819.
[234] Y. Yin, Y. Yang, L. Zhang, Y. Li, Z. Li, W. Lei, Y. Ma, Z. Huang, Facile synthesis of Au/Pd nano-dogbones and their plasmon-enhanced visible-to-NIR light photocatalytic performance, RSC Adv. 7 (2017) 36923–36928.
[235] X. Zhu, H. Jia, X.M. Zhu, S. Cheng, X. Zhuo, F. Qin, Z. Yang, J. Wang, Selective Pd deposition on au nanobipyramids and Pd site-dependent plasmonic photocatalytic activity, Adv. Funct. Mater. 27 (2017) 1700016.
[236] Y. Kang, Q. Xue, R. Peng, P. Jin, J. Zeng, J. Jiang, Y. Chen, Bimetallic aurh nanodendrites consisting of au icosahedron cores and atomically ultrathin rh nanoplate shells: synthesis and light-enhanced catalytic activity, NPG Asia Mater. 9 (2017).
[237] Y. Wenpeng, W. Ke, Y. Weimin, W. Hailing, L. Xianglong, Q. Lihua, Y. Tianshui, L. Zengquan, Z. Xiangji, B. Godfrey Okumu, Y. Songliu, J. Yingtao, Y. Zhilin, Nanoporous au-ag shell with fast kinetics: integrating chemical and plasmonic catalysis, Nanotechnology 28 (2017) 425704.
[238] J. Kou, C. Lu, J. Wang, Y. Chen, Z. Xu, R.S. Varma, Selectivity enhancement in heterogeneous photocatalytic transformations, Chem. Rev. 117 (2017) 1445–1514.
[239] R. Shukla, V. Bansal, M. Chaudhary, A. Basu, R.R. Bhonde, M. Sastry, Biocompatibility of gold nanoparticles and their endocytotic fate inside the cellular compartment: a microscopic overview, Langmuir 21 (2005) 10644–10654.
[240] M. Sharifi, S.H. Hosseinali, A.A. Saboury, E. Szegezdi, M. Falahati, Involvement of planned cell death of necroptosis in cancer treatment by nanomaterials: recent advances and future perspectives, J. Control. Release 299 (2019) 121–137.
[241] Y.-Y. Ma, K.-T. Jin, S.-B. Wang, H.-J. Wang, X.-M. Tong, D.-S. Huang, X.-Z. Mou, Molecular imaging of cancer with nanoparticle-based theranostic probes, Contrast Media Mol. Imaging 2017 (2017).
[242] M. Sarkis, E. Ghanem, K. Rahme, Jumping on the bandwagon: a review on the versatile applications of gold nanostructures in Prostate Cancer, Int. J. Mol. Sci. 20 (2019) 970.
[243] D. Kim, Y.Y. Jeong, S. Jon, A drug-loaded aptamer− gold nanoparticle bioconjugate for combined CT imaging and therapy of prostate cancer, ACS Nano 4 (2010) 3689–3696.
[244] C.-H. Li, T.-R. Kuo, H.-J. Su, W.-Y. Lai, P.-C. Yang, J.-S. Chen, D.-Y. Wang, Y.-C. Wu, C.-C. Chen, Fluorescence-guided probes of aptamer-targeted gold nanoparticles with computed tomography imaging accesses for in vivo tumor resection, Sci. Rep. 5 (2015) 15675.
[245] S. Khademi, S. Sarkar, S. Kharrazi, S.M. Amini, A. Shakeri-Zadeh, M.R. Ay, H. Ghadiri, Evaluation of size, morphology, concentration, and surface effect of gold nanoparticles on X-ray attenuation in computed tomography, Phys. Medica 45 (2018) 127–133.
[246] Y. Zhao, W. Liu, Y. Tian, Z. Yang, X. Wang, Y. Zhang, Y. Tang, S. Zhao, C. Wang, Y. Liu, J. Sun, Z. Teng, S. Wang, G. Lu, Anti-EGFR peptide-conjugated triangular gold nanoplates for computed tomography/photoacoustic imaging-Guided photothermal therapy of non-small Cell Lung Cancer, ACS Appl. Mater. Interfaces 10 (2018) 16992–17003.
[247] R. Popovtzer, A. Agrawal, N.A. Kotov, A. Popovtzer, J. Balter, T.E. Carey, R. Kopelman, Targeted gold nanoparticles enable molecular CT imaging of cancer, Nano Lett. 8 (2008) 4593–4596.
[248] N. Manohar, F.J. Reynoso, P. Diagaradjane, S. Krishnan, S.H. Cho, Quantitative imaging of gold nanoparticle distribution in a tumor-bearing mouse using benchtop x-ray fluorescence computed tomography, Sci. Rep. 6 (2016) 22079.
[249] F.J. Nicholls, M.W. Rotz, H. Ghuman, K.W. MacRenaris, T.J. Meade, M. Modo, DNA–gadolinium–gold nanoparticles for in vivo T1 MR imaging of transplanted human neural stem cells, Biomaterials 77 (2016) 291–306.
[250] R.J. Holbrook, N. Rammohan, M.W. Rotz, K.W. MacRenaris, A.T. Preslar, T.J. Meade, Gd (III)-dithiolane gold nanoparticles for T 1-weighted magnetic resonance imaging of the pancreas, Nano Lett. 16 (2016) 3202–3209.
[251] N. Rammohan, R.J. Holbrook, M.W. Rotz, K.W. MacRenaris, A.T. Preslar, C.E. Carney, V. Reichova, T.J. Meade, Gd (III)-gold nanoconjugates provide remarkable cell labeling for high field magnetic resonance imaging, Bioconjug. Chem. 28 (2016) 153–160.
[252] H. Ke, J. Wang, S. Tong, Y. Jin, S. Wang, E. Qu, G. Bao, Z. Dai, Gold nanoshelled liquid perfluorocarbon magnetic nanocapsules: a nanotheranostic platform for bimodal ultrasound/magnetic resonance imaging guided photothermal tumor ablation, Theranostics 4 (2014) 12.
[253] L. Henderson, O. Neumann, C. Kaffes, R. Zhang, V. Marangoni, M.K. Ravoori,

V. Kundra, J. Bankson, P. Nordlander, N.J. Halas, routes to potentially safer T1 magnetic resonance imaging contrast in a compact plasmonic nanoparticle with enhanced fluorescence, ACS Nano 12 (2018) 8214–8223.
[254] Y. Jin, J. Wang, H. Ke, S. Wang, Z. Dai, Graphene oxide modified PLA microcapsules containing gold nanoparticles for ultrasonic/CT bimodal imaging guided photothermal tumor therapy, Biomaterials 34 (2013) 4794–4802.
[255] H. Moon, D. Kumar, H. Kim, C. Sim, J.-H. Chang, J.-M. Kim, H. Kim, D.-K. Lim, Amplified photoacoustic performance and enhanced photothermal stability of reduced graphene oxide coated gold nanorods for sensitive photoacoustic imaging, ACS Nano 9 (2015) 2711–2719.
[256] L. Xu, C. Wan, J. Du, H. Li, X. Liu, H. Yang, F. Li, Synthesis, characterization, and in vitro evaluation of targeted gold nanoshelled poly (d, l-lactide-co-glycolide) nanoparticles carrying anti p53 antibody as a theranostic agent for ultrasound contrast imaging and photothermal therapy, J. Biomater. Sci. Polym. Ed. 28 (2017) 415–430.
[257] F. Zhao, J. Zhou, X. Su, Y. Wang, X. Yan, S. Jia, B. Du, A Smart responsive dual aptamers-targeted bubble-generating nanosystem for Cancer triplex therapy and ultrasound imaging, Small 13 (2017) 1603990.
[258] S. Goel, F. Chen, R. Hernandez, S. Graves, R. Nickles, W. Cai, Dynamic PET imaging of renal clearable gold nanoparticles, J. Nucl. Med. 57 (2016) 1094.
[259] C. Tsoukalas, G. Laurent, G.J. Sánchez, T. Tsotakos, R. Bazzi, D. Stellas, C. Anagnostopoulos, L. Moulopoulos, V. Koutoulidis, M. Paravatou-Petsotas, Initial in Vitro and in Vivo Assessment of Au@ DTDTPA-RGD Nanoparticles for Gd-MRI and 68Ga-PET Dual Modality Imaging, in: EJNMMI Physics, Nature Publishing Group, 2015, p. A89.
[260] M. Pretze, N.P. van der Meulen, C. Wängler, R. Schibli, B. Wängler, Targeted 64Cu-labeled gold nanoparticles for dual imaging with positron emission tomography and optical imaging, J. Label. Compd. Radiopharm. (2019) 0.
[261] S.B. Lee, Y. Li, I.-K. Lee, S.J. Cho, S.K. Kim, S.-W. Lee, J. Lee, Y.H. Jeon, In vivo detection of sentinel lymph nodes with PEGylated crushed gold shell @ radioactive core nanoballs, J. Ind. Eng. Chem. 70 (2019) 196–203.
[262] M.A. Wall, T.M. Shaffer, S. Harmsen, D.-F. Tschaharganeh, C.-H. Huang, S.W. Lowe, C.M. Drain, M.F. Kircher, Chelator-free radiolabeling of SERRS nanoparticles for whole-body PET and intraoperative raman imaging, Theranostics 7 (2017) 3068.
[263] K.C. Black, W.J. Akers, G. Sudlow, B. Xu, R. Laforest, S. Achilefu, Dual-radiolabeled nanoparticle SPECT probes for bioimaging, Nanoscale 7 (2015) 440–444.
[264] X. Li, C. Wang, H. Tan, L. Cheng, G. Liu, Y. Yang, Y. Zhao, Y. Zhang, Y. Li, C. Zhang, Gold nanoparticles-based SPECT/CT imaging probe targeting for vulnerable atherosclerosis plaques, Biomaterials 108 (2016) 71–80.
[265] B. Zhou, R. Wang, F. Chen, L. Zhao, P. Wang, X. Li, I. Bányai, Q. Ouyang, X. Shi, M. Shen, 99mTc-labeled RGD–polyethylenimine conjugates with entrapped gold nanoparticles in the cavities for dual-mode SPECT/CT imaging of Hepatic Carcinoma, ACS Appl. Mater. Interfaces 10 (2018) 6146–6154.
[266] L. Zhao, Y. Li, J. Zhu, N. Sun, N. Song, Y. Xing, H. Huang, J. Zhao, Chlorotoxin peptide-functionalized polyethylenimine-entrapped gold nanoparticles for glioma SPECT/CT imaging and radionuclide therapy, J. Nanobiotechnol. 17 (2019) 30.
[267] Y. Zhao, B. Pang, H. Luehmann, L. Detering, X. Yang, D. Sultan, S. Harpstrite, V. Sharma, C.S. Cutler, Y. Xia, Gold nanoparticles doped with 199Au atoms and their use for targeted cancer imaging by SPECT, Adv. Healthc. Mater. 5 (2016) 928–935.
[268] X. Huang, I.H. El-Sayed, W. Qian, M.A. El-Sayed, Cancer cell imaging and photothermal therapy in the near-infrared region by using gold nanorods, J. Am. Chem. Soc. 128 (2006) 2115–2120.
[269] I.H. El-Sayed, X. Huang, M.A. El-Sayed, Surface plasmon resonance scattering and absorption of anti-EGFR antibody conjugated gold nanoparticles in cancer diagnostics: applications in oral cancer, Nano Lett. 5 (2005) 829–834.
[270] V. Mani, B.V. Chikkaveeraiah, V. Patel, J.S. Gutkind, J.F. Rusling, Ultrasensitive immunosensor for cancer biomarker proteins using gold nanoparticle film electrodes and multienzyme-particle amplification, ACS Nano 3 (2009) 585–594.
[271] X. Huang, I.H. El-Sayed, W. Qian, M.A. El-Sayed, Cancer cells assemble and align gold nanorods conjugated to antibodies to produce highly enhanced, sharp, and polarized surface raman spectra: a potential cancer diagnostic marker, Nano Lett. 7 (2007) 1591–1597.
[272] A. Ambrosi, F. Airó, A. Merkoçi, Enhanced gold nanoparticle based ELISA for a breast cancer biomarker, Anal. Chem. 82 (2010) 1151–1156.
[273] H. Suo, Z. Gao, L. Xu, C. Xu, D. Yu, X. Xiang, H. Huang, Y. Hu, Synthesis of functional ionic liquid modified magnetic chitosan nanoparticles for porcine pancreatic lipase immobilization, Mater. Sci. Eng. 96 (2019) 356–364.
[274] H. Jing, Q. Zhang, N. Large, C. Yu, D.A. Blom, P. Nordlander, H. Wang, Tunable plasmonic nanoparticles with catalytically active high-index facets, Nano Lett. 14 (2014) 3674–3682.
[275] X. Huang, M.A. El-Sayed, Gold nanoparticles: optical properties and implementations in cancer diagnosis and photothermal therapy, J. Adv. Res. 1 (2010) 13–28.
[276] Y. Cheng, J.D. Meyers, A.-M. Broome, M.E. Kenney, J.P. Basilion, C. Burda, Deep penetration of a PDT drug into tumors by noncovalent drug-gold nanoparticle conjugates, J. Am. Chem. Soc. 133 (2011) 2583–2591.
[277] Y. Cheng, T.L. Doane, C.H. Chuang, A. Ziady, C. Burda, Near infrared light-triggered drug generation and release from gold nanoparticle carriers for photodynamic therapy, Small 10 (2014) 1799–1804.
[278] J.D. Meyers, Y. Cheng, A.M. Broome, R.S. Agnes, M.D. Schluchter, S. Margevicius, X. Wang, M.E. Kenney, C. Burda, J.P. Basilion, Peptide-targeted gold nanoparticles for photodynamic therapy of brain cancer, Part. Part. Syst. Charact. 32 (2015) 448–457.
[279] S.R. Panikkanvalappil, N. Hooshmand, M.A. El-Sayed, Intracellular assembly of nuclear-targeted gold nanosphere enables selective plasmonic photothermal therapy of cancer by shifting their absorption wavelength toward near-infrared region, Bioconjug. Chem. 28 (2017) 2452–2460.
[280] M.R. Ali, Y. Wu, Y. Tang, H. Xiao, K. Chen, T. Han, N. Fang, R. Wu, M.A. El-Sayed, Targeting cancer cell integrins using gold nanorods in photothermal therapy inhibits migration through affecting cytoskeletal proteins, Proc. Natl. Acad. Sci. 114 (2017) E5655–E5663.
[281] M.R. Ali, M.A. Rahman, Y. Wu, T. Han, X. Peng, M.A. Mackey, D. Wang, H.J. Shin, Z.G. Chen, H. Xiao, Efficacy, long-term toxicity, and mechanistic studies of gold nanorods photothermal therapy of cancer in xenograft mice, Proc. Natl. Acad. Sci. 114 (2017) E3110–e3118 201619302.
[282] A.S. Abdoon, E.A. Al-Ashkar, O.M. Kandil, A.M. Shaban, H.M. Khaled, M.A. El Sayed, M.M. El Shaer, A.H. Shaalan, W.H. Eisa, A.A.G. Eldin, Efficacy and toxicity of plasmonic photothermal therapy (PPTT) using gold nanorods (GNRs) against mammary tumors in dogs and cats, Nanomedicine 12 (2016) 2291–2297.
[283] M.R. Ali, Y. Wu, T. Han, X. Zang, H. Xiao, Y. Tang, R. Wu, F.M. Fernández, M.A. El-Sayed, Simultaneous time-dependent surface-enhanced raman spectroscopy, metabolomics, and proteomics reveal cancer cell death mechanisms associated with gold nanorod photothermal therapy, J. Am. Chem. Soc. 138 (2016) 15434–15442.
[284] M.R. Ali, H.R. Ali, C.R. Rankin, M.A. El-Sayed, Targeting heat shock protein 70 using gold nanorods enhances cancer cell apoptosis in low dose plasmonic photothermal therapy, Biomaterials 102 (2016) 1–8.
[285] M.A. Rahman, M.R. Ali, Z. Zhao, G.Z. Chen, M.A. El-Sayed, D.M. Shin, Optimizing the Antitumor Efficacy of AuNR-Assisted Plasmonic Photothermal Therapy and its Molecular Impact, AACR, 2016.
[286] M. Aioub, M.A. El-Sayed, A real-time surface enhanced raman spectroscopy study of plasmonic photothermal cell death using targeted gold nanoparticles, J. Am. Chem. Soc. 138 (2016) 1258–1264.
[287] Y. Cheng, A.C. Samia, J.D. Meyers, I. Panagopoulos, B. Fei, C. Burda, Highly efficient drug delivery with gold nanoparticle vectors for in vivo photodynamic therapy of cancer, J. Am. Chem. Soc. 130 (2008) 10643–10647.
[288] Y. Cheng, A.C. Samia, J. Li, M.E. Kenney, A. Resnick, C. Burda, Delivery and efficacy of a cancer drug as a function of the bond to the gold nanoparticle surface, Langmuir 26 (2009) 2248–2255.
[289] T.L. Doane, Y. Cheng, A. Babar, R.J. Hill, C. Burda, Electrophoretic mobilities of PEGylated gold NPs, J. Am. Chem. Soc. 132 (2010) 15624–15631.
[290] Y. Cheng, J.D. Meyers, R.S. Agnes, T.L. Doane, M.E. Kenney, A.M. Broome, C. Burda, J.P. Basilion, Addressing brain tumors with targeted gold nanoparticles: a new gold standard for hydrophobic drug delivery? Small 7 (2011) 2301–2306.
[291] H. Liu, T.L. Doane, Y. Cheng, F. Lu, S. Srinivasan, J.J. Zhu, C. Burda, Control of surface ligand density on PEGylated gold nanoparticles for optimized cancer cell uptake, Part. Part. Syst. Charact. 32 (2015) 197–204.
[292] I.H. El-Sayed, X. Huang, M.A. El-Sayed, Selective laser photo-thermal therapy of epithelial carcinoma using anti-EGFR antibody conjugated gold nanoparticles, Cancer Lett. 239 (2006) 129–135.
[293] X. Huang, P.K. Jain, I.H. El-Sayed, M.A. El-Sayed, Determination of the minimum temperature required for selective photothermal destruction of cancer cells with the use of immunotargeted gold nanoparticles, Photochem. Photobiol. 82 (2006) 412–417.
[294] J. Nam, N. Won, H. Jin, H. Chung, S. Kim, pH-induced aggregation of gold nanoparticles for photothermal cancer therapy, J. Am. Chem. Soc. 131 (2009) 13639–13645.
[295] X. Cheng, R. Sun, L. Yin, Z. Chai, H. Shi, M. Gao, Light-triggered assembly of gold nanoparticles for photothermal therapy and photoacoustic imaging of tumors in vivo, Adv. Mater. 29 (2017) 1604894.
[296] Y. Hu, X. Liu, Z. Cai, H. Zhang, H. Gao, W. He, P. Wu, C. Cai, J.-J. Zhu, Z. Yan, Enhancing the plasmon resonance absorption of multibranched gold nanoparticles in the near-infrared region for photothermal cancer therapy: theoretical predictions and experimental verification, Chem. Mater. 31 (2019) 471–482.
[297] R.K. Visaria, R.J. Griffin, B.W. Williams, E.S. Ebbini, G.F. Paciotti, C.W. Song, J.C. Bischof, Enhancement of tumor thermal therapy using gold nanoparticle–assisted tumor necrosis factor-α delivery, Mol. Cancer Ther. 5 (2006) 1014–1020.
[298] J. Shao, R.J. Griffin, E.I. Galanzha, J.-W. Kim, N. Koonce, J. Webber, T. Mustafa, A.S. Biris, D.A. Nedosekin, V.P. Zharov, Photothermal nanodrugs: potential of TNF-gold nanospheres for cancer theranostics, Sci. Rep. 3 (2013) 1293.
[299] R. Pang, M. Li, C. Zhang, Degradation of phenolic compounds by laccase immobilized on carbon nanomaterials: diffusional limitation investigation, Talanta 131 (2015) 38–45.
[300] S. Nikzad, G. Mahmoudi, P. Amini, M. Baradaran-Ghahfarokhi, A. Vahdat-Moaddab, S.M. Sharafi, L. Hojaji-Najafabadi, A. Hosseinzadeh, Effects of radiofrequency radiation in the presence of gold nanoparticles for the treatment of renal cell carcinoma, J. Ren. Inj. Prev. 6 (2017) 103.
[301] E.S. Day, L.R. Bickford, J.H. Slater, N.S. Riggall, R.A. Drezek, J.L. West, Antibody-conjugated gold-gold sulfide nanoparticles as multifunctional agents for imaging and therapy of breast cancer, Int. J. Nanomedicine 5 (2010) 445.
[302] G. Von Maltzahn, J.-H. Park, A. Agrawal, N.K. Bandaru, S.K. Das, M.J. Sailor, S.N. Bhatia, Computationally guided photothermal tumor therapy using long-circulating gold nanorod antennas, Cancer Res. 69 (2009) 3892–3900.
[303] Z. Zhang, J. Wang, X. Nie, T. Wen, Y. Ji, X. Wu, Y. Zhao, C. Chen, Near infrared laser-induced targeted cancer therapy using thermoresponsive polymer encapsulated gold nanorods, J. Am. Chem. Soc. 136 (2014) 7317–7326.
[304] N. Larson, A. Gormley, N. Frazier, H. Ghandehari, Synergistic enhancement of cancer therapy using a combination of heat shock protein targeted HPMA copolymer–drug conjugates and gold nanorod induced hyperthermia, J. Control. Release 170 (2013) 41–50.

[305] N. Frazier, R. Robinson, A. Ray, H. Ghandehari, Effects of heating temperature and duration by gold nanorod mediated plasmonic photothermal therapy on copolymer accumulation in tumor tissue, Mol. Pharm. 12 (2015) 1605–1614.
[306] S. Parida, C. Maiti, Y. Rajesh, K.K. Dey, I. Pal, A. Parekh, R. Patra, D. Dhara, P.K. Dutta, M. Mandal, Gold nanorod embedded reduction responsive block copolymer micelle-triggered drug delivery combined with photothermal ablation for targeted cancer therapy, Biochim. Biophys. Acta 1861 (2017) 3039–3052.
[307] M. Sharifi, M.R. Avadi, F. Attar, F. Dashtestani, H. Ghorchian, S.M. Rezayat, A.A. Saboury, M. Falahati, Cancer diagnosis using nanomaterials based electrochemical nanobiosensors, Biosens. Bioelectron. 126 (2019) 773–784.
[308] J. Wu, X. Wang, Q. Wang, Z. Lou, S. Li, Y. Zhu, L. Qin, H. Wei, Nanomaterials with enzyme-like characteristics (nanozymes): next-generation artificial enzymes (II), Chem. Soc. Rev. 48 (2019) 1004–1076.
[309] J. Song, X. Yang, O. Jacobson, L. Lin, P. Huang, G. Niu, Q. Ma, X. Chen, Sequential drug release and enhanced photothermal and photoacoustic effect of hybrid reduced GO-loaded ultrasmall gold nanorod vesicles for cancer therapy, ACS Nano 9 (2015) 9199–9209.
[310] D.V. Peralta, Z. Heidari, S. Dash, M.A. Tarr, Hybrid paclitaxel and gold nanorod-loaded human serum albumin nanoparticles for simultaneous chemotherapeutic and photothermal therapy on 4T1 breast cancer cells, ACS Appl. Mater. Interfaces 7 (2015) 7101–7111.
[311] P. Manivasagan, S.W. Jun, V.T. Nguyen, N.T.P. Truong, G. Hoang, S. Mondal, M. Santha Moorthy, H. Kim, T.T. Vy Phan, V.H.M. Doan, C.-S. Kim, J. Oh, A multifunctional near-infrared laser-triggered drug delivery system using folic acid conjugated chitosan oligosaccharide encapsulated gold nanorods for targeted chemo-photothermal therapy, J. Mater. Chem. B 7 (2019) 3811–3825.
[312] G. Terentyuk, E. Panfilova, V. Khanadeev, D. Chumakov, E. Genina, A. Bashkatov, V. Tuchin, A. Bucharskaya, G. Maslyakova, N. Khlebtsov, Gold nanorods with a hematoporphyrin-loaded silica shell for dual-modality photodynamic and photothermal treatment of tumors in vivo, Nano Res. 7 (2014) 325–337.
[313] B. Wang, J.-H. Wang, Q. Liu, H. Huang, M. Chen, K. Li, C. Li, X.-F. Yu, P.K. Chu, Rose-bengal-conjugated gold nanorods for in vivo photodynamic and photothermal oral cancer therapies, Biomaterials 35 (2014) 1954–1966.
[314] J. Song, X. Yang, O. Jacobson, P. Huang, X. Sun, L. Lin, X. Yan, G. Niu, Q. Ma, X. Chen, Ultrasmall gold nanorod vesicles with enhanced tumor accumulation and fast excretion from the body for cancer therapy, Adv. Mater. 27 (2015) 4910–4917.
[315] N. Wang, Z. Zhao, Y. Lv, H. Fan, H. Bai, H. Meng, Y. Long, T. Fu, X. Zhang, W. Tan, Gold nanorod-photosensitizer conjugate with extracellular pH-driven tumor targeting ability for photothermal/photodynamic therapy, Nano Res. 7 (2014) 1291–1301.
[316] M. Aioub, S.R. Panikkanvalappil, M.A. El-Sayed, Platinum-coated gold nanorods: efficient reactive oxygen scavengers that prevent oxidative damage toward healthy, untreated cells during plasmonic photothermal therapy, ACS Nano 11 (2017) 579–586.
[317] S.E. Skrabalak, J. Chen, L. Au, X. Lu, X. Li, Y. Xia, Gold nanocages for biomedical applications, Adv. Mater. 19 (2007) 3177–3184.
[318] X. Xia, M. Yang, L.K. Oetjen, Y. Zhang, Q. Li, J. Chen, Y. Xia, An enzyme-sensitive probe for photoacoustic imaging and fluorescence detection of protease activity, Nanoscale 3 (2011) 950–953.
[319] M. Hajfathalian, A. Amirshaghaghi, P.C. Naha, P. Chhour, J.C. Hsu, K. Douglas, Y. Dong, C.M. Sehgal, A. Tsourkas, S. Neretina, D.P. Cormode, Wulff in a cage gold nanoparticles as contrast agents for computed tomography and photoacoustic imaging, Nanoscale 10 (2018) 18749–18757.
[320] M. Hajfathalian, K.D. Gilroy, S.D. Golze, A. Yaghoubzade, E. Menumerov, R.A. Hughes, S. Neretina, A wulff in a cage: the confinement of substrate-based structures in plasmonic nanoshells, nanocages, and nanoframes using galvanic replacement, ACS Nano 10 (2016) 6354–6362.
[321] J. Chen, C. Glaus, R. Laforest, Q. Zhang, M. Yang, M. Gidding, M.J. Welch, Y. Xia, Gold nanocages as photothermal transducers for cancer treatment, Small 6 (2010) 811–817.
[322] Z. Wang, Z. Chen, Z. Liu, P. Shi, K. Dong, E. Ju, J. Ren, X. Qu, A multi-stimuli responsive gold nanocage–hyaluronic platform for targeted photothermal and chemotherapy, Biomaterials 35 (2014) 9678–9688.
[323] A. Srivatsan, S.V. Jenkins, M. Jeon, Z. Wu, C. Kim, J. Chen, R.K. Pandey, Gold nanocage-photosensitizer conjugates for dual-modal image-guided enhanced photodynamic therapy, Theranostics 4 (2014) 163.
[324] J. Chen, D. Wang, J. Xi, L. Au, A. Siekkinen, A. Warsen, Z.-Y. Li, H. Zhang, Y. Xia, X. Li, Immuno gold nanocages with tailored optical properties for targeted photothermal destruction of cancer cells, Nano Lett. 7 (2007) 1318–1322.
[325] L. Gao, J. Fei, J. Zhao, H. Li, Y. Cui, J. Li, Hypocrellin-loaded gold nanocages with high two-photon efficiency for photothermal/photodynamic cancer therapy in vitro, ACS Nano 6 (2012) 8030–8040.
[326] X.Q. Wang, F. Gao, X.Z. Zhang, Initiator-loaded gold nanocages as a light-induced free-radical generator for cancer therapy, Angew. Chem. 129 (2017) 9157–9161.
[327] C. Loo, A. Lowery, N. Halas, J. West, R. Drezek, Immunotargeted nanoshells for integrated cancer imaging and therapy, Nano Lett. 5 (2005) 709–711.
[328] D.P. O'Neal, L.R. Hirsch, N.J. Halas, J.D. Payne, J.L. West, Photo-thermal tumor ablation in mice using near infrared-absorbing nanoparticles, Cancer Lett. 209 (2004) 171–176.
[329] L.R. Hirsch, R.J. Stafford, J. Bankson, S.R. Sershen, B. Rivera, R. Price, J.D. Hazle, N.J. Halas, J.L. West, Nanoshell-mediated near-infrared thermal therapy of tumors under magnetic resonance guidance, Proc. Natl. Acad. Sci. 100 (2003) 13549–13554.
[330] Y. Ma, X. Liang, S. Tong, G. Bao, Q. Ren, Z. Dai, Gold nanoshell nanomicelles for potential magnetic resonance imaging, light-triggered drug release, and photothermal therapy, Adv. Funct. Mater. 23 (2013) 815–822.
[331] Y. Liu, X. Zhang, Z. Liu, L. Wang, L. Luo, M. Wang, Q. Wang, D. Gao, Gold nanoshell-based betulinic acid liposomes for synergistic chemo-photothermal therapy, Nanomedicine 13 (2017) 1891–1900.
[332] H. Wang, R. Zhao, Y. Li, H. Liu, F. Li, Y. Zhao, G. Nie, Aspect ratios of gold nanoshell capsules mediated melanoma ablation by synergistic photothermal therapy and chemotherapy, Nanomedicine 12 (2016) 439–448.
[333] M. Wang, Y. Liu, X. Zhang, L. Luo, L. Li, S. Xing, Y. He, W. Cao, R. Zhu, D. Gao, Gold nanoshell coated thermo-pH dual responsive liposomes for resveratrol delivery and chemo-photothermal synergistic cancer therapy, J. Mater. Chem. B 5 (2017) 2161–2171.
[334] S.-Y. Lee, M.-J. Shieh, Combined photothermo-chemotherapy using gold nanoshells on drug-loaded micelles for colorectal cancer treatment, Colloidal Nanoparticles for Biomedical Applications XIII, International Society for Optics and Photonics, 2018, p. 105070Y.
[335] H. Luo, M. Xu, X. Zhu, J. Zhao, S. Man, H. Zhang, Lung cancer cellular apoptosis induced by recombinant human endostatin gold nanoshell-mediated near-infrared thermal therapy, Int. J. Clin. Exp. Med. 8 (2015) 8758.
[336] R. Huschka, A. Barhoumi, Q. Liu, J.A. Roth, L. Ji, N.J. Halas, Gene silencing by gold nanoshell-mediated delivery and laser-triggered release of antisense oligonucleotide and siRNA, ACS Nano 6 (2012) 7681–7691.
[337] L. Ding, R. Sun, X. Zhang, Rap2b siRNA significantly enhances the anticancer therapeutic efficacy of adriamycin in a gold nanoshell-based drug/gene co-delivery system, Oncotarget 8 (2017) 21200.
[338] E. Morgan, D. Wupperfeld, D. Morales, N. Reich, Shape matters: gold nanoparticle shape impacts the biological activity of siRNA delivery, Bioconjug. Chem. 30 (2019) 853–860.
[339] S.J. Madsen, S.-K. Baek, A.R. Makkouk, T. Krasieva, H. Hirschberg, Macrophages as cell-based delivery systems for nanoshells in photothermal therapy, Ann. Biomed. Eng. 40 (2012) 507–515.
[340] A.J. Trinidad, S.J. Hong, Q. Peng, S.J. Madsen, H. Hirschberg, Combined concurrent photodynamic and gold nanoshell loaded macrophage-mediated photothermal therapies: an in vitro study on squamous cell head and neck carcinoma, Lasers Surg. Med. 46 (2014) 310–318.
[341] R. Cao-Milán, L.M. Liz-Marzán, Gold nanoparticle conjugates: recent advances toward clinical applications, Expert Opin. Drug Deliv. 11 (2014) 741–752.
[342] S. Her, D.A. Jaffray, C. Allen, Gold nanoparticles for applications in cancer radiotherapy: mechanisms and recent advancements, Adv. Drug Deliv. Rev. 109 (2017) 84–101.
[343] J.D. Mangadlao, X. Wang, C. McCleese, M. Escamilla, G. Ramamurthy, Z. Wang, M. Govande, J.P. Basilion, C. Burda, Prostate-specific membrane antigen targeted gold nanoparticles for theranostics of prostate cancer, ACS Nano 12 (2018) 3714–3725.
[344] T.A. Henderson, L.D. Morries, Near-infrared photonic energy penetration: can infrared phototherapy effectively reach the human brain? Neuropsychiatr. Dis. Treat. 11 (2015) 2191.
[345] S. Biffi, R. Voltan, E. Rampazzo, L. Prodi, G. Zauli, P. Secchiero, Applications of nanoparticles in cancer medicine and beyond: optical and multimodal in vivo imaging, tissue targeting and drug delivery, Expert Opin. Drug Deliv. 12 (2015) 1837–1849.
[346] D. Paithankar, B.H. Hwang, G. Munavalli, A. Kauvar, J. Lloyd, R. Blomgren, L. Faupel, T. Meyer, S. Mitragotri, Ultrasonic delivery of silica–gold nanoshells for photothermolysis of sebaceous glands in humans: nanotechnology from the bench to clinic, J. Control. Release 206 (2015) 30–36.
[347] G. Vincze, O. Szasz, A. Szasz, Generalization of the thermal dose of hyperthermia in oncology, Open J. Biophys. 5 (2015) 97.
[348] S. Kotb, A. Detappe, F. Lux, F. Appaix, E.L. Barbier, V.-L. Tran, M. Plissonneau, H. Gehan, F. Lefranc, C. Rodriguez-Lafrasse, Gadolinium-based nanoparticles and radiation therapy for multiple brain melanoma metastases: proof of concept before phase I trial, Theranostics 6 (2016) 418.
[349] F. Attar, M.G. Shahpar, B. Rasti, M. Sharifi, A.A. Saboury, S.M. Rezayat, M. Falahati, Nanozymes with intrinsic peroxidase-like activities, J. Mol. Liq. 278 (2019) 130–144.
[350] C. Zhang, S.Z. Jiang, C. Yang, C.H. Li, Y.Y. Huo, X.Y. Liu, A.H. Liu, Q. Wei, S.S. Gao, X.G. Gao, Gold@ silver bimetal nanoparticles/pyramidal silicon 3D substrate with high reproducibility for high-performance SERS, Sci. Rep. 6 (2016) 25243.
[351] T. Dobrovolskaya, V. Emelyanov, S. Danilova, V. Emelyanov, K. Butov, Assessment of Reliability of Recognition of Nanoparticles of Silver on Polyester Fibers on Two-dimensional Models and Experimental Data of the Raman Ranges, (2016).
[352] A.L. Nogueira, R.A. Machado, A.Z. de Souza, C.V. Franco, G.B. Dutra, Influence of process parameters and scalability of the semi-batch production of functionalized silver nanoparticles, Can. J. Chem. Eng. 94 (2016) 1472–1485.
[353] H.A. Zeinabad, A. Zarrabian, A.A. Saboury, A.M. Alizadeh, M. Falahati, Interaction of single and multi wall carbon nanotubes with the biological systems: tau protein and PC12 cells as targets, Sci. Rep. 6 (2016) 26508.
[354] L. Pishkar, S. Taheri, S. Makarem, H. Alizadeh Zeinabad, A. Rahimi, A.A. Saboury, M. Falahati, Studies on the interaction between nanodiamond and human hemoglobin by surface tension measurement and spectroscopy methods, J. Biomol. Struct. Dyn. 35 (2017) 603–615.
[355] Z. Aghili, S. Taheri, H.A. Zeinabad, L. Pishkar, A.A. Saboury, A. Rahimi, M. Falahati, Investigating the interaction of Fe nanoparticles with lysozyme by biophysical and molecular docking studies, PLoS One 11 (2016) e0164878.
[356] H.A. Zeinabad, E. Kachooei, A.A. Saboury, I. Kostova, F. Attar, M. Vaezzadeh, M. Falahati, Thermodynamic and conformational changes of protein toward interaction with nanoparticles: a spectroscopic overview, RSC Adv. 6 (2016)

105903–105919.
[357] G. Hajsalimi, S. Taheri, F. Shahi, F. Attar, H. Ahmadi, M. Falahati, Interaction of iron nanoparticles with nervous system: an in vitro study, J. Biomol. Struct. Dyn. 36 (2018) 928–937.
[358] S. Sweeney, A. Adamcakova-Dodd, P.S. Thorne, J.G. Assouline, Biocompatibility of multi-imaging engineered mesoporous silica nanoparticles: in vitro and adult and fetal in vivo studies, J. Biomed. Nanotechnol. 13 (2017) 544–558.
[359] A.S. Emrani, N.M. Danesh, P. Lavaee, M. Ramezani, K. Abnous, S.M. Taghdisi, Colorimetric and fluorescence quenching aptasensors for detection of streptomycin in blood serum and milk based on double-stranded DNA and gold nanoparticles, Food Chem. 190 (2016) 115–121.
[360] M.K. Lam, T. Gadzikwa, T. Nguyen, A. Kausar, B.S. Alladin-Mustan, M.D. Sikder, J.M. Gibbs-Davis, Tuning toehold length and temperature to achieve rapid, colorimetric detection of DNA from the disassembly of DNA–gold nanoparticle aggregates, Langmuir 32 (2016) 1585–1590.
[361] A.I. Dar, S. Walia, A. Acharya, Citric acid-coated gold nanoparticles for visual colorimetric recognition of pesticide dimethoate, J. Nanopart. Res. 18 (2016) 233.
[362] C. Cheng, H.-Y. Chen, C.-S. Wu, J.S. Meena, T. Simon, F.-H. Ko, A highly sensitive and selective cyanide detection using a gold nanoparticle-based dual fluorescence–colorimetric sensor with a wide concentration range, Sensors Actuators B Chem. 227 (2016) 283–290.
[363] J. Du, H. Du, X. Li, J. Fan, X. Peng, In-situ colorimetric recognition of arylamine based on chemodosimeter-functionalized gold nanoparticle, Sensors Actuators B Chem. 248 (2017) 318–323.
[364] M. Oishi, S. Sugiyama, An efficient particle-based DNA circuit system: catalytic disassembly of DNA/PEG-modified gold nanoparticle–magnetic bead composites for colorimetric Detection of miRNA, Small 12 (2016) 5153–5158.
[365] M. Nilam, A. Hennig, W.M. Nau, K.I. Assaf, Gold nanoparticle aggregation enables colorimetric sensing assays for enzymatic decarboxylation, Anal. Methods 9 (2017) 2784–2787.
[366] C.-C. Chang, C.-P. Chen, C.-Y. Chen, C.-W. Lin, DNA base-stacking assay utilizing catalytic hairpin assembly-induced gold nanoparticle aggregation for colorimetric protein sensing, Chem. Commun. 52 (2016) 4167–4170.
[367] J. Tashkhourian, M. Afsharinejad, A.R. Zolghadr, Colorimetric chiral discrimination and determination of S-citalopram based on induced aggregation of gold nanoparticles, Sensors Actuators B 232 (2016) 52–59.
[368] L. Yuan, X. Wang, Y. Fang, C. Liu, D. Jiang, X. Wo, W. Wang, H.-Y. Chen, Digitizing gold nanoparticle-based colorimetric assay by imaging and counting single nanoparticles, Anal. Chem. 88 (2016) 2321–2326.
[369] Y. Alnasser, C. Ferradas, T. Clark, M. Calderon, A. Gurbillon, D. Gamboa, U.S. McKakpo, I.A. Quakyi, K.M. Bosompem, D.J. Sullivan, Colorimetric detection of Plasmodium vivax in urine using msp10 oligonucleotides and gold nanoparticles, PLoS Negl. Trop. Dis. 10 (2016) e0005029.
[370] L. Gong, B. Du, L. Pan, Q. Liu, K. Yang, W. Wang, H. Zhao, L. Wu, Y. He, Colorimetric aggregation assay for arsenic (III) using gold nanoparticles, Microchim. Acta 184 (2017) 1185–1190.
[371] T.-S. Lai, T.-C. Chang, S.-C. Wang, Gold nanoparticle-based colorimetric methods to determine protein contents in artificial urine using membrane micro-concentrators and mobile phone camera, Sensors Actuators B 239 (2017) 9–16.
[372] X. Liu, Z. Wu, Q. Zhang, W. Zhao, C. Zong, H. Gai, Single gold nanoparticle-based colorimetric detection of picomolar mercury ion with dark-field microscopy, Anal. Chem. 88 (2016) 2119–2124.
[373] A. Marsella, P. Valentini, P. Tarantino, M. Congedo, P.P. Pompa, A gold nanoparticles-based colorimetric test to detect single nucleotide polymorphisms for improvement of personalized therapy of psoriasis, Biophotonics: Photonic Solutions for Better Health Care V, International Society for Optics and Photonics, 2016(pp. 98870P).
[374] H. Du, R. Chen, J. Du, J. Fan, X. Peng, Gold nanoparticle-based colorimetric recognition of creatinine with good selectivity and sensitivity, Ind. Eng. Chem. Res. 55 (2016) 12334–12340.
[375] R. Kumvongpin, P. Jearanaikool, C. Wilailuckana, N. Sae-ung, P. Prasongdee, S. Daduang, M. Wongsena, P. Boonsiri, W. Kiatpathomchai, S.S. Swangvaree, High sensitivity, loop-mediated isothermal amplification combined with colorimetric gold-nanoparticle probes for visual detection of high risk human papillomavirus genotypes 16 and 18, J. Virol. Methods 234 (2016) 90–95.
[376] H.-H. Deng, G.-L. Hong, F.-L. Lin, A.-L. Liu, X.-H. Xia, W. Chen, Colorimetric detection of urea, urease, and urease inhibitor based on the peroxidase-like activity of gold nanoparticles, Anal. Chim. Acta 915 (2016) 74–80.
[377] Y.-S. Borghei, M. Hosseini, M. Dadmehr, S. Hosseinkhani, M.R. Ganjali, R. Sheikhnejad, Visual detection of cancer cells by colorimetric aptasensor based on aggregation of gold nanoparticles induced by DNA hybridization, Anal. Chim. Acta 904 (2016) 92–97.
[378] H. Zhao, Y. Qu, F. Yuan, X. Quan, A visible and label-free colorimetric sensor for miRNA-21 detection based on peroxidase-like activity of graphene/gold-nanoparticle hybrids, Anal. Methods 8 (2016) 2005–2012.
[379] A. Safavi, R. Ahmadi, Z. Mohammadpour, Colorimetric sensing of silver ion based on anti aggregation of gold nanoparticles, Sensors Actuators B 242 (2017) 609–615.
[380] L. Wang, Z. Liu, X. Xia, C. Yang, J. Huang, S. Wan, Colorimetric detection of cucumber green mottle mosaic virus using unmodified gold nanoparticles as colorimetric probes, J. Virol. Methods 243 (2017) 113–119.
[381] C. Dong, G. Wu, Z. Wang, W. Ren, Y. Zhang, Z. Shen, T. Li, A. Wu, Selective colorimetric detection of Cr (III) and Cr (VI) using gallic acid capped gold nanoparticles, DTr 45 (2016) 8347–8354.
[382] A.V. Skinner, S. Han, R. Balasubramanian, Rapid selective colorimetric sensing of polyphosphates by ionic resorcinarene cavitand interdigitated gold nanoparticles, Sensors Actuators B 247 (2017) 706–712.
[383] D. Zhang, J. Yang, J. Ye, L. Xu, H. Xu, S. Zhan, B. Xia, L. Wang, Colorimetric detection of bisphenol a based on unmodified aptamer and cationic polymer aggregated gold nanoparticles, Anal. Biochem. 499 (2016) 51–56.
[384] Y. Huo, L. Qi, X.-J. Lv, T. Lai, J. Zhang, Z.-Q. Zhang, A sensitive aptasensor for colorimetric detection of adenosine triphosphate based on the protective effect of ATP-aptamer complexes on unmodified gold nanoparticles, Biosens. Bioelectron. 78 (2016) 315–320.
[385] Y. Xiong, M. Li, H. Liu, Z. Xuan, J. Yang, D. Liu, Janus PEGylated gold nanoparticles: a robust colorimetric probe for sensing nitrite ions in complex samples, Nanoscale 9 (2017) 1811–1815.
[386] P. Huang, J. Li, X. Liu, F. Wu, Colorimetric determination of aluminum (III) based on the aggregation of schiff base-functionalized gold nanoparticles, Microchim. Acta 183 (2016) 863–869.
[387] R.-D. Li, B.-C. Yin, B.-C. Ye, Ultrasensitive, colorimetric detection of microRNAs based on isothermal exponential amplification reaction-assisted gold nanoparticle amplification, Biosens. Bioelectron. 86 (2016) 1011–1016.
[388] J.-j. Li, X.-f. Wang, D.-q. Huo, C.-j. Hou, H.-b. Fa, M. Yang, L. Zhang, Colorimetric measurement of Fe3+ using a functional paper-based sensor based on catalytic oxidation of gold nanoparticles, Sensors Actuators B 242 (2017) 1265–1271.
[389] K. Tian, G. Siegel, A. Tiwari, A simple and selective colorimetric mercury (II) sensing system based on chitosan stabilized gold nanoparticles and 2, 6-pyridinedicarboxylic acid, Mater. Sci. Eng. 71 (2017) 195–199.
[390] T. Hu, S. Lu, C. Chen, J. Sun, X. Yang, Colorimetric sandwich immunosensor for Aβ (1–42) based on dual antibody-modified gold nanoparticles, Sensors Actuators B 243 (2017) 792–799.
[391] R. Ahirwar, P. Nahar, Development of a label-free gold nanoparticle-based colorimetric aptasensor for detection of human estrogen receptor alpha, Anal. Bioanal. Chem. 408 (2016) 327–332.
[392] N. Fahimi-Kashani, M.R. Hormozi-Nezhad, Gold-nanoparticle-based colorimetric sensor array for discrimination of organophosphate pesticides, Anal. Chem. 88 (2016) 8099–8106.
[393] Y. Yu, Y. Hong, P. Gao, M.K. Nazeeruddin, Glutathione modified gold nanoparticles for sensitive colorimetric detection of Pb2+ ions in rainwater polluted by leaking perovskite solar cells, Anal. Chem. 88 (2016) 12316–12322.
[394] A. Kumar, M. Bhatt, G. Vyas, S. Bhatt, P. Paul, Sunlight induced preparation of functionalized gold nanoparticles as recyclable colorimetric dual sensor for aluminum and fluoride in water, ACS Appl. Mater. Interfaces 9 (2017) 17359–17368.
[395] G. Song, F. Zhou, C. Xu, B. Li, A universal strategy for visual chiral recognition of α-amino acids with L-tartaric acid-capped gold nanoparticles as colorimetric probes, Analyst 141 (2016) 1257–1265.
[396] X. Gao, Y.-H. Tsou, M. Garis, H. Huang, X. Xu, Highly specific colorimetric detection of DNA oxidation biomarker using gold nanoparticle/triplex DNA conjugates, Nanomedicine 12 (2016) 2101–2105.
[397] G. Jian-feng, H. Chang-jun, Y. Mei, H. Dan-qun, L. Jun-jie, F. Huan-bao, L. Hui-bo, Y. Ping, Colorimetric sensing of chromium (VI) ions in aqueous solution based on the leaching of protein-stabled gold nanoparticles, Anal. Methods 8 (2016) 5526–5532.
[398] X. Ma, L. Song, N. Zhou, Y. Xia, Z. Wang, A novel aptasensor for the colorimetric detection of S. typhimurium based on gold nanoparticles, Int. J. Food Microbiol. 245 (2017) 1–5.
[399] Y. Mao, T. Fan, R. Gysbers, Y. Tan, F. Liu, S. Lin, Y. Jiang, A simple and sensitive aptasensor for colorimetric detection of adenosine triphosphate based on unmodified gold nanoparticles, Talanta 168 (2017) 279–285.
[400] F. Yuan, H. Zhao, X. Wang, X. Quan, Determination of oxytetracycline by a graphene—gold nanoparticle-based colorimetric aptamer sensor, Anal. Lett. 50 (2017) 544–553.
[401] F. Tanvir, A. Yaqub, S. Tanvir, W.A. Anderson, Colorimetric enumeration of bacterial contamination in water based on β-galactosidase gold nanoshell activity, Enzym. Microb. Technol. 99 (2017) 49–56.
[402] V.V. Kumar, S.P. Anthony, Highly selective colorimetric sensing of Hg2+ ions by label free AuNPs in aqueous medium across wide pH range, Sensors Actuators B 225 (2016) 413–419.
[403] H.-y. Shi, L. Yang, X.-y. Zhou, J. Bai, J. Gao, H.-x. Jia, Q.-g. Li, A gold nanoparticle-based colorimetric strategy coupled to duplex-specific nuclease signal amplification for the determination of microRNA, Microchim. Acta 184 (2017) 525–531.
[404] G. Li, C. Zeng, R. Jin, Chemoselective hydrogenation of nitrobenzaldehyde to nitrobenzyl alcohol with unsupported au nanorod catalysts in water, J. Phys. Chem. C 119 (2015) 11143–11147.
[405] L. Gao, C.N. Liang, H.H. Li, Z.X. Lu, Hierarchically templated synthesis of hollow nanoporous gold rods and TiO2-coated gold rods, ChemNanoMat 2 (2016) 1098–1103.
[406] J.-H. Lee, Z. Cheglakov, J. Yi, T.M. Cronin, K.J. Gibson, B. Tian, Y. Weizmann, Plasmonic photothermal gold bipyramid nanoreactors for ultrafast real-time bioassays, J. Am. Chem. Soc. 139 (2017) 8054–8057.
[407] B. Lu, C. Kan, S. Ke, H. Xu, Y. Ni, C. Wang, D. Shi, Geometry-dependent surface plasmonic properties and dielectric sensitivity of bimetallic Au@Pd nanorods, Plasmonics 12 (2017) 1183–1191.
[408] C.-Y. Chiu, P.-J. Chung, K.-U. Lao, C.-W. Liao, M.H. Huang, Facet-dependent catalytic activity of gold nanocubes, octahedra, and rhombic dodecahedra toward 4-nitroaniline reduction, J. Phys. Chem. C 116 (2012) 23757–23763.
[409] G. Fu, L. Ding, Y. Chen, J. Lin, Y. Tang, T. Lu, Facile water-based synthesis and catalytic properties of platinum-gold alloy nanocubes, CrystEngComm 16 (2014) 1606–1610.
[410] J.W. Park, S.W. Lai, S.O. Cho, Catalytic hydrogen generation from hydrolysis of ammonia borane using octahedral Au@Pt nanoparticles, Int. J. Hydrog. Energy 40

(2015) 16316–16322.
[411] S. Rej, K. Chanda, C.-Y. Chiu, M.H. Huang, Control of regioselectivity over gold nanocrystals of different surfaces for the synthesis of 1,4-disubstituted triazole through the click reaction, Chem. Eur. J. 20 (2014) 15991–15997.
[412] Y.S. Seo, E.-Y. Ahn, J. Park, T.Y. Kim, J.E. Hong, K. Kim, Y. Park, Y. Park, Catalytic reduction of 4-nitrophenol with gold nanoparticles synthesized by caffeic acid, Nanoscale Res. Lett. 12 (2017) 7.
[413] Q. Cui, A. Yashchenok, L. Li, H. Möhwald, M. Bargheer, Mechanistic study on reduction reaction of nitro compounds catalyzed by gold nanoparticles using in situ SERS monitoring, Colloids Surf. A Physicochem. Eng. Asp. 470 (2015) 108–113.
[414] Q. Cui, B. Xia, S. Mitzscherling, A. Masic, L. Li, M. Bargheer, H. Möhwald, Preparation of gold nanostars and their study in selective catalytic reactions, Colloids Surf. A Physicochem. Eng. Asp. 465 (2015) 20–25.
[415] A.-J. Wang, S.-F. Qin, D.-L. Zhou, L.-Y. Cai, J.-R. Chen, J.-J. Feng, Caffeine assisted one-step synthesis of flower-like gold nanochains and their catalytic behaviors, RSC Adv. 3 (2013) 14766–14773.
[416] D. Huang, X. Bai, L. Zheng, Ultrafast preparation of three-dimensional dendritic gold nanostructures in aqueous solution and their applications in catalysis and SERS, J. Phys. Chem. C 115 (2011) 14641–14647.
[417] M. Ying, Y. Edward Ng Siang, Facile synthesis of hierarchical gold nanostructures and their catalytic application, Nanotechnology 27 (2016) 325602.
[418] B. Liu, M. Yang, H. Li, Synthesis of gold nanoflowers assisted by a CH-CF hybrid surfactant and their applications in SERS and catalytic reduction of 4-nitroaniline, Colloids Surf. A Physicochem. Eng. Asp. 520 (2017) 213–221.
[419] K. Liu, L. Han, J. Zhuang, D.-P. Yang, Protein-directed gold nanoparticles with excellent catalytic activity for 4-nitrophenol reduction, Mater. Sci. Eng. 78 (2017) 429–434.
[420] L. Li, Z. Wang, T. Huang, J. Xie, L. Qi, Porous gold nanobelts templated by metal – surfactant complex nanobelts, Langmuir 26 (2010) 12330–12335.
[421] M. Chirea, A. Freitas, B.S. Vasile, C. Ghitulica, C.M. Pereira, F. Silva, Gold nanowire networks: synthesis, characterization, and catalytic activity, Langmuir 27 (2011) 3906–3913.
[422] R. Bhandari, M.R. Knecht, Synthesis, characterization, and catalytic application of networked Au nanostructures fabricated using peptide templates, Catal. Sci. Technol. 2 (2012) 1360–1366.
[423] H. Jia, J. An, X. Guo, C. Su, L. Zhang, H. Zhou, C. Xie, Deep eutectic solvent-assisted growth of gold nanofoams and their excellent catalytic properties, J. Mol. Liq. 212 (2015) 763–766.
[424] Y. Lu, J. Yuan, F. Polzer, M. Drechsler, J. Preussner, In situ growth of catalytic active Au – Pt bimetallic nanorods in thermoresponsive core – shell microgels, ACS Nano 4 (2010) 7078–7086.
[425] Y. Zheng, J. Tao, H. Liu, J. Zeng, T. Yu, Y. Ma, C. Moran, L. Wu, Y. Zhu, J. Liu, Y. Xia, Facile synthesis of gold nanorice enclosed by high-index facets and its application for CO oxidation, Small 7 (2011) 2307–2312.
[426] Y. Zhu, H. Qian, A. Das, R. Jin, Comparison of the catalytic properties of 25-atom gold nanospheres and nanorods, Chin. J. Catal. 32 (2011) 1149–1155.
[427] M.L. Tang, N. Liu, J.A. Dionne, A.P. Alivisatos, Observations of shape-dependent hydrogen uptake trajectories from single nanocrystals, J. Am. Chem. Soc. 133 (2011) 13220–13223.
[428] Y. Fu, Y. Lu, F. Polzer, M.C. Lux-Steiner, C.-H. Fischer, In-situ synthesis of stabilizer-free gold nanocrystals with controllable shape on substrates as highly active catalysts for multiple use, Adv. Synth. Catal. 358 (2016) 1440–1448.
[429] W. Ye, J. Yu, Y. Zhou, D. Gao, D. Wang, C. Wang, D. Xue, Green synthesis of Pt–Au dendrimer-like nanoparticles supported on polydopamine-functionalized graphene and their high performance toward 4- nitrophenol reduction, Appl. Catal. B Environ. 181 (2016) 371–378.
[430] Y. Yu, K. Kant, J.G. Shapter, J. Addai-Mensah, D. Losic, Gold nanotube membranes have catalytic properties, Microporous Mesoporous Mater. 153 (2012) 131–136.
[431] M.A. Sanchez-Castillo, C. Couto, W.B. Kim, J.A. Dumesic, Gold-nanotube membranes for the oxidation of CO at gas–water interfaces, Angew. Chem. 116 (2004) 1160–1162.
[432] B. Pal, R. Kaur, Facile synthesis of anisotropic au nanostructures by laser irradiation and study of their optical and electrokinetic properties, Part. Sci. Technol. 33 (2015) 139–144.
[433] Z. Lou, S. Kim, P. Zhang, X. Shi, M. Fujitsuka, T. Majima, In situ observation of single au triangular nanoprism etching to various shapes for plasmonic photocatalytic hydrogen generation, ACS Nano 11 (2017) 968–974.
[434] J. Joo, B.H. Kim, J.S. Lee, Synthesis of gold nanoparticle-embedded silver cubic mesh nanostructures using AgCl nanocubes for plasmonic photocatalysis, Small 13 (2017) 1701751.
[435] M.K. Gangishetty, A.M. Fontes, M. Malta, T.L. Kelly, R.W.J. Scott, Improving the rates of Pd-catalyzed reactions by exciting the surface plasmons of AuPd bimetallic nanotriangles, RSC Adv. 7 (2017) 40218–40226.
[436] C. Fang, H. Jia, S. Chang, Q. Ruan, P. Wang, T. Chen, J. Wang, (Gold core)/(titania shell) nanostructures for plasmon-enhanced photon harvesting and generation of reactive oxygen species, Energy Environ. Sci. 7 (2014) 3431–3438.
[437] Y. Horiguchi, T. Kanda, K. Torigoe, H. Sakai, M. Abe, Preparation of gold/silver/titania trilayered nanorods and their photocatalytic activities, Langmuir 30 (2014) 922–928.
[438] Y. Qu, R. Cheng, Q. Su, X. Duan, Plasmonic enhancements of photocatalytic activity of Pt/n-Si/Ag photodiodes using Au/Ag core/shell nanorods, J. Am. Chem. Soc. 133 (2011) 16730–16733.
[439] W.R. Erwin, A. Coppola, H.F. Zarick, P. Arora, K.J. Miller, R. Bardhan, Plasmon enhanced water splitting mediated by hybrid bimetallic Au-Ag core-shell nanostructures, Nanoscale 6 (2014) 12626–12634.
[440] T.-Y. Shin, S.-H. Yoo, S. Park, Gold nanotubes with a nanoporous wall: their ultrathin platinum coating and superior electrocatalytic activity toward methanol oxidation, Chem. Mater. 20 (2008) 5682–5686.
[441] S.-S. Li, P. Song, A.-J. Wang, J.-J. Feng, Neuron-like gold-palladium alloy nanostructures: rapid synthesis and applications in electrocatalysis and surface-enhanced raman scattering, J. Colloid Interface Sci. 482 (2016) 73–80.
[442] Y. Xu, P. Yiu, G. Shan, T. Shibayama, S. Watanabe, M. Ohnuma, W. Huang, C.H. Shek, 3D nanoporous gold with very low parting limit derived from au-based metallic glass and enhanced methanol electro-oxidation catalytic performance induced by metal migration, ChemNanoMat 4 (2017) 88–97.
[443] Y. Tang, Q. Liu, X. Yang, M. Wei, M. Zhang, Copper oxide coated gold nanorods like a film: a facile route to nanocomposites for electrochemical application, J. Electroanal. Chem. 806 (2017) 8–14.
[444] N.S.K. Gowthaman, S.A. John, Simultaneous growth of spherical, bipyramidal and wire-like gold nanostructures in solid and solution phases: SERS and electrocatalytic applications, CrystEngComm 19 (2017) 5369–5380.
[445] Y. Jiang, Y. Yan, Y. Han, H. Zhang, D. Yang, Core–shell and alloy integrating PdAu bimetallic nanoplates on reduced graphene oxide for efficient and stable hydrogen evolution catalysts, RSC Adv. 7 (2017) 43373–43379.
[446] X. Han, D. Wang, J. Huang, D. Liu, T. You, Ultrafast growth of dendritic gold nanostructures and their applications in methanol electro-oxidation and surface-enhanced raman scattering, J. Colloid Interface Sci. 354 (2011) 577–584.
[447] J.-J. Feng, A.-Q. Li, Z. Lei, A.-J. Wang, Low-potential synthesis of “clean” au nanodendrites and their high performance toward ethanol oxidation, ACS Appl. Mater. Interfaces 4 (2012) 2570–2576.
[448] S. Choi, Y. Moon, H. Yoo, Finely tunable fabrication and catalytic activity of gold multipod nanoparticles, J. Colloid Interface Sci. 469 (2016) 269–276.
[449] A. Li, Y. Chen, K. Zhuo, C. Wang, C. Wang, J. Wang, Facile and shape-controlled electrochemical synthesis of gold nanocrystals by changing water contents in deep eutectic solvents and their electrocatalytic activity, RSC Adv. 6 (2016) 8786–8790.
[450] N.Y. Hau, P. Yang, C. Liu, J. Wang, P.-H. Lee, S.-P. Feng, Aminosilane-Assisted Electrodeposition of Gold Nanodendrites and Their Catalytic Properties, 7 (2017), p. 39839.
[451] P. Song, L. Liu, J.-J. Feng, J. Yuan, A.-J. Wang, Q.-Q. Xu, Poly(ionic liquid) assisted synthesis of hierarchical gold-platinum alloy nanodendrites with high electrocatalytic properties for ethylene glycol oxidation and oxygen reduction reactions, Int. J. Hydrog. Energy 41 (2016) 14058–14067.
[452] S. Li, H. Xu, Z. Xiong, K. Zhang, C. Wang, B. Yan, J. Guo, Y. Du, Monodispersed porous flowerlike PtAu nanocrystals as effective electrocatalysts for ethanol oxidation, Appl. Surf. Sci. 422 (2017) 172–178.
[453] Y. Peng, L. Li, R. Tao, L. Tan, M. Qiu, L. Guo, One-pot synthesis of Au@Pt star-like nanocrystals and their enhanced electrocatalytic performance for formic acid and ethanol oxidation, Nano Res. (2017) 1–11.
[454] M. Taei, E. Havakeshian, F. Hasheminasab, A gold nanodendrite-decorated layered double hydroxide as a bifunctional electrocatalyst for hydrogen and oxygen evolution reactions in alkaline media, RSC Adv. 7 (2017) 47049–47055.
[455] D.-N. Li, A.-J. Wang, J. Wei, Q.-L. Zhang, J.-J. Feng, Facile synthesis of flower-like Au@AuPd nanocrystals with highly electrocatalytic activity for formic acid oxidation and hydrogen evolution reactions, Int. J. Hydrog. Energy 42 (2017) 19894–19902.
[456] H. Jia, G. Chang, H. Shu, M. Xu, X. Wang, Z. Zhang, X. Liu, H. He, K. Wang, R. Zhu, Y. He, Pt nanoparticles modified Au dendritic nanostructures: facile synthesis and enhanced electrocatalytic performance for methanol oxidation, Int. J. Hydrog. Energy 42 (2017) 22100–22107.
[457] J.-J. Feng, S.-S. Chen, X.-L. Chen, X.-F. Zhang, A.-J. Wang, One-pot fabrication of reduced graphene oxide supported dendritic core-shell gold@gold-palladium nanoflowers for glycerol oxidation, J. Colloid Interface Sci. 509 (2018) 73–81.
[458] S.-S. Chen, Z.-Z. Yang, A.-J. Wang, K.-M. Fang, J.-J. Feng, Facile synthesis of bimetallic gold-palladium nanocrystals as effective and durable advanced catalysts for improved electrocatalytic performances of ethylene glycol and glycerol oxidation, J. Colloid Interface Sci. 509 (2018) 10–17.
[459] R. Cao, T. Xia, R. Zhu, Z. Liu, J. Guo, G. Chang, Z. Zhang, X. Liu, Y. He, Novel synthesis of core-shell au-pt dendritic nanoparticles supported on carbon black for enhanced methanol electro-oxidation, Appl. Surf. Sci. 509 (509) (2018) 840–846.
[460] J. Zhang, P. Liu, H. Ma, Y. Ding, nanostructured porous gold for methanol electro-oxidation, J. Phys. Chem. C 111 (2007) 10382–10388.
[461] N. Zhao, Y. Wei, N. Sun, Q. Chen, J. Bai, L. Zhou, Y. Qin, M. Li, L. Qi, controlled synthesis of gold nanobelts and nanocombs in aqueous mixed surfactant solutions, Langmuir 24 (2008) 991–998.
[462] C.C. Mayorga-Martinez, M. Guix, R.E. Madrid, A. Merkoci, Bimetallic nanowires as electrocatalysts for nonenzymatic real-time impedancimetric detection of glucose, Chem. Commun. 48 (2012) 1686–1688.
[463] L.-L. He, P. Song, J.-J. Feng, W.-H. Huang, Q.-L. Wang, A.-J. Wang, Simple wet-chemical synthesis of alloyed PdAu nanochain networks with improved electrocatalytic properties, Electrochim. Acta 176 (2015) 86–95.
[464] T. Guo, G. Yu, Y. Zhang, H. Xiang, F. Chang, C.-J. Zhong, Synthesis of ultralong, monodispersed, and surfactant-free gold nanowire catalysts: growth mechanism and electrocatalytic properties for methanol oxidation reaction, J. Phys. Chem. C 121 (2017) 3108–3116.